# Study on a Resource-Saving Cloud based Long-Term ECG Monitoring System Using Machine Learning Algorithms

by

Ping Cheng

B.Eng., Northwestern Polytechnical University, 2009

M.Sc., Northwestern Polytechnical University, 2012

A Dissertation Submitted in Partial Fulfillment of the

Requirements for the Degree of

DOCTOR OF PHILOSOPHY

in the Department of Electrical and Computer Engineering

Study on a Resource-Saving Cloud based Long-Term ECG Monitoring System Using Machine Learning Algorithms

by

Ping Cheng

B.Eng., Northwestern Polytechnical University, 2009

M.Sc., Northwestern Polytechnical University, 2012

Supervisory Committee

---

Dr. Xiaodai Dong, Supervisor

(Department of Electrical and Computer Engineering)

---

Dr. Wu-Sheng Lu, Departmental Member

(Department of Electrical and Computer Engineering)

---

Dr. Yang Shi, Outside Member

(Department of Mechanical Engineering)

## ABSTRACT

Electrocardiogram (ECG) records the electrical impulses from myocardium, reflects the underlying dynamics of the heart and has been widely exploited to detect and identify cardiac arrhythmias. This dissertation examines a resource-saving cloud based long-term ECG (CLT-ECG) monitoring system which consists of an ECG raw data acquisition system, a mobile device and a serve. Three issues that are critically pertaining to the effectiveness and efficiency of the monitoring system are studied: the detection of life-threatening arrhythmias, the discrimination of normal and abnormal heartbeats to facilitate the resource-saving operation and the multi-class heartbeat classification algorithm for non-life-threatening arrhythmias.

The detection algorithm for life-threatening ventricular arrhythmias, which is critical to saving patients' lives, is investigated by exploiting personalized features. Two new personalized features, namely, aveCC and medianCC, are extracted based on the correlation coefficients between a patient-specific regular QRS-complex template and his/her real-time ECG data, characterizing subtle differences in the QRS complexes among different people. A small set of the most effective features is selected for efficient performance and real-time operation using Support Vector Machines (SVMs). The effectiveness of the proposed algorithm is validated in enhancing the performance under both the record-based and database-based data divisions. The classification algorithm achieves results outperforming the existing classification performances using top-two or top-three features.

A novel patient-specific arrhythmia detection algorithm, which discriminates the normal and abnormal heartbeats, is proposed using One-Class SVMs. Conventionally, CLT-ECG systems are used to solve problems such as the portable problem and the difficulty of capturing the intermittent arrhythmias. However, CLT-ECG systems are subject to several practical limitations: battery power restriction, network congestion and heavily redundant ECG data. To overcome these problems, a resource-saving CLT-ECG system is studied, in

which a novel arrhythmia detection algorithm closely related to the resource-saving rate is proposed and examined in detail. The proposed arrhythmia detection algorithm explores two types of variations: waveform change indicator (WCI), which reflects a change within one heartbeat; modified RR interval ratio (modRRIR), which characterizes the successive heartbeat interval variation. The overall classification result is obtained from combining the results separately adopting WCI and modRRIR. The proposed algorithm is validated using the public ECG database with a result outperforming others in the literature, as well as using the data collected from the ECG platform Heartcarer built in our research group.

Considering the multi-class classification in the cloud server, a patient-specific single-lead ECG heartbeat classification strategy is proposed to discriminate ventricular ectopic beats (VEBs) and Supraventricular Ectopic Beats (SVEBs). Two types of features are extracted: Intra-beat features characterize the distortion of the waveform within one heartbeat, while inter-beat features reflect the variation between successive heartbeats. A novel fusion strategy consisting of a global classifier and a local classifier is presented. The local classifier is obtained using the high-confidence heartbeats extracted from about 5-minute data of a specific patient, while the global classifier is trained by the public training data. The advantage of the developed strategy is that fully automatic classification is realized without the intervention of physicians. Finally, simulation results show that comparable or even better classification performance is achieved, which validates the effectiveness of the proposed strategy.

# Contents

# List of Tables

# List of Figures

# ACKNOWLEDGEMENTS

First of all, I would like to thank my supervisor, Prof. Xiaodai Dong, for her patient guidance and insightful instructions during my Ph.D study. In countless individual meetings with her, I have learnt how to think and conduct research as a Ph.D student. She is a decent and professional researcher and sets an excellent example for me. She is also a trusted friend who always provide comfort and encouragement whenever I am frustrated and upset. I will remember the time we were working together.

I also would like to thank the thesis committee members, Dr. Yang Shi and Dr. Wu-Sheng Lu for their constructive comments. I was lucky to have the opportunity to visit Dr. Yang Shi's group for half a year in 2011, and this experience greatly broadens my horizon. Dr. Yang Shi gave me a lot of valuable comments on my study, research and life. I took several courses instructed by Dr. Wu-Sheng Lu, and also discussed problems with him for many times. I sincerely express my gratitude for his dedication and kindness.

During my Ph.D studies, I am very lucky to have a lot of groupmates, officemates and friends around. I am grateful to their help and encouragement: Binyan Zhao, Ming Lei, Zheng Xu, Yongyu Dai, Leyuan pan, Guowei Zhang, Yiming Huo, Tong Xue, Le Liang, Guang Zeng, Wanbo Li, Weizheng Li, Yuejiao Hui, Jun Zhou, Weiheng Ni, Lan Xu, Tianyang Li, Farnoosh Talaei, Wenyan Yu, Yunlong Shao, Fang Chen, Zhu Ye, Xiao Ma, Mengyue Cai, Xiao Feng, and Po Zhang. With them, my research perspective becomes wide and my research life becomes colorful.

I also would like to thank Xiaotao Liu for his research encouragement and emotional support during the last stage of my Ph.D study.

Finally, but most importantly, I would like to thank my family members who are always with me whether I am sad or happy.

*Ping Cheng, Victoria, BC, Canada*

# DEDICATION

*To my family,*

*When involved in a dilemma,*

*Pick yourself up,*

*Brush yourself off,*

*Whisper a prayer,*

*And start where you let off.*

*Never, never, never give up.*

## Abbreviations

| | |
|---|---|
| **ECG** | Electrocardiogram |
| **CLT-ECG** | Cloud based Long-Term ECG |
| **SA Node** | Sinoatrial Node |
| **AV Node** | Atrioventricular Node |
| **NSR(s)** | Normal Sinus Rhythm(s) |
| **AAMI** | Association of the Advancement for Medical Instrumentation |
| **CUDB** | Creighton University Ventricular Tachyarrhythmia Database |
| **VFDB** | MIT-BIH Malignant Ventricular Arrhythmia Database |
| **MITDB** | MIT-BIH Arrhythmia Database |
| **VF** | Ventricular Fibrillation |
| **VFL** | Ventricular Flutter |
| **VT** | Ventricular Tachycardia |
| **VEB(s)** | Ventricular Ectopic Beat(s) |
| **SVEB(s)** | Supraventricular Ectopic Beat(s) |
| **aveCC** | Average of the Correlation Coefficients Calculated in One Segment |
| **medianCC** | Median of the Correlation Coefficients Calculated in One Segment |
| **RR Interval** | Time Duration between a R-peak to the Next R-peak |
| **WCI** | Waveform Change Index |
| **modRRIR** | Modified RR Interval Ratio |
| **SVM(s)** | Support Vector Machine(s) |
| **OC-SVM(s)** | One-Class Support Vector Machine(s) |

# Chapter 1

# Introduction

Hundreds of thousands of people worldwide are impacted by a variety of heart diseases, which can lead to various health issues or even cardiac deaths. Traditional hospital health examination and long-term personal care provided by doctors and nurses can not handle the growing number of patients and the resulting astronomical healthcare cost. A cloud based long-term electrocardiogram (CLT-ECG) system using a smartphone is emerging as an effective tool for long-term monitoring and urgent cardiac event alarming. With the availability of a large amount of data collected by an ambulatory electrocardiogram (ECG), signal processing of the ECG data for automatic identification of potential problems is becoming increasingly important. Thus, research work on CLT-ECG signal processing techniques draws many attentions from both academic researchers and cardiologists.

In general, ECG signal processing techniques are developed in two main directions, system design (for data acquisition, transmission, storage and display), and automatic ECG-based heart disease classification and diagnosis. A simple CLT-ECG system is shown in Fig. 1.1. The data stream originating from the ECG sensor board, is amplified, filtered, digitalized and finally transmitted to the cloud server/hospital database through the mobile device such as smartphones. The system design is determined by objectives of the automatic ECG

classification and diagnosis.

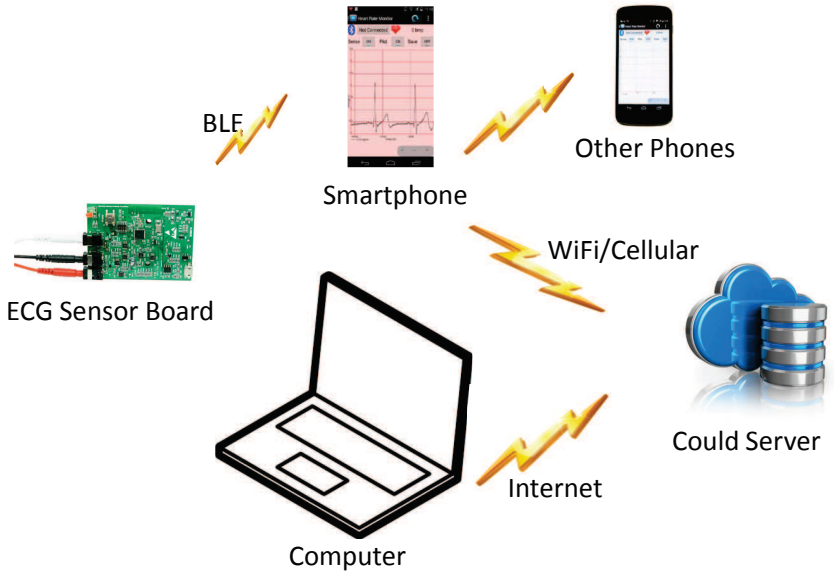


Figure 1.1: A CLT-ECG system overview.

Automatic ECG classification usually includes filtering, QRS detection, feature extraction and selection, and heartbeat/rhythm classification, as shown in Fig. 1.2. In the filtering process, the motion artifact problem is still not well solved, especially in wearable CLT-ECG systems, while other noise removal mechanisms achieve good performance. QRS detection is the first step to analyze an ECG signal. The commonly used methods for QRS detection are well developed, such as the Pan and Tompkins (P & T) algorithm and wavelet transform based methods. Feature extraction and selection are mainly for ECG classification such as diagnosing of certain heart diseases. Extracted features are from time domain, frequency domain or other domains/spaces. Feature selection techniques rank extracted features and choose the features with desired performance, which facilitates the following abnormal heartbeat detection or arrhythmia detection.

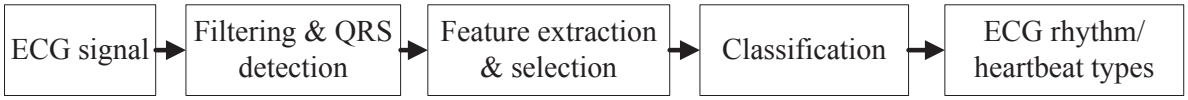


Figure 1.2: Diagram for automatic ECG classification.

How to assign the classification tasks to different parts of the whole CLT-ECG system, in order to make the system practical and resource-effective? And how to realize the tasks and improve the automatic classification performances? Based on what is mentioned above, the dissertation focuses on the final result when considering the CLT-ECG system design as well as the distributed implementation of the automatic ECG classification and diagnosis algorithm, to achieve the overall improvement on both system design and classification algorithms.

This chapter is organized as follows. The background of ECG, namely, the interpretation of cardiac electrophysiology, the fundamentals of ECG lead signals, ECG arrhythmias closely related with ECG waveforms, and a general CLT-ECG system scheme, is introduced in Section 1.1. Then three research issues, namely, life-threatening arrhythmia detection, anomaly-trigged CLT-ECG data transmission and non-life-threatening arrhythmia detection, are stated separately under the proposed CLT-ECG scheme in Section 1.2. Finally, the contributions and the organization of the thesis are presented in Section 1.3.

## 1.1 Background

ECG signal serves as the basis for all the subsequent research objectives, such as feature extraction and classification. Thus, the background of ECG, namely, cardiac electrophysiology, ECG lead signals, and ECG arrhythmias, is presented as follows.

### 1.1.1 Cardiac Electrophysiology

The cardiac electrophysiology can be interpreted in two different levels. At the cellular level, the ECG signal stems from an electrochemical activity. Under the resting condition, there is a negative potential inside the cell and a positive potential outside the cell, called resting potentials. Stimulated by a current, potentials of the inside and the outside of the cell are both changed towards the opposite potentials, named action potentials. In one heartbeat, the original action potential is generated by a group of autorhythmic cells inside the sinoatrial (SA) node in the right atrium, propagated to the left atrium, and finally conducted to the ventricles through the atrioventricular (AV) node between the right ventricle and the right atrium (Fig. 1.3). Depolarization of heart cells happens along with the conduction process and repolarization of cells occurs when recovering from an action status to a resting status.

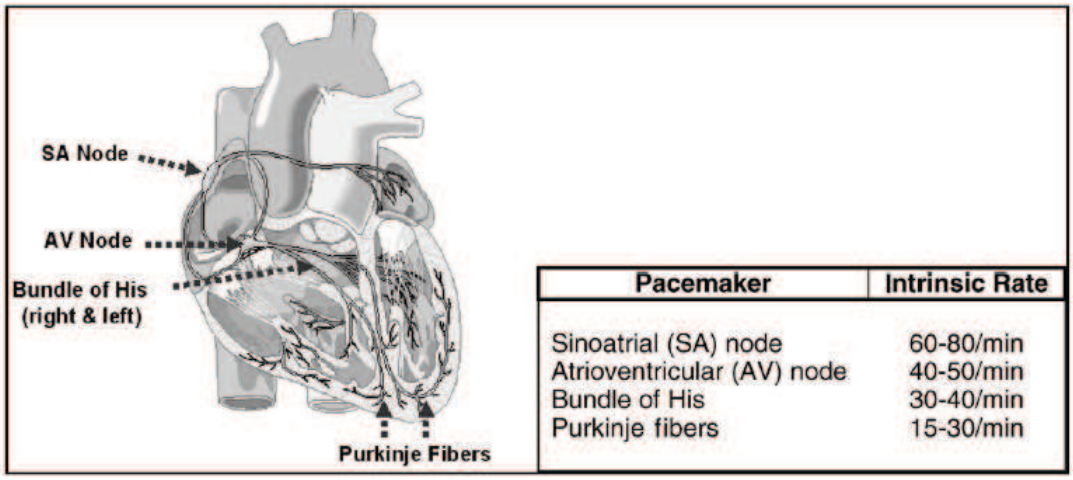


Figure 1.3: Specialized neural-like conductive tissues and their approximate intrinsic rates [1].

At the body surface level, the morphology of the ECG signal is related to the depolarization and repolarization processes, as well as the contraction and recovery of the atria and the ventricles. One ECG morphology record of Lead II in Fig. 1.4 is taken as an example of normal sinus rhythms (NSRs). P wave describes the depolarization process from the right atrium to the left atrium and from the SA node to the AV node, corresponding to the

contraction of the atria; QRS-complex represents the depolarization of ventricles with the ventricular contraction and hidden atrial repolarization; T wave reflects the repolarization of the ventricles together with the ventricular recovery; P-R interval and S-T interval are the transition durations; P-R interval is the atrial transition duration; Q-T interval is the ventricular transition duration of the depolarization and repolarization processes; U wave is seldom seen and used as a reference in the clinical diagnosis.

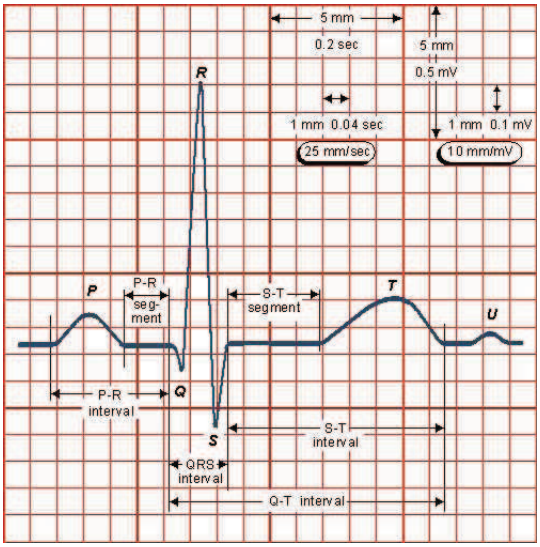


Figure 1.4: ECG waveform of a single heartbeat [2].

### 1.1.2 Electrocardiogram Leads and Electrode Placement

In the previous section, the generation and conduction of the ECG signal are illustrated, as well as the ECG waveform during one heartbeat from Lead II. In the following, the measurement of the ECG signal and the interpretation of different lead signals are generally introduced.

One typical traditional ECG system is the standard 12-lead ECG system, mainly used in hospitals for a short-term inspection. As shown in Fig. 1.5, 10 body surface potentials collected by 10 electrodes placed at the fixed points, i.e., 4 limb voltages (RA, LA, RL, and LL) and 6 precordial voltages (V1,V2,V3,V4,V5,and V6), are collected at the same time.

12-lead ECG signals obtained from 10 electrode potentials are grouped into three sets as follows.

- 3 limb leads: Lead I, Lead II and Lead III, respectively calculated by LA-RA, LL-RA and LL-LA, i.e., the potential difference from the left arm to the the right arm, from the left leg to the the right arm and from the left leg to the left arm.
- 3 augmented limb leads: aVR, aVL, aVF, respectively calculated by $\frac{3}{2}$(RA-Vw), $\frac{3}{2}$(LA-Vw), and $\frac{3}{2}$(LL-Vw), where Vw = $\frac{1}{3}$(RA+LA+LL).
- 6 precordial leads: V1,V2,V3,V4,V5 and V6.

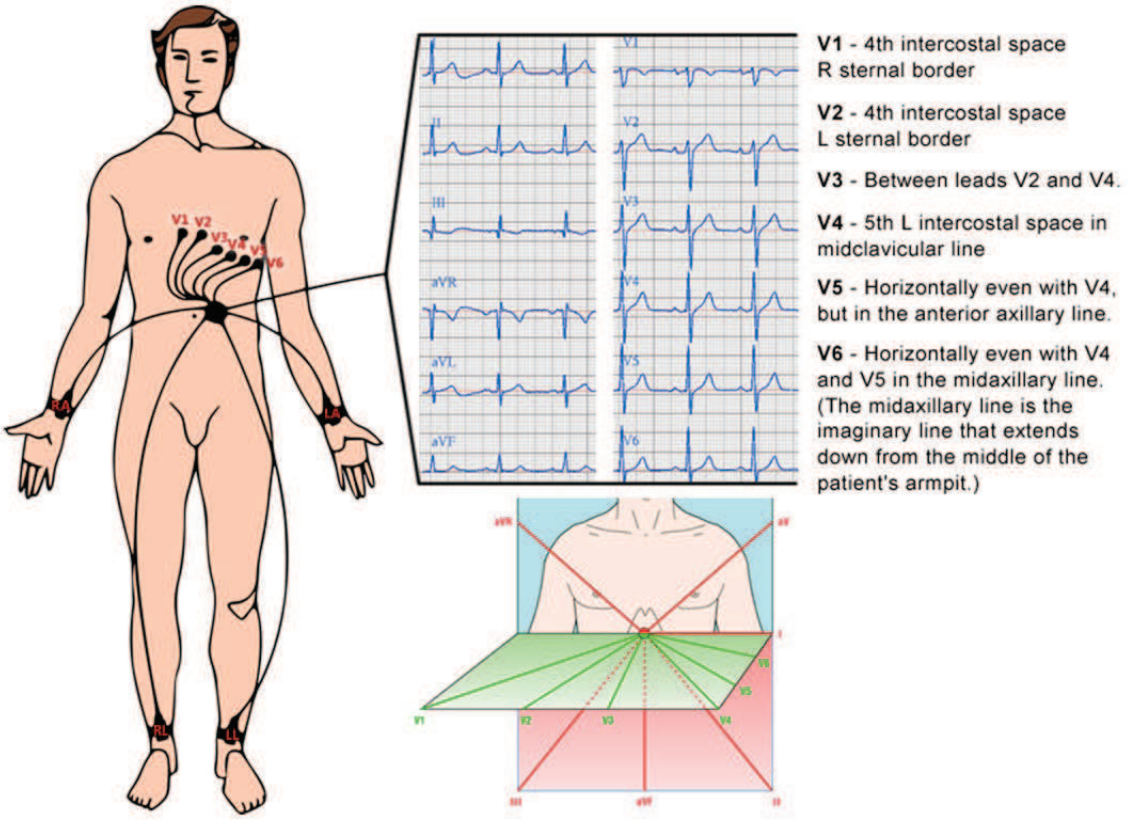


Figure 1.5: Electrode placement for the standard 12-lead ECG [3].

In CLT-ECG monitoring systems, less electrodes will be used for portable and real-time usage. The ECG electrode placement will be arranged according to the limb leads as the

limb leads usually have larger signal power. For some patients are diagnosed to have certain specific heart disease symptoms, the electrode placement will be changed accordingly.

### 1.1.3 ECG Arrhythmias

ECG arrhythmias are caused by the heart disorder, different from NSRs. Generally, NSRs result from the normal pacemaker and the subsequent successful electrical impulse propagation downward along the conductive tissues as shown in Fig. 1.3. The pacemaker is the electrical excitation signal originating from the SA node. An arrhythmia happens while there are problems in the pacemaker and/or the impulse conduction. According to the pathologies, arrhythmias can be divided into 6 types. Each type has a few typical morphologic features and consists of a few heart diseases which are described in [4] and are summarized in Tables 1.1 and 1.2.

These arrhythmias mentioned above can be grouped into two sets according to the emergency level in practice, namely, life-threatening arrhythmias and non-life-threatening arrhythmias. Life-threatening arrhythmias are also known as shockable rhythms, such as VF. These arrhythmias may cause sudden cardiac arrest or death if no immediate therapy is provided within a few minutes, especially in an out-of-hospital situation. Henceforth, continuous monitoring and real-time detection for these critical heart arrhythmias are necessary, which will help achieve a high probability of survival for patients. On the other hand, the detection of the non-life-threatening arrhythmia detection can save a lot of workload and provide diagnosis reference for cardiologists and experts before deterioration.

### 1.1.4 ECG Systems

The traditional standard 12-lead wired ECG system mentioned in Subsection 1.1.2, has 10 electrodes connected to the surface of patients' body using wires and the 12 lead signals are obtained by differential operation. Such a relatively complex system with so many leads is

Table 1.1: Arrhythmia information I.

| **Rhythm Type** | **Pathologies** | **Morphlogical Features and Disease** |
|---|---|---|
| NSRs | The pacemaker is in sinoatrial node and works well | Normal sinus P-wave, QRS-complex and T-wave morphologies |
| Sinus Node Arrhythmias | The pacemaker is in sinoatrial node but works abnormally | Usually normal sinus P-wave morphology as the P wave is generated from the S-A node as usual<br>• Sinus Arrhythmia<br>• Sinus Bradycardia<br>• Sinus Arrest<br>• Sino-Atrial Exit Block |
| Atrial Arrhythmias | The pacemaker is in the atria | Different P-wave morphology but normal QRS-complex and T-wave morphologies, as the P-wave is generated outside the S-A node but the other two waves originate from ventricles excited by a normal A-V node<br>• Wandering Atrial Pacemaker (WAP)<br>• Premature Atrial Contraction (PAV)<br>• Atrial Tachycardia (Ectopic and Multifocal)<br>• Atrial Flutter<br>• Atrial Fibrillation |
| Junctional Arrhythmias | The pacemaker is in the A-V junction. | Normal QRS-complex and T-wave morphologies but abnormal P-wave morphology, as the pacemaker in the A-V junction triggers the depolarization of ventricles according to the normal pathway but the depolarization of atria may be conducted along the opposite direction of the normal P wave, from the A-V node to atria<br>• Premature Junctional Contractions (PJC)<br>• Junctional Escape Rhythm<br>• Non-Paroxysmal Junctional Tachycardia<br>• Paroxysmal Supraventricular Tachycardia (PSVT) |

Table 1.2: Arrhythmia information II.

| **Rhythm Type** | **Pathologies** | **Morphlogical Features and Disease** |
|---|---|---|
| Ventricular Arrhythmias | The pacemaker is in the bundle branches, Purkinje network, or ventricular myocardium | Wider bizarre QRS-complex as the impulse is conducted along abnormal pathway and goes through non-specialized myocardium with a slower speed and an irregular direction<br>• Premature Ventricular Contractions (PVC)<br>• Ventricular Tachycardia (VT)<br>• Ventricular Fibrillation (VF)<br>• Ventricular Escape Rhythm (Idioventricular Rhythm)<br>• Accelerated Idioventricular Rhythm<br>• Ventricular Asystole |
| Atrioventricular Blocks | The impulse is blocked in the A-V junction | A prolonged P-R interval and even no QRS-complex, as the propagation of the impulse is delayed or totally prevented along the conduction pathway to the ventricles<br>• First Degree AV Block<br>• Second Degree Type I AV Block<br>• Type II AV Block<br>• Second Degree AV Block<br>• Third Degree AV Block (Complete AV Block)<br>• Pacemaker Rhythm (Implant) |
| Bundle Branch and Fascicular | The impulse is blocked in the bundle of branches and subbranches (fascicles) | Wider abnormal QRS-complex, as a block of the impulse appears in the buddle of his, one of the bundle branches, or only one subbranch such as one fascicle of the left branch<br>• Right Bundle Branch Block (RBBB)<br>• Left Bundle Branch Block<br>• Left Anterior Fascicular Block (Left Anterior hemiblock)<br>• Left Posterior Fascicular Block (Left Posterior Hemiblock) |

mainly used in hospitals for a meticulous inspection and examination by physicians.

Alternative to wired multi-lead ECG systems, a relatively simple CLT-ECG system that is portable to use outside hospitals and suitable for long-term monitoring can provide many additional values not achievable in today's hospital ECGs. As shown in Fig. 1.1, this CLT-ECG has fewer leads, and can be further simplified to just have one lead or up to three leads. Thus such a tiny equipment is very portable and wearable for convenient long-time continuous monitoring. Furthermore, the use of smartphones can easily display and store the ECG curves, and transmit the data to a remote cloud server for storage, access and further processing. Thus, there is no need for patients to frequently drop by certain hospitals to check their heart status, as their ECG monitoring data could be automatically uploaded and handily checked by a family doctor. More importantly, an alert will be sent to an ambulance or a monitoring station, when life-threatening arrhythmias are automatically detected during the real-time monitoring process. The most commonly-used lead signal is Lead II, followed by Lead I and Lead III.

## 1.2 Research Issues

Current research efforts focus on the design of continuous cardiac monitoring systems and the performance improvement of ECG arrhythmia detection/classification methods [5–7]. The widespread use of previously proposed systems and techniques has been restricted by several factors. Firstly, limited battery power makes continuous data transmission not realizable for long-term ECG recording [8]. Secondly, WiFi/cellular network congestion and disconnection incidents may cause ECG systems down and no service can be provided, when these ECG systems rely on online automatic diagnosis from a remote health center and need all the ECG data to be transmitted remotely [9]. This potential situation is dangerous when life-threatening arrhythmias happen. Thirdly, a large number of heartbeats in the ECG stream

are normal, occupying lots of memories and being redundant for diagnosis, leading to heavy workload for doctors or physicians to review [5]. According to the limitations of the current CLT-ECG system, a task-based resource-saving system scheme is proposed. Under this scheme, three concerned research issues are presented, for realizing fully-automatic ECG classification and diagnosis.

### 1.2.1 The Proposed Cloud based Long-Term ECG Monitoring System

Fig. 1.6 presents the overall data processing structure of the resource-saving CLT-ECG monitoring system. The cloud based ECG monitoring system is simply composed of three functional blocks: an ECG sensor board, a mobile device, and the cloud server. The raw ECG signal is pre-filtered and collected in the ECG sensor part, and then is transmitted to the mobile where the ECG beats are determined whether or not they should be uploaded wirelessly to the cloud server, after a life-threatening arrhythmia detection process. In the cloud server, further analysis is conducted to facilitate the specific diagnosis.

The arrhythmia diagnosis task in this ECG monitoring system is realized by three-stage distributed processing, namely, online life-threatening arrhythmia detection, anomaly-trigged ECG data transmission and online arrhythmia classification/diagnosis. These three stages are described as follows. In the first stage, a fast life-threatening arrhythmia detection algorithm is realized on the patient's smartphones or PDAs, and an alarm is sent if a life-threatening arrhythmia is detected through WiFi or mobile data. In the second stage, the normal and abnormal classification is conducted to identify the ECG data surrounding the detected abnormal cardiac heartbeats and the anomaly-trigged transmission to the remote health center is realized, while a large number of redundant normal ECG heartbeats will be discarded. Finally, a high accuracy heartbeat classification using advanced classification techniques or strategies is implemented in the third part, taking advantage of strong com-

puting ability and large memories of the cloud server. Each possible abnormal heartbeat is classified into a specific type of arrhythmias, and diagnosis suggestions are provided by physicians.

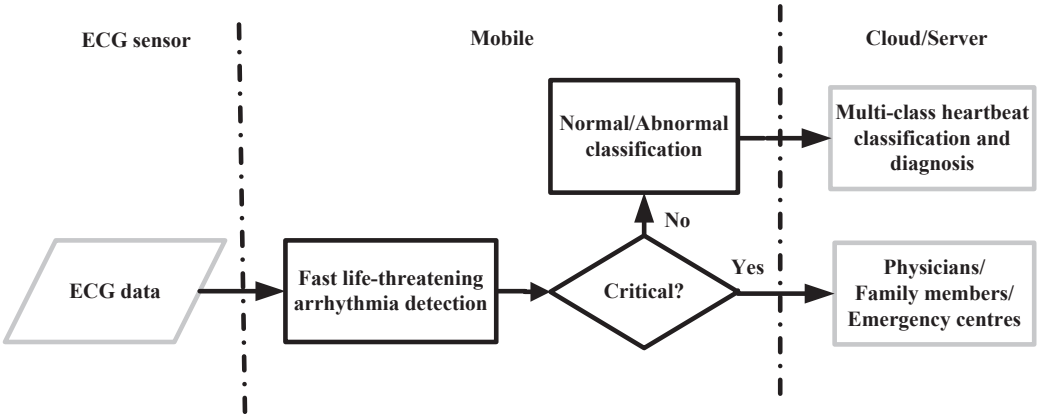


Figure 1.6: Resource-saving CLT-ECG data processing.

### 1.2.2 Life-Threatening Arrhythmia Detection

Life-threatening ventricular arrhythmias such as ventricular fibrillation (VF), ventricular flutter (VFL), and rapid ventricular tachycardia (VT) *et al.*, may cause sudden cardiac arrest or death if no immediate therapy is provided within a few minutes [10–12], especially in an out-of-hospital situation. Henceforth, continuous monitoring and real-time detection for these critical heart arrhythmia are necessary, which will help achieve a high probability of survival for patients.

Many research efforts have been dedicated into this area. The detection performance using a single feature for the life-threatening arrhythmias is limited mainly by the inter-patient ECG variation. Multi-features and multi-classifiers in a large number of algorithms are intensively explored to improve VA detection performance. However, few of them simultaneously consider both the detection performance and real-time performance, as well as patient-specific information.

We are motivated to 1) propose new personalized ECG features using the patient-specific

ECG heartbeat waveform, in order to reduce the impact of inter-patient ECG variation; 2) select a small set of the most effective features from the newly-extracted and previously-existing features, aiming to meet the requirement of real-time application.

### 1.2.3 Resource-Saving System Strategy

An anomaly-trigged CLT-ECG transmission system is proposed according to practical needs. To realize the anomaly-trigged ECG data transmission, the key step is to separate the normal heartbeat types from the abnormal ones.

There are generally two types of methods in the literature, that is, syntactic methods and machine learning based methods. Syntactic methods identify the abnormal heartbeats by comparing certain extracted features with a set of clinical or practical-verified rules, with explicit physical meanings and is easily interpreted. However, the performance of syntactic methods heavily relies on the accuracy and the types of the extracted features, while seldom considering the relationship among features.

Rather than syntactic methods, machine learning based methods can make a prediction on an unknown heartbeat based on a whole set of extracted features, taking the relationship of these features into consideration, thus, decreasing the impact of a certain single feature. Comparing with unsupervised learning, supervised learning has a higher classification accuracy and is more popular in academic purpose when an amount of pre-labeled normal and abnormal heartbeats are provided. However, in practical usage, most heartbeats in an ECG data stream are normal ones, and complete information about abnormal ECG heartbeats is not easy to obtain in terms of the appearance time and the types, which has a big impact on the performance of supervised learning. Deep learning, another group of machine learning methods, such as deep long short-term memory networks, convolutional neural networks and general regression neural networks, is limited by the high computing complexity and implicit interpretation. Thus, a simple unsupervised learning seems more suitable for the anomaly-

trigged ECG data transmission, to combine the advantages of both syntactic methods and machine learning based methods.

Hence, a novel normal and abnormal classification method is proposed for a resource-saving CLT-ECG system, assisting in anomaly-trigged transmission. This method is expected to have explicit physical meanings and can be easily interpreted, as well as considering the relationship between features. More importantly, this proposed method is less impacted by the electrode placement variation, which measures the relative changes between consecutive heartbeats.

### 1.2.4 Cloud based Non-Life-Threatening Arrhythmia Classification

In the CLT-ECG monitoring system, besides timely alarming for certain critical heart diseases and efficiently transmitting real-time ECG data streams, the most concerned problem is the automatic patient-specific ECG heartbeat classification. Earlier detection for non-life-threatening ECG arrhythmias is important for specific therapy, before degrading to life-threatening arrhythmias.

Other than the general classification of normal and abnormal heartbeats for data transmission, automatic ECG heartbeat classification is expected to conduct fine classification and provide more detailed reference information for clinical diagnosis, which does not strictly require real-time performance and is not sensitive to the computing complexity. Thus, the automatic classification task is suitable to implement in the cloud server under the proposed system scheme, preferring a higher classification performance accuracy.

According to the Association of the Advancement for Medical Instrumentation (AAMI) standard, up to 16 types of heartbeats are grouped into five categories, namely, V (ventricular ectopic beats (VEBs)), S (supraventricular ectopic beats (SVEBs)), F (fusion beats), Q (unknown beats) and N (beats not included in V, S, F and Q). Among these five categories,

VEBs and SVEBs draw most attention in the academic research as well as clinical practice.

A lot of research efforts have been dedicated to the detection of VEBs and SVEBs using the global classifier, the local classifier, or the combination of them. The global classifier generally refers to the classifier trained with ECG data from the public ECG database, excluding the current test subject data. The local classifier generally refers to the classifier trained with only the ECG data from the test subject, which is separated from the test data of the same subject. However, due to the inter-patient variation, the classification performance by the global classifier is not consistent for different individuals. Besides, even if a local classifier is combined with the global classifier, the classification performance is hardly effectively improved when there are no desired abnormal heartbeats appearance in the training data from the tested subject. A new patient-specific automatic ECG heartbeats classification method for non-life-threatening arrhythmias is thus proposed.

## 1.3 Contributions and Organization

In Chapter 2, to realize the real-time life-threatening arrhythmia detection, firstly, a set of new personalized, simple temporal features are proposed based on the correlation coefficients between a patient-specific QRS-complex template and the heartbeats of the same patient. Using Support Vector Machines (SVMs), classification performance of different feature combinations is studied. The best two-feature combination and the best three-feature combination which include the newly-proposed features aveCC and medianCC respectively, outperform the previous top-two and top-three feature combinations.

In Chapter 3, a novel normal and abnormal classification algorithm is proposed for the proposed resource-saving CLT-ECG monitoring system, to realize the anomaly-trigged data transmission. Considering the explicit physical meanings and classification performance, one unsupervised learning method using One-Class SVMs (OC-SVMs) is explored on two

categories of features, one morphological feature WCI, and one RR interval based feature modRRIR. Different from the existing waveform based morphological features, WCI indicates the change happened in any of P-segment, QRS-segment and T-segment in a complete heartbeat, avoiding neglecting the change in P-segment and T-segment caused by QRS-segment or noise. Finally, an appropriate combination scheme is designed to achieve an acceptable detection rate of the abnormal heartbeats.

In Chapter 4, a fully-automatic patient-specific classification method is proposed in terms of inter-patient and intra-patient variations. A set of intra-beat features and a set of inter-beat features are extracted using static measurement and dynamic measurement, respectively. A fusion strategy of the global classifier and the local classifier is also proposed to realize the fully-automatic classification. The method is verified in the simulation result.

In Chapter 5, the conclusion and the future work of this dissertation are presented. The conclusion separately summarizes the results obtained from Chapters 2-4. The future work proposes two promising research directions: exploitation of disease-specific features and integration of experienced 'classifiers' and development of behavior-adaptive arrhythmia classification algorithms.

# Chapter 2

# Life-Threatening Ventricular Arrhythmia Detection with Personalized Features

The timely detection of life-threatening ventricular arrhythmias (VAs) is critical to saving a patient's life. General features characterizing ECG waveforms are extracted for VA detection. To take into account the subtle differences in the QRS-complexes among different people, new personalized features are proposed in this chapter based on the (SVM) correlation coefficient between a patient-specific regular QRS-complex template and his/her real-time ECG data. Small sets of the most effective features are chosen with SVMs from 11 newly-extracted and 15 previously-existing features, for efficient performance and real-time operation. Our proposed new features aveCC and medianCC are verified to be effective to enhance the performance of existing features under both the record-based and database-based data divisions. Through 50-time random record-based data divisions, all combinations of two features and three features are tested. The top two-feature combination is VFleak and aveCC, which achieves an area under curve value (AUC) of $98.56\% \pm 0.89\%$, specificity

(SP) of $94.80\% \pm 2.15\%$ and accuracy (ACC) of $94.66\% \pm 1.97\%$; the top three-feature combination is VFleak, MEA and aveCC, which obtains an AUC of $98.98\% \pm 0.58\%$, SP of $95.56\% \pm 1.45\%$, ACC of $95.46\% \pm 1.36\%$; these results outperform the previous top-two and top-three feature combinations. Similar results are obtained on the database-based data division.

## 2.1 Introduction

VF, VFL and rapid VT, are life-threatening ventricular arrhythmias (VAs), which may cause sudden cardiac arrest and even death if timely therapy is not conducted within a few minutes [10–12]. A high quality, easily implementable, fast ventricular arrhythmia (VA) detection algorithm will help achieve a high probability of survival from out-of-hospital heart attack incidents. Henceforth, many research efforts have been dedicated to developing effective VA detection algorithms, aiming to achieve a trade-off between classification performance and real-time performance.

A large number of algorithms for VA detection have been proposed and evaluated in the literature. Detection methods using a single effective feature are proposed, of which features are extracted in temporal/morphologic domains [13–15], spectral domain [16–18] or other domains [11, 19–21]. Jekova *et al.* [22] conduct comparative assessment of five previously-existing VA detection algorithms. Amann *et al.* [11] evaluate multiple algorithms for VA detection, to verify the proposed algorithm using a single feature. However, the detection performance by using one single feature is limited [23]. One of the key reasons is that the ECG signals vary from one person to another [24], and also change according to different body movements or emotional status even for the same person [25].

To improve VA detection performance, multi-feature classification is investigated, with the aim to obtain the most effective feature set by feature selection techniques [23, 26–

29] or classifier-based methods [30–32]. Recent studies about multi-feature VA detection are presented in [23, 26, 31], using a large number of ECG data from the public databases and achieving superior performance over that of a single feature. Li *et al.* [31] select a subset of nine features from 14 features using genetic algorithm, further two most effective features using SVMs. Alonso-Atienza *et al.* [23] propose a new filter-type feature selection technique, obtaining nine features to build a simplified high-performance SVM detector for VA detection. Figuera *et al.* [26] explore the difference in the detection of shockable rhythms involving public and out-of-hospital cardiac arrest data. Thirty previously-defined ECG features and five state-of-the-art machine learning classifiers are investigated. Papers [23, 26, 31] obtain desired feature sets from the previously existing features, and show generalized classification results, however, without considering any patient-specific information.

In recent years, personalized medicine has received increasing attention, especially as the Internet based wearable technology allows a significant amount of personal data to be collected. Aramendi *et al.* [33] assess the performance of two spectral and two morphological features for adult and paediatric VA detection and the result shows that the morphological parameters present significant differences between the adult and paediatric patients because of the faster heart rates of the paediatric rhythms. Irusta *et al.* [34] propose a high-temporal resolution algorithm to discriminate shockable from nonshockable rhythms in adults and children. Both [33] and [34] show the individual differences in two distinct populations of adults and children.

Some research on personalized ECG classification consider training with a patient's own ECG records [35, 36], using known general existing features in the literature. One drawback of these methods is that a patient's data cannot include all kinds of arrhythmia events, and hence is limited in arrhythmia training varieties and data size. Furthermore, these methods do not examine deeper the characteristics of individual ECG waveforms which are unique to each person and can be used as a personal identification signature [37], missing potential

effective personalized ECG features.

In this chapter, we are motivated to 1) propose new personalized ECG features using the patient-specific ECG heart beat waveform; 2) select a small set of the most effective features from the newly-extracted and previously-existing features, aiming to meet the requirement of real-time application. The newly-extracted personalized features are based on the correlation between a patient's regular QRS-complex template extracted from the pre-selected regular/normal sinus rhythms (NSRs) and the incoming ECG signal for VA detection.

Since our proposed VA detection method is correlation based, the applications of correlation in ECG signal processing are firstly reviewed here. Correlation based techniques have been widely used in the past, mainly in three types of applications: 1) heart rate detection [38]; 2) alignment method for heart beats [39]; 3) ECG classification [12, 29, 40, 41]. For ECG classification, Dutta *et al.* [40] present a cross-correlation based three-class ECG classification algorithm, to separate normal beats, PVC beats and other beats. They extract 20 features from the magnitude and the phase of the cross-spectral density which is calculated from the Fourier transform of the cross-correlation sequences between each beat signal and one normal reference beat signal. For VA detection, Chen *et al.* divide the incoming ECG signal into short fixed-length segments and calculate the autocorrelation function (ACF) of each segment [11, 29]. If the peak magnitudes of the ACF as a function of time lags do not pass a linear regression test, it is then determined that the test rhythm is subject to VF. Chin *et al.* [12] classify ECG segments based on the correlation coefficients between the testing segment and the pre-extracted templates respectively for VT and VF, as well as NSR. However, VF is a random-like signal and a fixed template of VF cannot be very accurate. The classification performance is therefore not very good. Hammed *et al.* [41] use a hard correlation threshold at 0.85 to distinguish the normal and abnormal beats. Such fixed threshold cannot easily adapt to personalized ECG data, noise levels and measurement platforms.

In general, correlation based approaches have two drawbacks: 1) the correlation result is directly affected by noise and interference in the ECG signal; 2) calculation of the correlation coefficients/function can be time-consuming because of the sliding operation in template matching.

Keeping these in mind, we explore new ways to obtain correlation coefficients (CCs) between the normal ECG template and testing ECG signal with reduced complexity, and search for effective CC based features for VA classification using public ECG databases. The result has potential usage in the surface CLT-ECG monitoring [42] and automated external defibrillator (AED). In particular, the contributions of this chapter are summarized as follows.

- This chapter proposes to extract a range of new personalized, simple temporal features originating from the correlation coefficients between a patient-specific QRS-complex template and the heart beats of the same patient.

- This chapter studies classification performances using different feature combinations, and the best two-feature combination and the best three-feature combination which include the newly-proposed feature aveCC and medianCC respectively, outperform those mentioned in current reported methods [23, 31].

The rest of this chapter is organized as follows. Section 2.2 introduces the ECG databases, the data preprocessing and feature extraction. Section 2.3 presents personalized feature extraction. Section 2.4 introduces the classification algorithm SVM. Section 2.5 conducts simulation and shows the superiority of the proposed method. Section 2.6 concludes this chapter.

Table 2.1: Database introduction (segment length: 8 seconds).

| Database | Record index | Number | $f_s$ (Hz) | VA segments | Non-VA segments | Total segments |
|---|---|---|---|---|---|---|
| VFDB | 1-22 | 22 | 250 | 1027 | 4737 | 5764 |
| MITDB | 23-70 | 48 | 360 | 20 | 10780 | 10800 |
| CUDB | 71-105 | 35 | 250 | 464 | 1710 | 2174 |
| Total | 1-105 | 105 | N/A | 1511 | 17227 | 18738 |

## 2.2 Data Preparation

### 2.2.1 Database Information

Three commonly-used ECG databases are used in this chapter: MIT-BIH arrhythmia database (MITDB) [43], Creighton University Ventricular Tachyarrhythmia Database (CUDB) [44], and MIT-BIH Malignant Ventricular Arrhythmia Database (VFDB) [45]. MITDB is composed of 48 records from different patients and each record contains 30-minute 2-channel ECG data with the sampling rate of 360 Hz. CUDB includes 35 records of 8-minute single-channel ECG data, of which the sampling frequency is 250 Hz. VFDB includes 22 records of 30-minute 2-channel ECG data with the sampling rate of 250 Hz. In this study, only the first channels of records in MITDB and VFDB are used. Moreover, the four paced records in MITDB have been kept. The specifications about these three databases are presented in Table 2.1.

### 2.2.2 Data Preprocessing

The ECG data records are inevitably contaminated by external noises [46] and the ECG signals of interest fall in a specific frequency range. Henceforth, it is necessary to process the raw ECG data before feature extraction is conducted. To this end, the databases downloaded from the online sources [43–45] are preprocessed in the same way as in [23]: 1) the mean value is subtracted from the measured ECG signal; 2) the signal is filtered using a five-order moving average filter; 3) the baseline wander is removed using a high-pass filter with the 1 Hz

cut-off frequency; 4) the high-frequency noise is eliminated using a second-order Butterworth low-pass filter with the cut-off frequency at 30 Hz.

The preprocessed data are segmented and labeled as VAs or non-VAs by the following labeling rule [23]. VAs include VF, VFL and VT, whereas non-VAs consist of all other rhythms. The rule of segment labeling is: one segment is labeled as +1 if no less than 50% of the data inside this segment are VAs; otherwise, this segment is labeled as -1. The segment length is 8 seconds by default. As can be observed in Table 2.1, MITDB contains very few VA rhythms whereas CUDB includes a lot. The reason that MITDB is still included in the dataset, is to verify general classification performance of the proposed method when up to 15 other rhythms of MITDB are present at the same time.

### 2.2.3 Feature Extraction

Each feature characterizes the corresponding segment, distinguishing a VA segment from a non-VA segment. In the literature, many different types of features extracted from an ECG data segment have been studied, and some of them are summarized in Table 2.2. Basically, these features can be divided into three types, temporal/morphological features, spectral features and complexity features.

In this chapter, we propose five correlation coefficient related features and six R-peak related features for VA detection. These new features are highlighted in bold in Table 2.2. aveCC, devCC, minCC, maxCC and medianCC are correspondingly the average, the standard deviation, the minimum, the maximum and the median of CCs calculated in one segment; aveRR, devRR, minRR, maxRR, and medianRR respectively represent the average, the standard deviation, the minimum, the maximum, and the median of RR intervals in one segment; numPeaks is the number of R-peaks in one ECG segment. Details about these features are elaborated in Section 2.3.

Table 2.2: Features extracted.

| Class | Features |
|---|---|
| Temporal/Morphological features | • Threshold crossing interval (TCI) [14] |
| | • Threshold crossing sample count (TCSC) [13] |
| | • Auxiliary counts (Count2) [18] |
| | • Standard exponential (STE) [11] |
| | • Modified exponential (MEA) [11] |
| | • Mean absolute value (MAV) [15] |
| | • **aveCC, devCC, minCC, maxCC, medianCC** |
| | • **numPeaks** |
| | • **aveRR, devRR, minRR, maxRR, medianRR** |
| Spectral features | • VF filter (VFleak) [18] |
| | • Spectral algorithm (M, A2 and A3) [16] |
| | • Median Frequency (FM) [17] |
| Complexity features | • Complexity measurement (CM) [19] |
| | • Phase space reconstruction (PSR) [20] |
| | • Hilbert transform (HILB) [47] |
| | • Sample entropy (SpEn) [21] |

## 2.3 Personalized Feature Extraction

It is well known that each person has a unique QRS-complex [37]. If we use a person's regular QRS-complex as a normal template, correlating the person's ECG data samples with the template would give us a subtle indicator how similar the measured beat and the regular beat template are. In the case of severe arrhythmia events such as VAs, the similarity, in other

words, the correlation coefficient will distribute randomly. Therefore, the CC related features are potentially useful incorporating the patient-specific ECG signature for VA classification. As mentioned in the introduction, traditional sliding operation for template matching in the CC calculation is computational complex.

Here we propose to simplify the CC calculation and extract new features based on the CC set from one segment. Considering the fact that QRS-complex detection is required in most ECG applications, R-peak positions would already be known after QRS detection. Therefore, we propose to simplify the CC calculation by circumventing sample sliding. Instead, align the detected R-peak with the template R-peak and compute the correlation coefficient between the QRS template and the beat corresponding to each R-peak in the segment. For segment based feature extraction, there are multiple R-peaks and hence multiple CCs in one segment. Next we try to obtain effective features based on these coefficients. There are several ways to derive a CC feature from the CC set of one segment. For example, the median, the average, the standard deviation, the minimum or the maximum of the set are all tested. aveCC and medianCC will be shown later to achieve the superior performances.

To be more specific, the CC related feature extraction is implemented by two successive stages: the QRS-complex detection and the CC related feature extraction. Besides, six R-peak related features are extracted at the same time as a comparison. The details of the two-stage feature extraction are presented next.

### 2.3.1 QRS Detection

QRS detection is the first stage for the personalized feature extraction. The objective of QRS detection is to identify the R-peaks. The QRS-complexes are detected by the well-known Pan and Tompkins (P & T) QRS-complex detection algorithm [48]. The preprocessed ECG signal goes through operations of bandpass filtering, derivative, squaring and moving-window integration. The QRS detection identifies a windowed ECG waveform as the QRS-complex,

with the window length approximately the same as the maximum possible width of a QRS-complex. Then a peak detector finds the maximum point within this window as the R peak. The details are described in [39].

In this stage, six RR related features are extracted for one segment, namely, aveRR, devRR, minRR, maxRR, medianRR and numPeaks.

### 2.3.2 New Feature Extraction after QRS Detection

Based on the QRS detection, the second stage about the CC related feature extraction is introduced. The average normal QRS-complex template for each person is obtained with QRS detection. The feature extraction procedure and the qualitative analysis of the CC related features are described as follows.

The general flow-chart of the proposed feature extraction algorithm is shown in Fig. 2.1: first, data preprocessing such as filtering and data segmentation is conducted when raw real-time ECG data come in; then, for each segment, the QRS detection are applied and a set of R peaks is located; based on the RR set, six R-peak related features are calculated; meanwhile, with each detected R peak as a fiducial point, each value of a CC set is obtained from aligning the prepared QRS-complex template with the corresponding detected QRS-complex and calculating the correlation coefficient of the two time series (Fig. 2.2); based on the CC set, five CC related features are extracted. The mathematical description of the feature extraction is introduced in Algorithm 1. The ECG segment to determine the template was manually selected for each record, and in practice this can be done in an initialization phase in a portable ECG monitor or holter. Thus the QRS-complex template is established after the QRS detection in our simulation as described by Step 3 in Algorithm 1. Automatic determination and update of the template can be designed for real-time ECG as future work.

As shown in Figs. 2.3-2.5, the detected R-peaks by the P & T algorithm are marked using

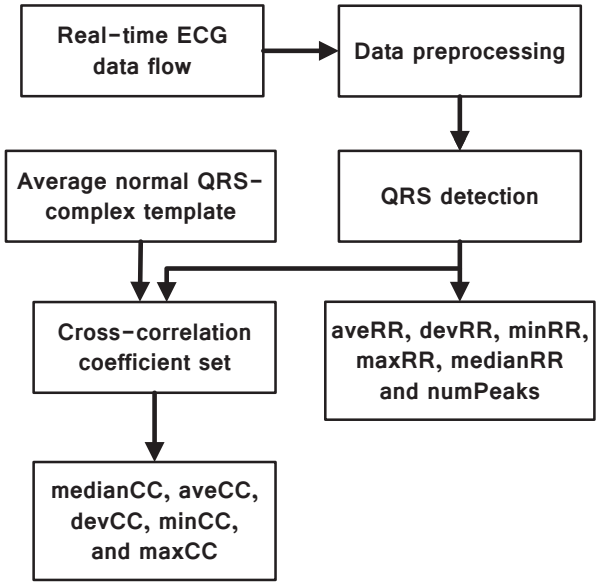


Figure 2.1: General flow-chart for extracting the RR related features and the CC related features.

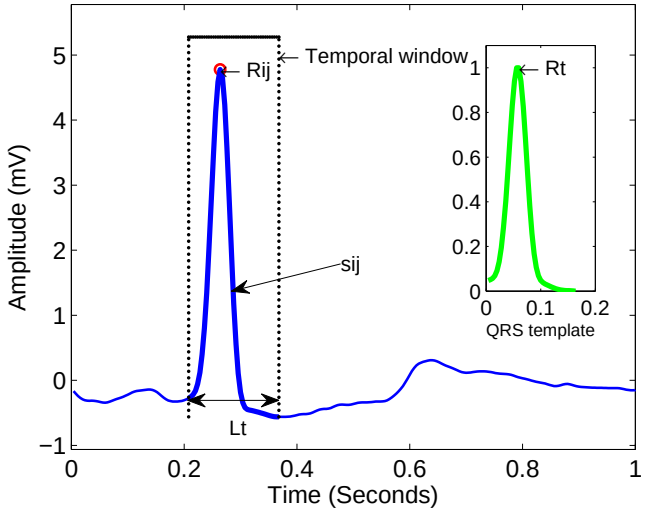


Figure 2.2: CC related feature extraction.

red circles, including real R-peaks and mistakenly detected R-peaks. For the NSR segments, the detected R-peaks are almost the real R-peaks based on the fact that QRS detection rate is high [48]. However, the random property of a VA segment leads to the randomness for

detected R-peaks. Given the fact that the detected R-peak positions in VA segments are random, the CC calculated from the R-peak alignment will be low because the VA waveform has dissimilar shapes to the average normal template. As shown in Fig. 2.6, the values of medianCC are generally high for non-VA segments while they are in the low range for VA segments on the complete dataset.

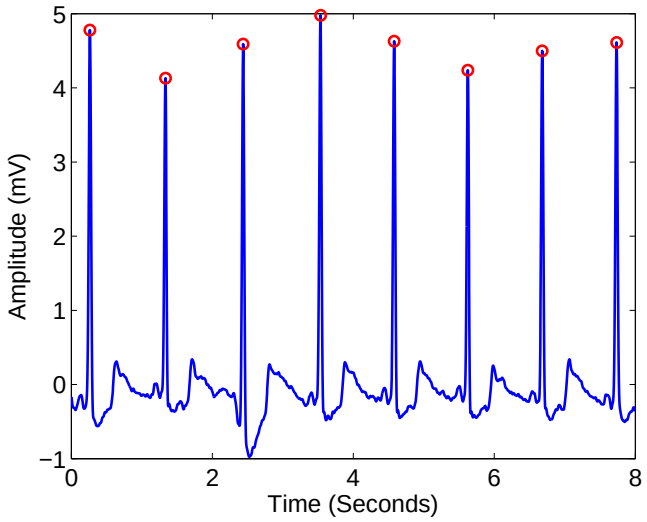


Figure 2.3: One segment of NSR from the first record in CUDB.

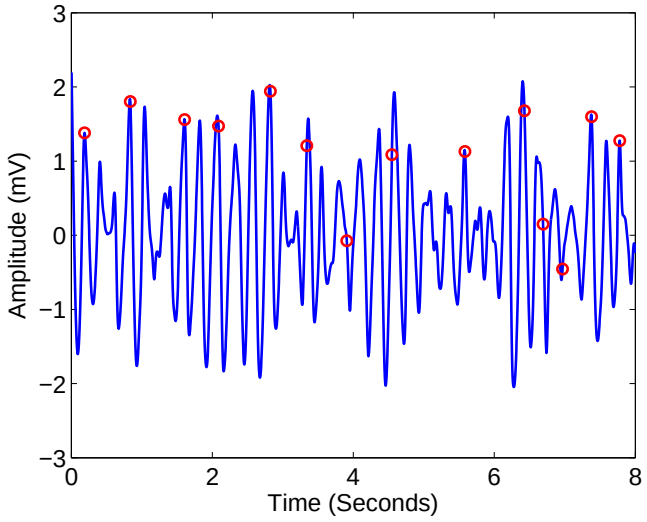


Figure 2.4: One segment of VF from the first record in CUDB.

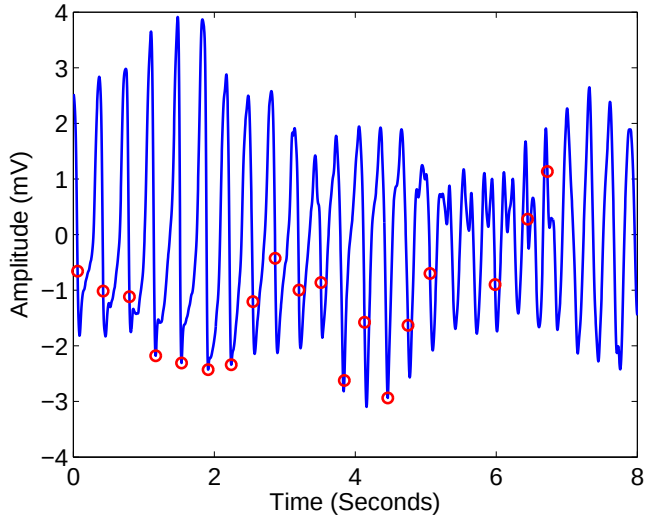


Figure 2.5: One segment of VT from the third record in VFDB.

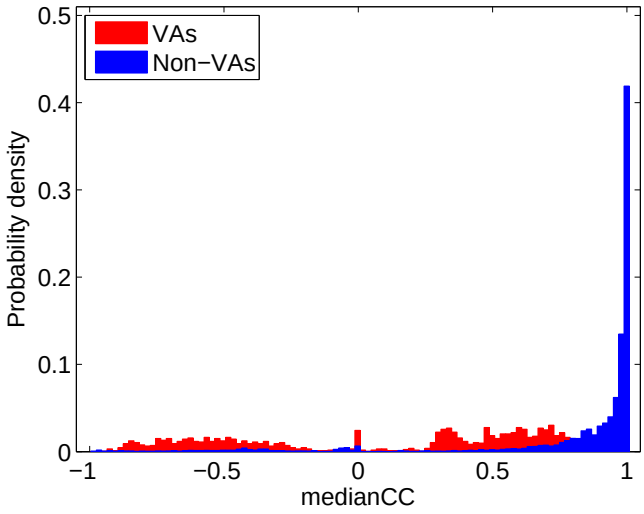


Figure 2.6: The probability histogram of medianCC on the complete dataset.

**Algorithm 1** Personalized feature extraction

1: Identify the R-peaks in each segment. Real-time ECG data flow is firstly divided into segments of a fixed length of $L_s$ seconds ($L_s = 8$ s by default). For the $i^{\text{th}}$ segment, $J_i$ R-peaks are detected by the P & T QRS-complex algorithm. Thus, the R-peak set is denoted as $\mathbf{R}_i = \{R_{i1}, R_{i2}, \ldots, R_{ij}, \ldots, R_{iJ_i}\},\ j = 1, 2, \cdots, J_i$. According to the fiducial point $R_{ij}$, the $j^{\text{th}}$ QRS-complex time series under the temporal window of $L_t$ milliseconds ($L_t$ is set as 160 ms according to the statistical QRS-complex duration of normal beats), is expressed as $\mathbf{s}_j = \{s_{j1}, s_{j2}, \ldots, s_{jk}, \ldots, s_{jK}\}$, $s_{jk}$ represents the $k^{\text{th}}$ ECG data sample, $k = 1, 2, \cdots, K$, and $K = L_t * f_s$, as shown in Fig. 2.2.

2: Calculate the RR set for the $i^{\text{th}}$ segment and extract the RR related features based on the RR set. The RR set is calculated by

$$\begin{aligned} &\mathbf{r}_i = r_1, r_2, \ldots, r_j, \ldots, r_{J_i-1}, \\ &r_j = R_{i(j+1)} - R_{ij}. \end{aligned} \tag{2.1}$$

The RR related features are obtained by

$$\begin{aligned} &aveRR_i = \frac{1}{J_i - 1} \sum_{j=1}^{J_i-1} r_j; \\ &devRR_i = \frac{1}{\sqrt{J_i - 2}} \left\| \mathbf{r}_i - aveRR_i \right\|_2 (\|\cdot\|_2 - L_2 \text{ norm}); \\ &minRR_i = \mathbf{min}(\mathbf{r}_i);\ maxRR_i = \mathbf{max}(\mathbf{r}_i); \\ &medianRR_i = \mathbf{median}(\mathbf{r}_i);\ numPeaks_i = J_i. \end{aligned} \tag{2.2}$$

3: Extract the normalized average normal QRS-complex template for each patient. A pre-selected normal segment from each record is denoted as the $t^{\text{th}}$ segment. Then in the template segment, a series of $J_t$ R-peaks is detected and denoted as $\mathbf{R}_t$. The corresponding $J_t$ QRS-complex time series are aligned by R-peaks, averaged, and normalized into the range of [0,1]. The normalized average QRS-complex template is expressed by

$$\overline{\mathbf{s}} = \{\overline{s}_1, \overline{s}_2, \cdots, \overline{s}_k, \cdots, \overline{s}_K\}. \tag{2.3}$$

4: Calculate the CC set for the $i^{th}$ segment and extract the CC related features based on the CC set. The CC set is calculated by

$$\mathbf{c}_i = \{c_1, c_2, \ldots, c_j, \ldots, c_{J_i}\},\ c_j = \frac{\sum_{k=1}^{K} \overline{s}_k s_{jk}}{\|\overline{\mathbf{s}}\|_2 \|\mathbf{s}_j\|_2}. \tag{2.4}$$

The CC related features are obtained by

$$\begin{aligned} &medianCC_i = \mathbf{median}(\mathbf{c}_i);\ aveCC_i = \frac{1}{J_i}\sum_{j=1}^{J_i} c_j; \\ &devCC_i = \frac{1}{\sqrt{J_i - 1}} \|\mathbf{c}_i - aveCC_i\|_2 ; \\ &minCC_i = \mathbf{min}(\mathbf{c}_i);\ maxCC_i = \mathbf{max}(\mathbf{c}_i). \end{aligned} \tag{2.5}$$

5: Repeat from Step 2 to Step 4 to get CC related values for all the segments.

6: End.

## 2.4 Classification Algorithm

SVM is a widely used and effective algorithm in the literature [49,50]. Among the numerous variants of SVMs, the soft-margin SVM using a Gaussian kernel function is widely adopted in practical classification problems. This method can classify data having non-linear relationship with features, and also non-separable data with a designed or minimum error rate [51]. The SVM model is confirmed through two-stage operations: the first stage is to train this model on the training set; the second stage is to evaluate the classification performance of the model on the test set. The model with desired performance is finally determined. The basic SVM operation is described as follows.

Given any feature vectors $\mathbf{x}_i \in \mathbb{R}^{M\times 1}$ and the corresponding labels $y_i \in \{+1, -1\}$ on the

training set, the following optimization problem is solved

$$\begin{aligned} &\min_{\mathbf{w},b,s_i} \frac{1}{2}\|\mathbf{w}\|^2 + \tau \sum_{i=1}^{N} s_i \\ &\text{subject to } y_i(\mathbf{w}^{\mathrm{T}}\phi(\mathbf{x}_i) + b) \geq 1 - s_i, \\ &s_i \geq 0 \text{ for } i = 1, ..., N, \end{aligned} \tag{2.6}$$

where the weight vector $\mathbf{w} \in \mathbb{R}^{M\times 1}$, $\mathbf{x}_i \in \mathbb{R}^{M\times 1}$, $\phi(\mathbf{x}_i)$ is a linear or nonlinear transformation of $\mathbf{x}_i$, $\phi(\mathbf{x}_i) \in \mathbb{R}^{M\times 1}$, $s_i$ represents the violation value of data pair $(\mathbf{x}_i, y_i)$ to the classification boundaries, $\tau$ is the cost parameter for the violation chosen by users, and $b$ is an unknown constant.

By using Lagrange multipliers, the Lagrange dual problem of (2.6) is expressed as

$$\begin{aligned} &\min_{\mu_1,\mu_2,\cdots,\mu_N} \frac{1}{2}\sum_{i,j=1}^{N} \mu_i y_i \mu_j y_j K_G(\mathbf{x}_i, \mathbf{x}_j) - \sum_{i=1}^{N} \mu_i \\ &\text{subject to } \sum_{i=1}^{N} \mu_i y_i = 0,\ 0 \leq \mu_i \leq \tau, \end{aligned} \tag{2.7}$$

where $\mu_i$ is a Lagrange multiplier corresponding to the constraints of (2.6), $K_G(\mathbf{x}_i, \mathbf{x}_j) = e^{-\|\mathbf{x}_i - \mathbf{x}_j\|^2/2\sigma^2}$, is called a Gaussian kernel and $\sigma$ is a user-defined parameter. After solving (2.7) and obtaining the Lagrange multiplier set, the first stage of SVM classification is completed.

The second stage for SVM classification is to evaluate the performance of the classification model. For any known feature vector $\hat{\mathbf{x}}$ on the test set, the predicted label $\hat{y}$ is obtained as

$$\hat{y} = \text{sign}(\sum_{i=1}^{N} \mu_i y_i K_G(\mathbf{x}_i, \hat{\mathbf{x}}) + b). \tag{2.8}$$

By comparing the predicted labels with the true labels on the whole test set, the classification performance is analysed by calculating performance indices. There are several

commonly-used statistical indices to characterize the classification performance, such as the sensitivity (SE), the specificity (SP), the accuracy (ACC), the area under the curve (AUC), the false positive rate (FPR), the positive prediction (PP) and the balanced error rate (BER) [23].

## 2.5 Simulation

In this section, the effectiveness of the proposed personalized features for VA classification using SVM are evaluated through simulation. A total number of 105 records are considered in this chapter. In order to guarantee the data independence between the training dataset and the test dataset [52], a record-based data division and a database-based data division are both employed. As seen in Table 2.1, the classification problem we deal with is a binary classification of unbalanced data. To solve the unbalanced classification problem, $\tau$ in the SVM optimization problem (Eq. (6)) is assigned different values for the VA (positive) class and the non-VA (negative) class, according to the practical proportion of these two classes in the training set. (Note: Features or feature combinations in the following tables are sorted by AUC.)

For the record-based data division [31], the whole dataset is divided by randomly choosing 70% records (74 records) as the training set and the left 30% records (31 records) as the test set. This data division procedure is repeated 50 times. The SVM classifier is trained on the training set and validated on the test set. The mean and the standard deviation of the 50-time classification performances on the test set are calculated and presented in tables. The performances are sorted descendingly according to AUC values for different feature combinations.

First, Table 2.3 shows the classification performance using SVM with a single feature. TCSC performs well in terms of BER and AUC. VFleak ranks the best in SP, PP and ACC.

Our proposed feature medianCC achieves the highest SE among all the features.

Table 2.4 shows the classification performance using two features chosen from the feature set. There are 171 two-feature combinations in total. The top-ten feature combinations with the highest AUC values are presented. Our proposed feature aveCC and medianCC, combined with VFleak respectively, achieve the best two AUC values, whereas the combination of aveCC and VFleak also obtains the highest SP and ACC.

Table 2.5 shows the classification performance with three-feature combinations. Among 969 three-feature combinations, the new features, aveCC and medianCC, separately working with VFleak and MEA, achieve the highest two AUC values, which is consistent with the results presented in Table 2.4. The combination of VFleak, MEA and aveCC performs the best in terms of SP, PP, ACC, BER and AUC, with an acceptable SE, compared with two top-three combinations mentioned in the previously existing chapters, i.e., the combination of TCSC, VFleak and SpEn [23], and the combination of Count2, VFleak and A3 [31]. Furthermore, in the top-ten combinations with the highest AUC values, aveCC appears four times and medianCC appears five times, only after VFleak.

For the database-based data division, we do simulations to test three-feature combinations, namely, any two databases as the training set and the third one as the test set. As there are only a few VA segments in the MITDB database (shown in Table 2.1), MITDB database is only used in the training sets, combined with CUDB or VFDB, involving up to 15 other rhythms as kind of interference.

For data from CUDB as the test set, among 969 three-feature combinations, the best three-feature combination are (medianCC, MAV, SpEn); medianCC and aveCC appear respectively 6 times and 5 times in the top-ten three-feature combinations, as shown in Table 2.6. For data from VFDB as the test set, the best ones are (VFleak, medianCC, MEA); medianCC and aveCC appear respectively 4 times and 3 times, as shown in Table 2.7.

The limitation of the proposed method is that our used QRS-complex template is not

designed to be adaptive in this chapter. This is not a problem when using the open source databases, as the regular normal beat signals do not vary much in each record. Besides, the template we used is the QRS-complex (R complex), which is known as a function of distance, other than the heart rate. So the R complex remains fairly constant with changes in heart rate, other than the P complex or the T complex [37]. In the real time online application of this template, the patient-specific fixed template should be further verified at different heart rates.

Table 2.3: Performance of single feature on test sets.

| feature 1 | SE (%) | SP (%) | PP (%) | ACC (%) | BER (%) | AUC (%) |
|---|---|---|---|---|---|---|
| **TCSC** | 95.64 ± 2.77 | 92.23 ± 3.25 | 51.94 ± 12.02 | 92.54 ± 2.98 | **6.06 ± 2.18** | **97.45 ± 1.34** |
| **VFleak** | 90.00 ± 4.80 | **95.65 ± 2.47** | **64.89 ± 14.39** | **95.25 ± 2.35** | 7.17 ± 2.83 | 97.17 ± 1.84 |
| MAV | 95.57 ± 2.54 | 91.62 ± 3.10 | 49.81 ± 11.59 | 91.97 ± 2.84 | 6.40 ± 2.02 | 97.03 ± 1.71 |
| PSR | 93.13 ± 3.13 | 91.60 ± 2.83 | 48.84 ± 11.71 | 91.74 ± 2.57 | 7.63 ± 1.93 | 96.32 ± 1.38 |
| HILB | 87.95 ± 10.33 | 90.94 ± 3.55 | 46.09 ± 12.03 | 90.64 ± 2.96 | 10.56 ± 4.61 | 95.85 ± 1.49 |
| SpEn | 88.55 ± 9.78 | 89.43 ± 3.98 | 42.44 ± 11.91 | 89.29 ± 3.37 | 11.01 ± 4.45 | 95.23 ± 2.01 |
| A2 | 80.41 ± 6.44 | 95.07 ± 3.03 | 60.41 ± 16.66 | 93.94 ± 2.77 | 12.26 ± 3.36 | 93.50 ± 2.67 |
| **medianCC** | **97.28 ± 1.58** | 84.51 ± 3.47 | 34.94 ± 9.02 | 85.51 ± 3.18 | 9.11 ± 1.73 | 92.54 ± 2.32 |
| MEA | 84.85 ± 9.74 | 85.25 ± 4.24 | 33.33 ± 9.59 | 85.14 ± 3.57 | 14.95 ± 4.39 | 92.26 ± 2.24 |
| TCI | 87.53 ± 4.58 | 83.71 ± 4.15 | 31.88 ± 10.09 | 84.03 ± 3.79 | 14.38 ± 2.76 | 92.16 ± 2.33 |
| aveCC | 93.28 ± 4.87 | 83.87 ± 3.59 | 33.13 ± 8.51 | 84.59 ± 3.20 | 11.42 ± 2.36 | 92.14 ± 2.31 |
| Count2 | 85.36 ± 5.24 | 84.72 ± 4.19 | 33.09 ± 11.08 | 84.76 ± 3.84 | 14.96 ± 3.00 | 91.11 ± 2.52 |
| A3 | 78.31 ± 8.30 | 88.17 ± 3.38 | 36.67 ± 11.17 | 87.34 ± 2.99 | 16.76 ± 4.12 | 90.32 ± 3.48 |
| M | 83.79 ± 6.08 | 84.90 ± 3.58 | 32.59 ± 9.90 | 84.80 ± 3.34 | 15.65 ± 3.49 | 89.94 ± 3.36 |
| numPeaks | 75.42 ± 6.89 | 89.43 ± 4.13 | 39.19 ± 12.19 | 88.38 ± 3.71 | 17.58 ± 3.45 | 88.69 ± 3.74 |
| FM | 80.02 ± 8.63 | 70.54 ± 6.06 | 19.04 ± 5.72 | 71.21 ± 5.42 | 24.72 ± 4.01 | 83.52 ± 4.29 |
| STE | 58.12 ± 6.18 | 91.86 ± 3.14 | 39.25 ± 13.96 | 89.19 ± 2.68 | 25.01 ± 3.15 | 80.33 ± 3.46 |
| CM | 68.67 ± 12.92 | 73.36 ± 10.67 | 19.79 ± 8.29 | 72.72 ± 9.31 | 28.99 ± 5.47 | 78.56 ± 6.86 |
| maxRR | 17.34 ± 20.82 | 87.24 ± 16.89 | NaN ± NaN | 81.11 ± 13.55 | 47.71 ± 3.52 | 61.78 ± 5.26 |

Table 2.4: Performance of combinations of two features on test sets.

| feature 1 | feature 2 | SE (%) | SP (%) | PP (%) | ACC (%) | BER (%) | AUC (%) |
|---|---|---|---|---|---|---|---|
| VFleak | **aveCC** | 92.60 ± 5.27 | **94.80 ± 2.15** | 60.62 ± 11.27 | **94.66 ± 1.97** | 6.30 ± 2.67 | **98.56 ± 0.89** |
| VFleak | **medianCC** | 93.18 ± 4.92 | 94.45 ± 2.34 | 59.33 ± 12.00 | 94.38 ±2.15 | 6.18 ± 2.60 | 98.55 ± 0.94 |
| TCSC | TCI | 94.80 ± 3.33 | 92.79 ± 3.36 | 54.00 ± 13.04 | 92.98 ± 3.07 | 6.20 ± 2.30 | 98.38 ± 0.79 |
| TCSC | MEA | **95.06 ± 2.90** | 92.59 ± 3.32 | 53.31 ± 12.59 | 92.82 ± 3.03 | 6.17 ± 2.14 | 98.37 ± 0.74 |
| TCSC | SpEn | 94.82 ± 3.37 | 92.99 ± 3.27 | 54.67 ± 12.94 | 93.17 ± 3.00 | 6.10 ± 2.28 | 98.36 ± 0.82 |
| MAV | SpEn | 94.40 ± 3.41 | 93.12 ± 3.35 | 55.23 ± 13.64 | 93.26 ± 3.08 | 6.24 ± 2.33 | 98.35 ± 0.87 |
| TCSC | VFleak | 94.51 ± 4.51 | 93.47 ± 2.95 | 56.13 ± 12.58 | 93.60 ± 2.73 | **6.01 ± 2.69** | 98.24 ± 1.05 |
| VFleak | SpEn | 91.46 ± 5.26 | 94.77 ± 2.84 | **60.90 ± 14.79** | 94.54 ± 2.71 | 6.89 ± 3.16 | 98.24 ± 1.14 |
| TCSC | Count2 | 93.59 ± 4.11 | 92.90 ± 3.36 | 54.07 ± 12.98 | 92.99 ± 2.99 | 6.76 ± 2.24 | 98.19 ± 1.01 |
| MAV | MEA | 94.32 ± 3.07 | 92.74 ± 3.35 | 53.73 ± 13.05 | 92.90 ± 3.05 | 6.47 ± 2.10 | 98.19 ± 0.95 |
| TCSC | SpEn [23] | 94.82 ± 3.37 | 92.99 ± 3.27 | 54.67 ± 12.94 | 93.17 ± 3.00 | 6.10 ± 2.28 | 98.36 ± 0.82 |
| VFleak | Count2 [31] | 88.96 ± 5.85 | 95.98 ± 2.29 | 66.33 ± 14.45 | 95.46 ± 2.12 | 7.53 ± 3.04 | 97.65 ± 1.38 |

Table 2.5: Performance of combinations of three features on test sets.

| feature 1 | feature 2 | feature 3 | SE (%) | SP (%) | PP (%) | ACC (%) | BER (%) | AUC (%) |
|---|---|---|---|---|---|---|---|---|
| VFleak | MEA | **aveCC** | 93.87 ± 3.80 | **95.56 ± 1.45** | **63.81 ± 10.53** | **95.46 ± 1.36** | **5.28 ± 2.00** | **98.98 ± 0.58** |
| VFleak | **medianCC** | MEA | 93.93 ± 3.94 | 95.50 ± 1.58 | 63.59 ± 11.21 | 95.40 ± 1.47 | 5.29 ± 2.07 | 98.96 ± 0.62 |
| VFleak | **medianCC** | SpEn | 93.44 ± 4.51 | 95.08 ± 2.19 | 62.12 ± 12.09 | 94.98 ± 2.05 | 5.74 ± 2.45 | 98.94 ± 0.68 |
| VFleak | **aveCC** | TCI | 93.48 ± 4.16 | 95.44 ± 1.61 | 63.20 ± 10.58 | 95.31 ± 1.53 | 5.54 ± 2.23 | 98.92 ± 0.66 |
| VFleak | SpEn | **aveCC** | 93.07 ± 4.97 | 95.06 ± 2.17 | 61.90 ± 11.79 | 94.93 ± 2.00 | 5.93 ± 2.61 | 98.91 ± 0.68 |
| VFleak | **medianCC** | TCI | 93.85 ± 4.25 | 95.36 ± 1.68 | 63.00 ±10.89 | 95.27 ± 1.58 | 5.39 ± 2.28 | 98.90 ±0.69 |
| VFleak | **medianCC** | Count2 | 92.86 ± 4.59 | 95.16 ± 1.85 | 61.97 ± 11.62 | 95.02 ± 1.64 | 5.99 ± 2.22 | 98.87 ± 0.65 |
| VFleak | Count2 | **aveCC** | 92.85 ± 4.51 | 95.27 ± 1.77 | 62.49 ± 11.18 | 95.11 ± 1.57 | 5.94 ± 2.15 | 98.87 ± 0.64 |
| VFleak | **aveCC** | CM | 93.59 ± 4.49 | 95.06 ± 2.20 | 62.31 ± 11.59 | 94.98 ± 2.01 | 5.68 ± 2.34 | 98.83 ± 0.78 |
| TCSC | VFleak | **medianCC** | **95.22 ± 3.78** | 94.10 ± 2.69 | 58.84 ± 12.42 | 94.23 ± 2.48 | 5.34 ± 2.25 | 98.80 ± 0.66 |
| TCSC | VFleak | SpEn [23] | 93.98 ± 4.61 | 93.68 ± 3.07 | 57.09 ± 13.48 | 93.75 ± 2.85 | 6.17 ± 2.77 | 98.63 ± 0.86 |
| Count2 | VFleak | A3 [31] | 88.69 ± 5.88 | 96.00 ± 2.31 | 66.49 ± 14.49 | 95.47 ± 2.14 | 7.65 ± 3.05 | 97.65 ± 1.38 |

Table 2.6: Evaluation performance on CUDB with VFDB and MITDB as the training set.

| feature 1 | feature 2 | feature 3 | SE (%) | SP (%) | PP (%) | ACC (%) | BER (%) | AUC (%) |
|---|---|---|---|---|---|---|---|---|
| **medianCC** | MAV | SpEn | 89.66 | 89.47 | 69.80 | 89.51 | 10.44 | **96.17** |
| MAV | Count2 | **aveCC** | 93.10 | 84.97 | 62.70 | 86.71 | 10.96 | 96.08 |
| MAV | SpEn | **aveCC** | 88.15 | 89.59 | 69.68 | 89.28 | 11.13 | 96.05 |
| **medianCC** | MAV | Count2 | 92.67 | 85.32 | 63.14 | 86.89 | 11.00 | 96.03 |
| **medianCC** | Count2 | **aveCC** | **94.18** | 87.43 | 67.02 | 88.87 | **9.20** | 95.92 |
| Count2 | **aveCC** | FM | 92.46 | 87.49 | 66.72 | 88.55 | 10.03 | 95.90 |
| **medianCC** | Count2 | FM | **94.18** | 87.31 | 66.82 | 88.78 | 9.25 | 95.78 |
| TCSC | **medianCC** | SpEn | 89.22 | 85.79 | 63.01 | 86.52 | 12.49 | 95.78 |
| VFleak | Count2 | **aveCC** | 83.84 | **92.22** | **74.52** | 90.43 | 11.97 | 95.77 |
| **medianCC** | Count2 | CM | 86.64 | 91.52 | 73.49 | **90.48** | 10.92 | 95.70 |

Table 2.7: Evaluation performance on VFDB with CUDB and MITDB as the training set.

| feature 1 | feature 2 | feature 3 | SE (%) | SP (%) | PP (%) | ACC (%) | BER (%) | AUC (%) |
|---|---|---|---|---|---|---|---|---|
| VFleak | **medianCC** | MEA | **97.47** | 90.63 | 69.27 | 91.85 | 5.95 | **98.46** |
| VFleak | **medianCC** | TCI | **97.47** | 90.42 | 68.80 | 91.67 | 6.06 | 98.40 |
| VFleak | **medianCC** | Count2 | 96.88 | 90.12 | 68.01 | 91.33 | 6.50 | 98.34 |
| VFleak | MEA | **aveCC** | 97.18 | 90.12 | 68.08 | 91.38 | 6.35 | 98.31 |
| VFleak | **aveCC** | TCI | 97.18 | 89.70 | 67.16 | 91.03 | 6.56 | 98.28 |
| VFleak | Count2 | MEA | 95.62 | 92.65 | 73.83 | 93.18 | **5.86** | 98.23 |
| A2 | Count2 | MEA | 92.60 | **93.01** | **74.18** | 92.94 | 7.19 | 98.22 |
| VFleak | Count2 | **aveCC** | 95.91 | 90.35 | 68.31 | 91.34 | 6.87 | 98.16 |
| VFleak | **medianCC** | SpEn | **97.47** | 84.99 | 58.47 | 87.21 | 8.77 | 98.10 |
| VFleak | Count2 | TCI | 95.33 | 92.67 | 73.83 | **93.15** | 6.00 | 98.09 |

## 2.6 Conclusion

This chapter has proposed two new simple, effective, personalized temporal features named aveCC and medianCC for VA detection. These two features have been selected and verified among 11 newly-extracted features and 15 previously-validated existing features. Combined with one or two other features, aveCC or medianCC works well with SVM classifiers under both the record-based data division and the database-based data division of well-known public ECG databases.

Through 50-times record-based data division, the effectiveness of our proposed features have been validated by the statistic results on the test sets. The top two two-feature combinations are VFleak with aveCC, and VFleak with medianCC. The top two three-feature combinations are respectively aveCC and medianCC combined with VFleak and MEA.

For database-based data division, the three-feature combination of medianCC, MAV, and SpEn ranks atop when testing on CUDB with VFDB and MITDB as the training set. And the combination of VFleak, medianCC, and MEA ranks first when testing on VFDB with CUDB and MITDB as the training set.

In conclusion, these simple two or three features involving aveCC or medianCC achieve the best classification performances using SVMs, compared to other feature combinations. These features, especially aveCC and medianCC, have explicit physical meanings and low implementation complexity. The top two-feature and three-feature combinations enable accurate, low complexity, fast and personalized VA detection, leading to potential usage in real time ECG detection applications to improve the prediction of sudden cardiac death.

# Chapter 3

# A Novel Normal and Abnormal Heartbeat Classification Method for a Resource-Saving Cloud based Long-Term ECG Monitoring System

Continuous and noncontinuous remote healthcare monitoring of patients are enabled by the blooming Internet of Things (IoT) technology. However, long-term ECG systems are subject to several practical limitations: battery power restriction, network congestion and heavily-redundant ECG data. To overcome these problems, a novel simple normal and abnormal heartbeat classification algorithm is proposed for CLT-ECG monitoring systems, to decrease the redundant normal heartbeats in data transmission. The proposed algorithm explores two types of variations, intra-beat variation and inter-beat variation, namely, the waveform change indicator (WCI) and the modified RR interval ratio (modRRIR), to predict a heartbeat change. WCI indicates a waveform change in P/QRS/T segments, and is calculated by applying OC-SVMs on tens of personal normal heartbeats. modRRIR characterizes the

successive heartbeat interval variation, and is obtained from the ratio of consecutive three heartbeats, other than the absolute value of RR intervals. WCI and modRRIR are firstly tuned separately, and then combined to separate normal heartbeats from abnormal ones. The proposed method is evaluated using the publicly available MITDB database and achieves an overall accuracy of 78.4%, sensitivity of 76.5%, specificity of 93.2%, and positive predictive value of 98.9%, which outperforms the results in the literature. Furthermore, the strategy is also validated using the data collected from the ECG platform Heartcarer built in our research group.

## 3.1 Introduction

ECG records the electrical impulses from myocardium and is of great value in discovering cardiac arrhythmias which are caused by different heart disorders, impacting people's health and life. Some mild arrhythmias have several obvious symptoms such as lightheadedness and shortness of breath [5]. A few serious arrhythmias may degrade, and even lead to stroke or sudden cardiac death. For example, VF is life-threatening if emergent therapy is not conducted within a few minutes [53]. Early detection and timely therapy feedbacks for arrhythmias are critical to improving patients' health or even saving lives. However, not all arrhythmias can be confirmed in a routine physical exam in a cardiac health center or a hospital by traditional snapshot ECG testing, as they may occur infrequently or asymptomatic [6]. Therefore, long-term ECG monitoring of patients' heart status is extremely useful to arrhythmia detection and diagnosis.

The anomaly-trigged ECG data transmission part in the proposed system scheme is critical to the resource-saving objective, and is the research focus of this chapter. The proposed system realizes resource saving by discarding redundant normal rhythms whereas an acceptable abnormal detection rate should be guaranteed. A lot of research efforts have

been dedicated to developing normal and abnormal classification methods. The available methods can be categorized into two types: syntactic methods and the machine learning based methods.

Syntactic methods identify arrhythmia heartbeats by applying a set of clinical or practically-verified rules to certain extracted features [54–58]. The advantage of this method is that the features extracted usually have explicit physical meanings. In [57], the heart block and ventricular premature complexes are detected when the PR interval and the QRS duration exceed certain thresholds, respectively. In [58], a multistage cardiac event change detection algorithm is proposed, where abnormal beats are discriminated by respectively comparing each feature with its corresponding pre-set public threshold. Henceforth, the accuracy of this method is heavily influenced by the extracted feature types and accuracy, which also explains that advanced signal processing techniques are usually required in the syntactic methods [59–61]. Furthermore, the relationship among different features is ignored in the syntactic methods.

Rather than syntactic methods, machine learning based methods do not deeply rely on precise features of the heartbeat. By feeding a set of features into a machine learning scheme, the machine learning algorithms will yield a decision, which automatically takes into consideration the relationship among different features. The machine learning methods have been widely used in the classification of different types of arrhythmias [62–66], However, most machine learning algorithms used in the literature are supervised learning, and a large amount of pre-labeled ECG heartbeats including normal and abnormal heartbeats are required to train the classification model, which is not practical in real world applications. Most heartbeats in the ECG data stream are usually normal heartbeats. To obtain labeled abnormal heartbeats for training is not easy even if experts available for labeling. Deep learning, another group of machine learning methods, recently becomes more popular in ECG heartbeat classification, such as deep long short-term memory networks [67], convolutional neural networks [68] and

general regression neural network [69]. However, high computing complexity, requirement of labeled data for training and lack of physical network interpretation limit the usage of deep learning methods in the proposed resource-saving ECG monitoring system scheme.

Features extracted from ECG data are indispensable to both syntactic methods and machine learning based methods. Many sets of features used in heartbeat classification are studied in different domains [62, 70], such as time domain, morphological domain, frequency domain, *et al.* Temporal and morphological features are intuitively observed and explicitly analyzed. Thereinto, the whole waveform of a single heartbeat as a set of features keeps all the information and is studied in previous works [6, 67]. It is noted that P/QRS/T segments correspond to depolarization of the atrium, the depolarization of the ventricle and the repolarization of the ventricle, respectively. The waveform variation of each of these three segments indicates different types of heart anomalies. In [6], an unknown heartbeat is predicted to be a normal or abnormal using the dynamic time warping method to measure the waveform difference between this heartbeat and a pre-selected beat template. In [67], without elaborate preprocessing, every sampling point of one whole heartbeat is treated as a feature, and the classification is realized by exploiting a deep learning architecture that takes the whole ECG beat as the input. However, due to the intrinsic amplitude difference, a significant variation of the P/T segments might be counteracted and neglected due to a slight variation of the QRS-segment when P/R/T segments work together within one heartbeat as an entity.

In this chapter, a novel anomaly detection algorithm is presented only using several normal heartbeats for training, aimed for the proposed resource-saving CLT-ECG monitoring system where labeled patient-specific abnormal training heartbeats are not available. As mentioned above, any change among the P/QRS/T segments may indicate a potential abnormal heartbeat, as well as the heartbeat interval variation. Thus, this algorithm explores two types of variations to characterize a heartbeat change, a morphological variation

identification named WCI, and an interval-based feature named modRRIR. WCI is an intra-beat variation detection, which reflects the morphology change of the P/QRS/T segments other than one whole heartbeat using OC-SVMs. modRRIR, based on RR interval ratio (RRIR) [58], is an inter-beat feature, characterizing the successive heartbeat interval variation. An abnormal heartbeat is detected by combining two predictions separately from WCI and modRRIR. The contributions of the chapter are summarized as follows.

- WCI for P/QRS/T segments of one heartbeat, is explored. The waveform change of any of these three segments refers to a certain type of heartbeat anomalies. Thus, it is expected that exploiting the WCI of the three segments yields a better performance than that of exploiting the whole heartbeat.

- The feature modRRIR is proposed as a complementary feature to WCI. modRRIR can detect the successive abnormal beats which cannot be handled by RRIR.

- A combination scheme is designed to achieve a high detection rate of abnormal heartbeats and an as high as possible resource-saving rate simultaneously.

The rest of the chapter is organized as follows. Section 3.2 presents the architecture of the proposed CLT-ECG monitoring system. Section 3.3 introduces the MITDB database used in the simulation. Section 3.4 proposes a novel arrhythmia detection strategy. Section 3.5 validates the effectiveness of the proposed arrhythmia detection strategy on both the MITDB database and the data from our Heartcarer platform. Finally, Section 3.6 concludes this chapter.

## 3.2 Objective

The resource-saving objective is realized by transmitting almost all abnormal heartbeats while limiting the transmission of normal beats as much as possible, considering an acceptable

computational complexity. It is the key concern in this chapter and corresponds to the second stage of the abnormal heartbeat detection during the anomaly-trigged ECG data transmission. The second stage is essential to discriminate the normal and the abnormal beats. To achieve this objective, the following procedure is performed: 1) the ECG data are pre-filtered to remove noise; 2) the ECG beat is detected and segmented; 3) algorithms are explored to classify each beat as normal or abnormal. The objective is to keep as many abnormal heartbeats as possible and at the same time to discard as many normal beats as possible.

Pertaining to the performance regarding the resource-saving rate of the CLT-ECG monitoring system is the classification algorithm adopted to discriminate the normal beats and the abnormal beats. It is desirable that such a classification algorithm achieves a high detection rate for the abnormal and normal beats simultaneously, which is the research scope of this chapter.

## 3.3 Data Preparation

### 3.3.1 Database Information

The MITDB database is one of the most commonly-used public ECG databases, as mentioned in the previous chapter. This database is composed of 48 records from different patients and each record contains 30-minute 2-channel ECG data with a sampling rate of 360 Hz. Following the record partition method proposed by De Chazal *et al.* [71], these records are grouped into two sets, DS1 and DS2, respectively, usually for training a classification mode and validating/testing the classification performance of this trained mode. In this chapter, records in the set DS2 are used to verify our proposed method.

### 3.3.2 Data Preprocessing

The ECG data are inevitably contaminated by external noises [46] and the signal of interest falls in a specific frequency range [72]. Thus, to better reflect the dynamics of the heart, the raw ECG data are preprocessed to eliminate the influence of the external noise, which further facilitates the feature extraction of each heartbeat thereafter. To this end, the database downloaded from the online source [43] is preprocessed in the following way: 1) the baseline wander is removed using a high-pass filter with the 1 Hz cut-off frequency; 2) the high-frequency noise is eliminated using a second-order Butterworth low-pass filter with the cut-off frequency at 40 Hz.

### 3.3.3 Beat Types

In the MITDB database, each ECG beat is annotated manually by experts as one of the 16 heartbeat types. In the remote cloud based ECG monitoring device, it is desirable to transmit the ECG abnormal beats. According to [73], heartbeat types in the binary classification scene, namely, normal and abnormal, are listed in Table 3.1.

Table 3.1: Heartbeat type mapping from the MITDB database to the binary classification scene.

| Normal vs. Abnormal | ECG Heartbeat Types |
|---|---|
| Normal | Normal Beat (NOR), Left Bundle Branch Block (LBBB),<br>Right Bundle Branch Block (RBBB), Atrial Escape Beat (AE), Nodal (Junctional) Escape Beat (NE). |
| Abnormal | Atrial Premature Contraction (APC), Premature Ventricular Contraction (PVC),<br>Paced Beat (PACE), Aberrated Atrial Premature Beat (AP), Ventricular Flutter Wave (VF),<br>Fusion of Ventricular and Normal Beat (VFN), Blocked Atrial Premature Beat (BAP),<br>Fusion of Paced and Normal Beat (FPN),<br>Ventricular Escape Beat (VE), Nodal (Junctional) Premature Beat (NP),<br>Unclassificable Beat (UN). |

### 3.3.4 Performance Metrics

Performance evaluation of a classification algorithm is usually realized by comparing the predicted labels with the ground truth labels (given in the database) on the test set. Commonly-used statistical indices that characterize the classification performance include SE, SP, ACC, PP, etc. In the proposed resource-saving cloud based ECG monitoring system, normal heartbeats are treated as positive instances while abnormal heartbeats as negative instances, as shown in Table 3.2. SE and SP respectively represent the detection rate of normal heartbeats and abnormal heartbeats. Conventionally, SE and SP are more or less equally important, and both contribute to the final classification accuracy resulting in the tradeoff between SE and SP. In the resource-saving application scenario, resource-saving rate corresponds to the detection rate of normal heartbeats, namely, the value of SE. Different from the conventional thinking, we want to guarantee a very high abnormal heartbeat detection rate (i.e., SP), while identifying as many normal heartbeats possible (proportional to SE). In other words, we want to make sure that abnormal beats are always transmitted and stored to the cloud server, even if some normal beats are also inevitably transmitted due to misclassification as abnormal beats. Slightly lower SE simply means the percentage of normal ECG data exempted from transmission and storage are not as much, which is acceptable in the resource-saving CLT-ECG application. Even a SE of 50%, i.e., above a resource-saving rate of 50%, for 24 hours's monitoring, ensures an obvious resource saving in the whole ECG system.

Table 3.2: Statistical indices.

| | Detected Normal | Detected Abnormal |
|---|---|---|
| Annotated Normal | TP | FN |
| Annotated Abnormal | FP | TN |

## 3.4 A Novel Arrhythmia Classification Strategy

A novel arrhythmia detection strategy for the CLT-ECG application is proposed in this section. The strategy aims to achieve an acceptable resource-saving rate while keeping heartbeats of interest and the potentially useful ECG signal as much as possible. As mentioned in [6], advanced signal processing techniques are beneficial to the classification performance but a high computation complexity will be introduced, which might not be suitable at the long-term ECG application side. Furthermore, some undiscovered ECG signal information is unintentionally removed by complicated preprocessing, before the high-resolution heart disease analysis is conducted at the side of the diagnostic cloud server. For example, in [58] the ECG beat will be discarded if it is evaluated as having a bad quality using the signal quality assessment method. In the proposed method, all the ECG beats are processed with the intention that the so-call bad ECG beats may provide additional information for the diagnosis. Furthermore, our proposed strategy realizes the normal and abnormal classification with a simple unsupervised method OC-SVMs, only using lightly-filtered ECG waveforms without advanced signal processing techniques and with explicit physical meanings.

The proposed strategy is elaborated in three subsections. The first part introduces the OC-SVM algorithm; the second part explains WCI obtained from OC-SVMs which indicates any change in one heartbeat in terms of separate P-segment, QRS-segment and/or T-segment using OC-SVMs, and modRRIR derived from the RR-interval as an improvement feature based on the RRIR feature proposed in [58]. The last part illustrates in detail the decision-making procedure.

### 3.4.1 One Class Support Vector Machines

The OC-SVM algorithm is a commonly-used unsupervised machine learning algorithm, which can be used to predict an unseen heartbeat to be a normal or abnormal heartbeat based on a

learning model trained using a small number of normal heartbeats. The OC-SVMs algorithm is essentially constructed to be a two-class algorithm according to Scholkopf's methodology. Let $\{\mathbf{x}_1, \mathbf{x}_2, \cdots, \mathbf{x}_N\}$ denote the training set of $N$ normal heartbeats, then the training of the OC-SVM model is realized as follows

$$\begin{aligned} &\min_{\mathbf{w}, s_i, \rho} \frac{1}{2}\|\mathbf{w}\|^2 - \rho + \frac{1}{\nu N}\sum_{i=1}^{N} s_i \\ &\text{subject to} \quad (\mathbf{w}^{\mathrm{T}}\phi(\mathbf{x}_i)) \geq \rho - s_i, \\ &\qquad\qquad s_i \geq 0 \text{ for } i = 1, \cdots, N, \end{aligned} \tag{3.1}$$

where $\mathbf{x}_i \in \mathbb{R}^{M\times 1}$ is one training sample with $M$ features; $\mathbf{w} \in \mathbb{R}^{M\times 1}$ is the weighting vector; $\phi(\mathbf{x}_i) \in \mathbb{R}^{M\times 1}$ is a transformation operator; $N$ is the number of training samples; $s_i$ represents the slack variable of the $i^{\text{th}}$ training sample with respect to the separating boundaries; $\nu$ is the regularization parameter which represents the upper bound of the fraction of outliers and the lower bound of the number of support vectors, and $\rho$ is a bias item.

Given any testing feature vector $\hat{\mathbf{x}}$, the decision value

$$\text{WCI\_d} = \mathbf{w}^{\mathrm{T}}\phi(\hat{\mathbf{x}}) - \rho,\ \text{d} \in \{\text{P},\ \text{R},\ \text{T}\}. \tag{3.2}$$

It is worth noting that the training size $N$ and the parameter $\nu$ are important factors that impact the classification performance, which is investigated in the simulation part.

### 3.4.2 Wave Change Indicator and Modified RR Interval Ratio

The intra-beat indicator WCI, and the inter-beat feature modRRIR are extracted below. WCI reflects the heartbeat change in terms of separate P-segment, QRS-segment and T-segment by exploiting the OC-SVM classifier. modRRIR is a modified feature based on the feature RRIR proposed in [58], which indicates the prematurity of the heartbeat [74].

Before performing feature extraction, the R-peak in each heartbeat needs to be localized in advance. The P & T QRS detector with high accuracy is available in the literature [48]. Since the QRS detection is not the focus of this chapter, in the simulation part, the R-peaks annotated in the MITDB database are used for the sake of comparison, while in the experimental validation using our Heartcarer ECG platform, the R-peaks are extracted using the P & T QRS detector.

1) Waveform Change Indicator

Inspired by [6, 67], each of the sampling points that compose an ECG heartbeat waveform is treated as one feature, contributing to distinguishing a normal beat from a potential abnormal beat. Generally, a single heartbeat is composed of three main segments, namely, P-segment, QRS-segment and T-segment. Morphological changes of different segments may provide an indication for different anomaly types. For example, the disappearance or abnormality of the P-segment is associated with atrial fibrillation (AF). However, compared with the QRS-segment with high amplitude and large energy, P-segment and T-segment is easily ignored in the presence of a slight variation of the QRS-segment during arrhythmia detection. Thus, the shape change indices of the three segments, are separately calculated according to Eq. (3.2), namely, decision values WCI_P, WCI_R and WCI_T, and are then combined to obtain WCI of the current heartbeat. The procedures of extracting WCI is introduced as follows.

Before proceeding, the method to divide each heartbeat into a P-segment, a QRS-segment and a T-segment, is firstly illustrated in Fig. 3.1. According to general characteristics of ECG heartbeat waveforms, a group of typical window lengths is used to segment each ECG heartbeat. Given the detected R-peak position, a complete heartbeat is confirmed surrounding its R-peak, ranging from 220 ms before the R-peak to 500 ms after the R-peak. Each beat is divided as three segments, P-segment, QRS-segment and T-segment. When the QRS-segment of 160 ms is acquired from 53 ms before the R-peak to 107 ms after the R-peak, the

P-segment and the T-segment are determined accordingly. This way to segment heartbeats is just an example to illustrate the process. Such a segmentation is applicable to situations with a faster or a slower heart rate, as well as a different group of window lengths, as relative changes of consecutive heartbeats are generally evaluated in the proposed algorithm.

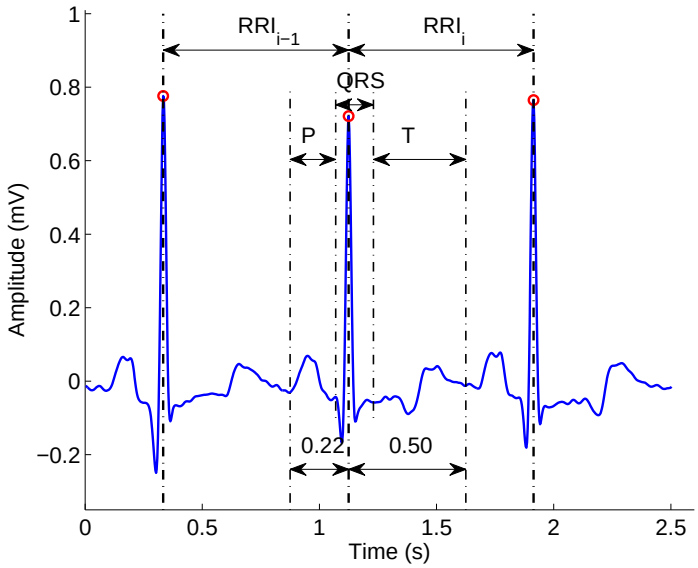


Figure 3.1: ECG beat segmentation (Record 100 in the MITDB database).

After beat segmentation, a prediction making is conducted by exploring WCI for each heartbeat. The WCI feature is obtained through the work flow shown in Fig. 3.2. At the beginning, pre-selected $N$ normal beats are used to train OC-SVM classification models for P-segments, R-segments and T-segments respectively, i.e., ocsvm_P, ocsvm_QRS, and ocsvm_T. An unknown new heartbeat can be predicted to be normal or abnormal based on the three pre-trained classifier mode outputs, i.e., decision values WCI_P, WCI_QRS, and WCI_T separately for the P/QRS/T segments. This heartbeat is evaluated as an abnormal beat if any of the three WCI values indicates a potential abnormality. The threshold $\theta_1$ for WCI values of these three segments can be consistent or different, which is appropriately tuned so that a better SP can be achieved according to the application demand. In detail, if any output of these three OC-SVM classifiers is larger than $\theta_1$, this unknown heartbeat is

predicted to be 'Normal' and denoted by WCI of 0; otherwise 'Abnormal' with WCI of 1.

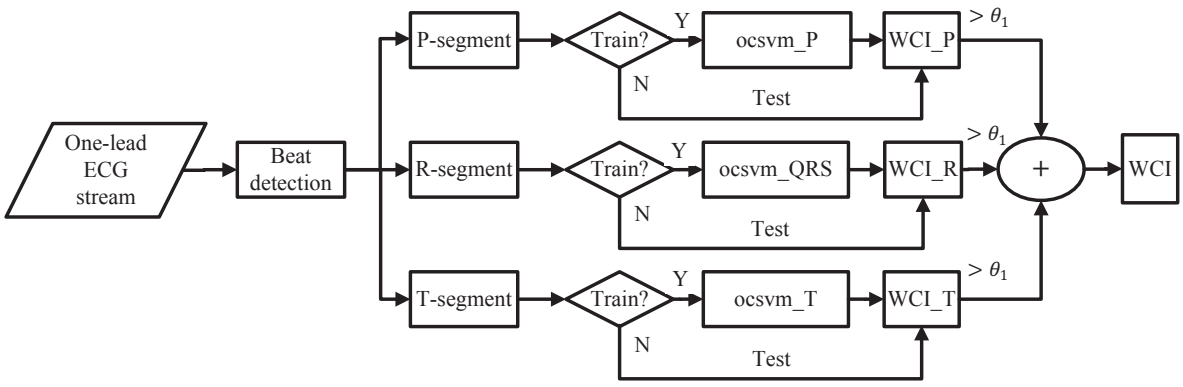


Figure 3.2: Waveform change indicator.

2) Modified RR Interval Ratio (modRRIR)

RR interval is an important feature that reflects the heartbeat variability, specifically, atrial premature contraction. Thus, it is in some sense a good indicator to predict a heartbeat to be normal or abnormal. A RR-interval based feature, RRIR, is presented in [58] to detect real-time changes of cardiac events. RRIR represents the ratio calculated by two consecutive RR interval $RRI_{i-1}$ and $RRI_i$, denoted as $\mathbf{min}\{RRI_{i-1}, RRI_i\}/\mathbf{max}\{RRI_{i-1}, RRI_i\}$. If $RRIR < \theta_2$, the current heartbeat is predicted to be abnormal; otherwise, it is predicted to be normal. RRIR works fine when a single abnormal heartbeat occurs among a duration of normal heartbeats, e.g., for abnormal heartbeats in Record 100.

However, when abnormal heartbeats occur continuously, RRIR fails to detect the cardiac event changes. For example, one waveform segment of continuous abnormal heartbeats (AF beats) is shown in Fig. 3.3, and the correspondingly calculated RRIR and modRRIR are displayed in the rectangular box of Fig. 3.4. It is noted that the most abnormal heartbeats in Fig. 3.3 can not be identified by RRIR values, as these abnormal RR intervals (RRIs) do not change too much although these RRIs are extremely small.

To overcome this problem, RRIR is modified in this chapter as follows: if the $i^{\text{th}}$ heartbeat

is classified as an abnormal beat, $RRI_i = RRI_{i-1}$, where $RRI_i$ and $RRI_{i-1}$ represent the $i^{\text{th}}$ and $(i-1)^{\text{th}}$ RR intervals, respectively. Table 3.4 presents the arrhythmia detection results on Record 209, which shows the superiority of modRRIR compared with RRIR.

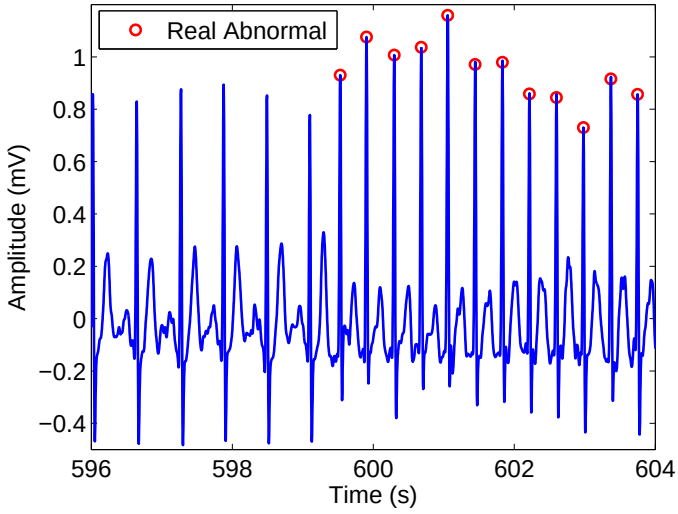


Figure 3.3: Waveform of the segment corresponding to the rectangular box presented in Fig. 3.4.

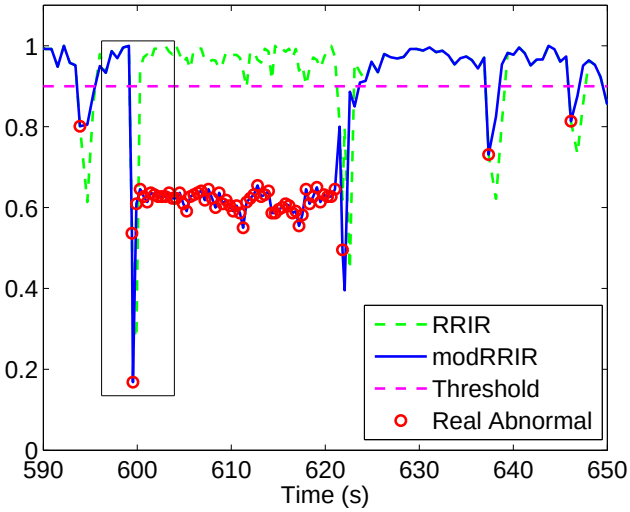


Figure 3.4: Performance comparison between modRRIR and RRIR on Record 209, $\theta_2 = 0.9$.

Table 3.3: Arrhythmia detection performance of Record 209, $\theta_2 = 0.9$.

| | ACC | SE | SP | PP |
|---|---|---|---|---|
| RRIR | 80.7 | 86.5 | 45.1 | 90.6 |
| modRRIR | 92.3 | 91.3 | 98.6 | 99.7 |

A prediction is made based on modRRIR for an unknown heartbeat as normal or abnormal when compared with the threshold $\theta_2$. The value of $\theta_2$ for modRRIR is decided according to the final classification performance, complementary to the prediction WCI.

### 3.4.3 Decision Making Algorithm

With WCI and modRRIR extracted above, an unknown heartbeat is finally predicted to be normal or abnormal by combining the two predictions conducted using WCI and modRRIR, respectively. One beat is labeled as abnormal if any of these two pre-decisions is identified as abnormal. The details of this arrhythmia detection strategy are shown in Algorithm 2.

## 3.5 Simulation and Experiment

This section verifies the proposed novel binary classification strategy using the MITDB database. Firstly, the training length $N$ and the parameter $\nu$ for initializing the OC-SVM mode are analyzed and determined thereafter. Then, the classification performance of the proposed strategy is investigated.

### 3.5.1 Determination of the Training Size $N$ and the Parameter $\nu$

Before the OC-SVM algorithm is applied to the heartbeat to extract the features, the parameter $\nu$ and the training size $N$ need to be determined in advance. In this part, we study the impact of the training size $N$ and the parameter $\nu$ on the overall heartbeat classification

**Algorithm 2** Heartbeat Classification: Normal vs. Abnormal

**Input**

*signal* - raw ECG data stream;

$\theta_1$ - threshold value for WCI;

$\theta_2$ - threshold value for modRRIR;

$N$ - training size;

$I$ - the total number heartbeats in one record;

$M$ - number of sampling points in one segmented heartbeat;

$\nu$ - one OC-SVM parameter.

**Output**

*idxNormal* - the indices of detected abnormal heartbeats.

1: Filter the raw ECG data *signal* as mentioned in Subsection 3.3.2.
2: Identify R-peaks by the P & T QRS-complex algorithm, denoted as

$$\mathbf{R} = \{R_1, R_2, \ldots, R_i, \ldots, R_I\},\ i = 1, 2, \cdots, I.$$

3: Segment the lightly-filtered signal as shown in Fig. 3.1, to obtain a beat array with aligning R-peaks as $\mathbf{X} = \{\mathbf{x}_i | \mathbf{x}_i \in \mathbb{R}^{M\times 1}, i = 1, 2, \cdots, I\},\ \mathbf{X} \in \mathbb{R}^{M\times I}$.
4: Train classification models separately for P-segments, QRS-segments and T-segments for the pre-selected $N$ normal heartbeats using the patient-specific training subset, i.e.,

$$\begin{aligned} ocsvm\_P &= \textbf{ocsvm\_train}(\mathbf{X}(1:P, 1:N)) \\ ocsvm\_QRS &= \textbf{ocsvm\_train}(\mathbf{X}((P+1):T, 1:N)) \\ ocsvm\_T &= \textbf{ocsvm\_train}(\mathbf{X}((T+1):M, 1:N)) \end{aligned}$$

where $P$ and $T$ represent the end points of the P-segment and the QRS-segment for one heartbeat, respectively.
5: $i := N + 1$
6: **while** $i \leq I$ **do**
7: The RR interval $RRI_i = R_i - R_{i-1}$
8: **if** $i > N + 2$ **then**
9: $modRRIR_i = \min(RRI_i, RRI_{i-1}) / \max(RRI_i, RRI_{i-1})$,
10: **end if**
11: **if** $RRIR_i > \theta_2$ **then**
12: $idxNormal \leftarrow idxNormal \bigcup i$
13: $RRI_i = RRI_{i-1}$
14: **end if**

Calculate decision values separately for different segments of Beat $i$
  $WCI\_P$ = **ocsvm_predict**($\mathbf{X}(1:P,i), ocsvm\_P$)
  $WCI\_R$ = **ocsvm_predict**($\mathbf{X}((P+1):T,i), ocsvm\_QRS$)
  $WCI\_T$ = **ocsvm_predict**($\mathbf{X}((T+1):M,i), ocsvm\_T$)
**if** $WCI\_P > \theta_1$ || $WCI\_R > \theta_1$ || $WCI\_T > \theta_1$ **then**
  $idxNormal \leftarrow idxNormal \bigcup i$
**end if**
$i = i + 1$
**end while**
Return $idxNormal$.

performance, and then choose appropriate values for the following implementation. The overall performance is calculated with the aggregated classification counts of each record. Records in DS2 are selected following the record division scheme proposed in [71].

Fig. 3.5 shows the impact of training size $N$ on the heartbeat classification performance, given a fixed parameter $\nu = 0.02$, when the OC-SVM algorithm is applied. It can be observed that ACC and SE decrease slightly along with the training size ranging from 10 to 90 beats, and then stabilize at around 78% and 76%, respectively. Meanwhile, SP and PP increase a little bit as the training size increases. Similar trend relating the training size and the classification performance can also be observed when the parameter $\nu$ varies, which indicates that the classification performance is not that sensitive when the training size changes. Fig. 3.6 shows how the parameter $\nu$ affects the classification performance when the training size $N = 20$. It is noted that the parameter $\nu$ in the OC-SVM algorithm represents the upper bound for the outlier in the training set. Intuitively, When the parameter $\nu$ increases, more normal heartbeats are treated as outliers in the training process. On the contrary, more normal beats can not be identified in the test stage, leading to a decrease of SE and an indirect increase of SP, as demonstrated in Fig. 3.6.

It is noted from Fig. 3.5 and Fig. 3.6 that PP is always high, and the influence of the training size $N$ and the parameter $\nu$ are negligible, which is an advantage of applying the proposed strategy. Particularly, PP of close to 100% and high SP mean few abnormal beats

are mistakenly detected as normal ones. Based on the above analysis, the training size $N$ and the parameter $\nu$ are chosen as 20 and 0.02, respectively, for the following implementation.

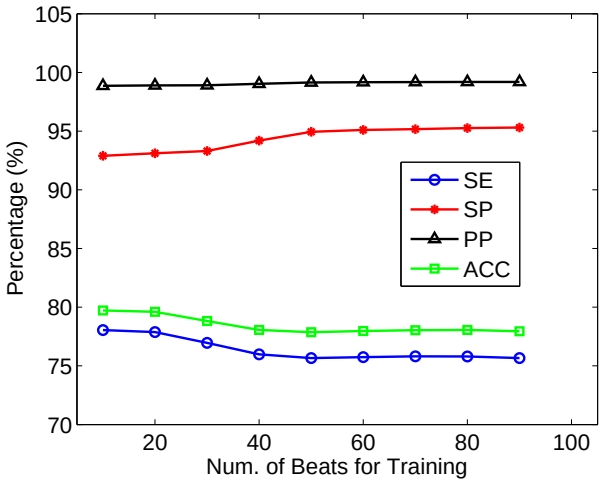


Figure 3.5: Overall performance vs. training size on DS2 ($\nu = 0.02, \theta_1 = 0$).

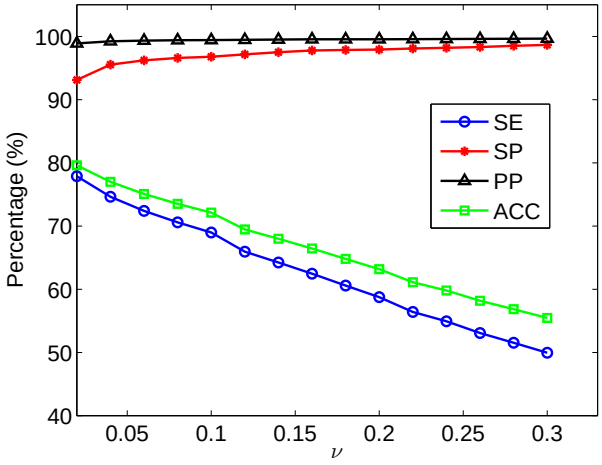


Figure 3.6: Overall performance vs. $\nu$ on DS2 ($N = 20, \theta_1 = 0$).

### 3.5.2 Performance Analysis Using the MITDB Database

After the training size $N$ and the parameter $\nu$ are determined, it is now ready to apply the proposed strategy on the MITDB database. In this part, the heartbeat classification

performance is presented in detail, and the comparison with the results in the literature is also conducted.

Table 3.4 presents the heartbeat classification results, record by record, by exploiting the feature WCI, the feature modRRIR and both of the two features, respectively. It can be observed that SP by exploiting both features outperforms that of exploiting one of the two features, indicating that a high abnormal detection rate is achieved. The procedure is as follows: after obtaining the classification results by exploiting the feature WCI, an appropriate threshold is chosen for the modRRIR such that a comparable SE is obtained compared to that of using WCI. Since the two features characterize the heartbeat in different aspects, an appropriate combination of the abnormal beats yields a high abnormal beat detection rate. It is also worth noting that most of the records have a very high SP above 90% as well as a tiptop PP value, which is consistent with the expectation in the resource-saving CLT-ECG application. In addition, a few records have low SP values because of their own specialities. For example, in Record 103, there are only two abnormal beats, so a low SP doesn't matter too much. And Record 102 has no abnormal beats so its SP is denoted as '-'.

Table 3.4: Heartbeat classification performance for each record ($\nu = 0.02, N = 20, \theta_1 = -0.025, \theta_2 = 0.68$).

| Record | Normal | Abnormal | WCI | | | | modRRIR | | | | Combined | | | |
|---|---|---|---|---|---|---|---|---|---|---|---|---|---|---|
| | | | ACC | SE | SP | PP | ACC | SE | SP | PP | ACC | SE | SP | PP |
| 100 | 2237 | 34 | 98.6 | 99.9 | 9.10 | 98.7 | 97.8 | 98.9 | 26.5 | 98.9 | 98.3 | 99.3 | 30.3 | 99 |
| 103 | 2080 | 2 | 99.1 | 99.2 | 0 | 99.9 | 98.9 | 99 | 0 | 99.9 | 98.7 | 98.8 | 0 | 99.9 |
| 105 | 2524 | 46 | 75.5 | 75.2 | 93.3 | 99.8 | 95.5 | 95.9 | 71.7 | 99.5 | 74.1 | 73.6 | 100 | 100 |
| 111 | 2121 | 1 | 60 | 60 | 100 | 100 | 98.6 | 98.6 | 0 | 100 | 59.4 | 59.3 | 100 | 100 |
| 113 | 1787 | 6 | 99.9 | 99.9 | 100 | 100 | 97.7 | 97.7 | 100 | 100 | 98.3 | 98.2 | 100 | 100 |
| 117 | 1532 | 1 | 54.4 | 54.4 | 100 | 100 | 89.9 | 89.9 | 100 | 100 | 45.1 | 45.1 | 100 | 100 |
| 121 | 1859 | 2 | 94.2 | 94.2 | 50 | 99.9 | 96.5 | 96.5 | 50 | 99.9 | 91.4 | 91.5 | 50 | 99.9 |
| 123 | 1513 | 3 | 99.7 | 99.7 | 100 | 100 | 95.8 | 95.8 | 100 | 100 | 96.2 | 96.2 | 100 | 100 |
| 200 | 1742 | 857 | 94.1 | 93 | 96.4 | 98.1 | 52 | 68.6 | 18.2 | 63 | 74.9 | 64.2 | 96.5 | 97.4 |
| 202 | 2059 | 75 | 93.5 | 93.9 | 82.7 | 99.3 | 58.2 | 56.7 | 97.3 | 99.8 | 55.6 | 53.9 | 100 | 100 |
| 210 | 2421 | 227 | 98.6 | 98.6 | 98.7 | 99.9 | 85.8 | 88.9 | 52 | 95.2 | 89.4 | 88.5 | 98.7 | 99.9 |
| 212 | 2746 | 0 | 63.9 | 63.9 | - | 100 | 98.3 | 98.3 | - | 100 | 62.9 | 62.9 | - | 100 |
| 213 | 2639 | 610 | 95.2 | 99.1 | 78.4 | 95.2 | 80.1 | 97 | 7 | 81.9 | 93.3 | 96.5 | 79.8 | 95.4 |
| 214 | 2001 | 259 | 98.5 | 98.6 | 97.7 | 99.7 | 87.2 | 85.9 | 97.3 | 99.6 | 86.9 | 85.2 | 100 | 100 |
| 219 | 2080 | 205 | 98.9 | 99.1 | 96.6 | 99.7 | 86.7 | 88.1 | 72.2 | 97 | 88.6 | 87.8 | 96.6 | 99.6 |
| 221 | 2029 | 396 | 99.8 | 99.8 | 100 | 100 | 18.5 | 21.2 | 4.50 | 53.3 | 34.4 | 21.5 | 100 | 100 |
| 222 | 2272 | 209 | 47.9 | 43.8 | 92.8 | 98.5 | 72.9 | 72.1 | 82.3 | 97.8 | 46.3 | 41.7 | 95.7 | 99 |
| 228 | 1686 | 365 | 89.2 | 87 | 99.2 | 99.8 | 73.7 | 78.6 | 50.7 | 88 | 75.6 | 70.5 | 99.2 | 99.7 |
| 231 | 1566 | 5 | 99.6 | 99.7 | 80 | 99.9 | 98.4 | 98.5 | 80 | 99.9 | 98.8 | 98.8 | 80 | 99.9 |
| 232 | 397 | 1381 | 85.5 | 80.6 | 86.8 | 62.6 | 2.90 | 1.50 | 3.30 | 0.400 | 69 | 0.300 | 87.8 | 0.600 |
| 233 | 2229 | 848 | 99.2 | 99.2 | 99.2 | 99.7 | 66.7 | 88.2 | 10.3 | 72.1 | 90.8 | 87.6 | 99.2 | 99.6 |
| 234 | 2698 | 53 | 99.1 | 99.2 | 92.5 | 99.8 | 94.4 | 95.6 | 34 | 98.7 | 95.2 | 95.2 | 92.5 | 99.8 |
| Total | 44218 | 5585 | 88.5 | 88.1 | **92.1** | 98.9 | 79.0 | 85.9 | **24.6** | 90.0 | 78.4 | 76.5 | **93.2** | 98.9 |

Table 3.5 compares the classification results with a few algorithms in the literature under the same test record subset, according to Table 10 in Luz's survey paper [75]. It can be seen from Table 3.5 that compared with the published results, comparable SE with a SP of 93.2% is achieved. Furthermore, the PP and ACC of the proposed strategy outperform that of the

published results.

Table 3.5: Performance comparison with the methods in the literature on DS2 ($\nu = 0.02, N = 20, \theta_1 = -0.025, \theta_2 = 0.68$).

| Method | ACC | SE | SP | PP |
|---|---|---|---|---|
| Ye *et al.* [76] | 75.2 | 80.2 | 78.2 | - |
| Yu and Chou [77] | 75.2 | 78.3 | 79.2 | - |
| Yu and Chen [78] | 73.9 | 81.5 | 74.2 | - |
| Guler and Obeyli [79] | 66.7 | 69.2 | 72.1 | - |
| Song *et al.* [80] | 76.3 | 78.0 | 83.9 | - |
| **Proposed method** | **78.4** | 76.5 | **93.2** | 98.9 |

### 3.5.3 Experimental Study

In this part, the proposed strategy is further studied using the Heartcarer ECG platform built in our research group. We first introduce the Heartcarer ECG platform and then present the experimental results.

1) Heartcarer ECG Platform

A CLT-ECG monitoring system, Heartcarer ECG platform, is built to conduct remote heart monitoring. As shown in Fig. 1.1, it mainly consists of an ECG sensor board, an Android smartphone, and an ECG cloud server. The ECG sensor board collects the raw ECG signal, conducts some pre-processing (amplification, filtering, etc.), and then transmits the signal to the smartphone using Bluetooth low-energy technique. On the smartphone, the proposed algorithm is exploited to discriminate the abnormal and normal beats, and the segments containing these detected abnormal beats are uploaded to the cloud server and stored as the way as shown in Fig. 3.7. To further classify the data stored on the cloud server into different arrhythmia types, some advanced signal processing techniques can be applied, which is out of the research scope of this chapter.

The ECG sensor board has four electrodes with a sampling rate of $f_s = 250$ Hz and a resolution of 8 bits. Generally the ECG waveforms of Lead I and Lead II could be obtained, as shown in Fig. 3.8. To keep a consistent setting with the simulation, the signal from Lead II is used in the experiment.

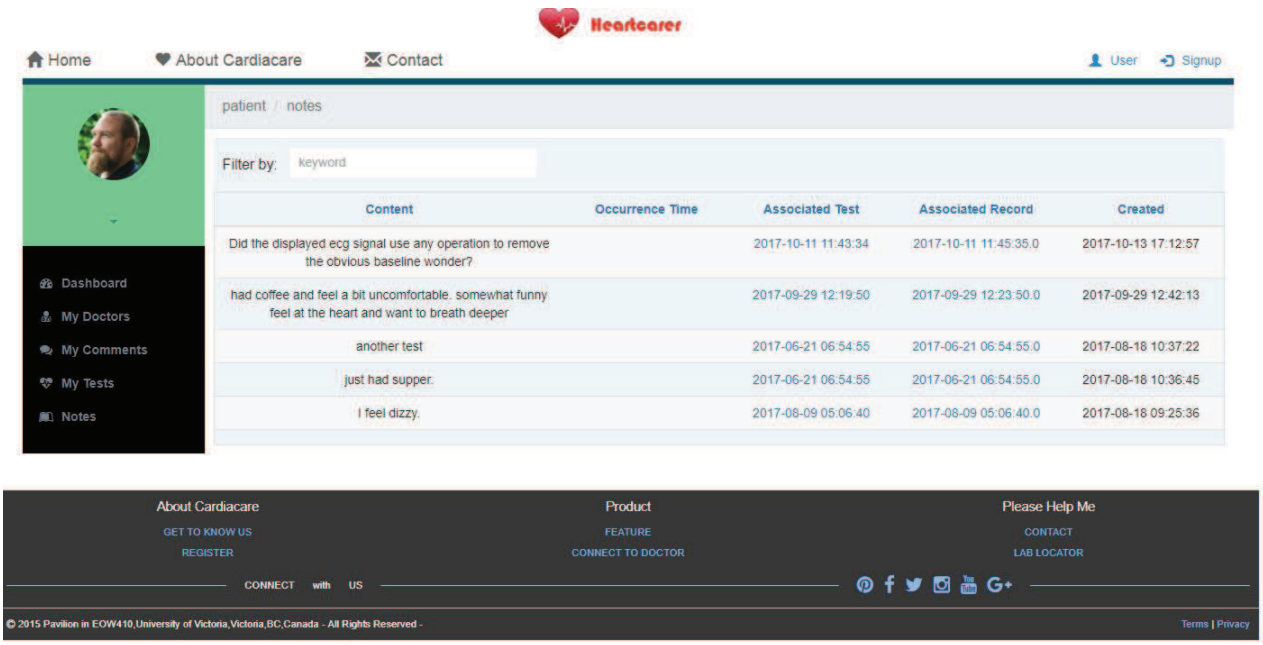


Figure 3.7: A snapshot for the Heartcarer website.


Figure 3.8: Heartcarer ECG waveform records for one subject.

2) Experimental Validation

The experimental data are collected from two volunteering subjects, one healthy person and the other one with long QT syndrome. The ECG record from the healthy subject includes 167 normal beats, as shown in Fig. 3.9. WCI and modRRIR are extracted from each heartbeat, the first 20 beats are fed into the OC-SVM classifier as the training set. Then the trained model is used to perform classification on the test set. It turns out that a detection rate of 78.2% is obtained, which is comparable to the simulation performance. The other ECG record, which is collected from the subject with long QT syndrome, has a total of 149 beats, and these beats are examined carefully one-by-one and annotated as normal and abnormal within our research group. The waveforms of the non-regular and regular beats are demonstrated in Fig. 3.10 and Fig. 3.11, respectively. Similarly, the first 20 beats are

used as the training set for the OC-SVM classifier, and the remaining beats as test data. Finally, implementation of Algorithm 2 yields a SE of 99.1%, SP of 100%, PP of 100%, and ACC of 99.2%. Here possible reasons for a higher SE compared to the simulation results are: 1) only one type of arrhythmia exists in the subject and 2) the abnormal beats and the normal beats from this subject differ significantly.

Both of the experiments above show the effectiveness of the proposed algorithm, i.e., a large amount of transmission power and cloud server storage can be saved. In practice, several beats before and after the detected abnormal/non-regular beats are suggested to be transmitted as reference to conduct further diagnosis. Thus, to keep enough normal/regular heartbeats as reference, the practical transmission resource-saving rate may be tuned lower. Even though, such a resource-saving scheme is beneficial for the remote, long-term cloud based ECG monitoring platform.

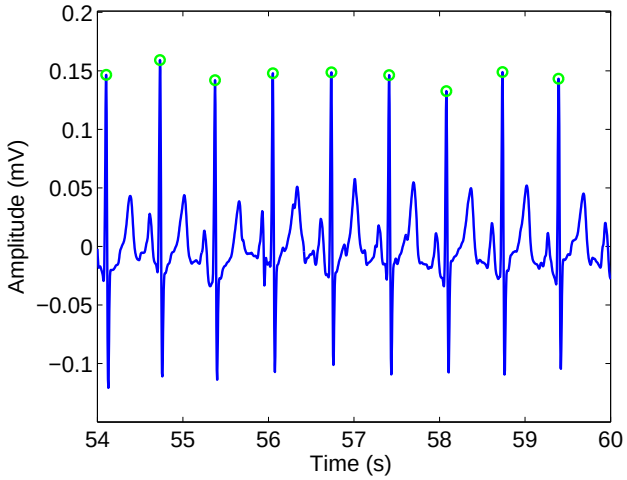


Figure 3.9: ECG data from a healthy subject by Heartcarer.

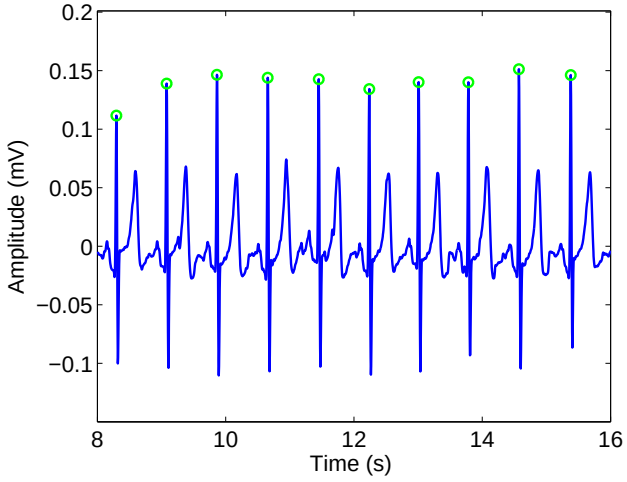


Figure 3.10: Regular ECG pattern from a subject with long QT syndrome by Heartcarer.

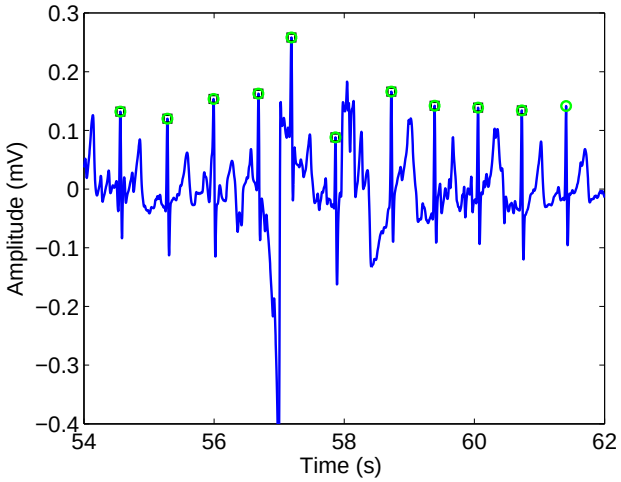


Figure 3.11: Irregular ECG pattern from a subject with long QT syndrome by Heartcarer.

### 3.5.4 Limitation

The limitation of the proposed normal and abnormal classification method is that the personal training subset, namely $N$, is required to be labeled with manual assistance. However, this requirement is as little as possible in this chapter, and is more practical and convenient for the patient himself/herself to implement since most of heartbeats are normal or regular heartbeats, e.g., sweeping with a finger to confirm several normal heartbeats on the

smartphone screen. Besides, labeling a small amount of personal training subset might be performed by a global classifier with good generalization ability.

## 3.6 Conclusion

This chapter presents a resource-saving CLT-ECG monitoring system structure and then studies a novel binary ECG arrhythmia detection algorithm that is critical to the resource-saving performance. WCI, an intra-beat waveform variation indicator, and modRRIR, an inter-beat feature, are introduced and extracted, respectively. Based on the above two results, a detailed algorithm to perform classification is presented. The proposed classification algorithm is evaluated using the MITDB database, and it turns out that a significant improvement is achieved in terms of ACC and PP, compared to the results in the literature. Furthermore, the proposed algorithm is verified on the experimental platform built in our research group, using the data collected from a healthy subject and a subject with long QT syndrome.

In the future, the proposed work will be examined and potentially applied in two directions. One direction is that the proposed patient-specific local classifier can be modified to realize fully automatic personal normal and abnormal classification, by selecting the high-confidence local training data using a global classifier; the other direction is that the proposed local classifier can be used to pre-select the data for the multi-type classification in the cloud server.

# Chapter 4

# A Patient-Specific Single-Lead ECG Heartbeat Classification

This chapter studies an automatic patient-specific heartbeat classification strategy to discriminate ventricular ectopic beats (VEBs) and supraventricular ectopic beats (SVEBs), two of the AAMI recommended heartbeat classes. Two sets of features, the intra-beat features and inter-beat features are extracted. Intra-beat features characterize the distortion of the waveform within one heartbeat, while inter-beat features reflect the variation between successive heartbeats. The effectiveness of the extracted feature set is verified by the simulation result of the global classifier for VEB detection. A novel fusion strategy consisting of a global classifier and a local classifier is presented which incorporates the patient-specific information and thus can potentially improve the classification performance. The local classifier is obtained using the high-confidence heartbeats extracted from the first above 5-minute data of a specific patient, where the high-confidence heartbeats are the heartbeats that are classified to a certain type by the global classifier with a high probability. The advantage of the developed strategy is that fully-automatic classification is realized without the intervention of physicians. Furthermore, simulation results show that comparable or even better classifi-

cation performance is achieved, which validates the effectiveness of the proposed strategy.

## 4.1 Introduction

The ECG signal characterizes the underlying dynamics of the heart and contains a wealth of information, reflecting the overall cardiovascular health condition. ECG signal has been exploited to automatically detect and identify the cardiac arrhythmias [81] which means irregular or abnormal dynamics of the heart. Cardiac arrhythmias are usually categorized into life-threatening arrhythmias and non-life-threatening arrhythmias. The detection of life-threatening arrhythmias is critical and extensive results with high classification performance have been achieved [16, 23, 32, 53, 82, 83]. For the non-life-threatening arrhythmias, they happen infrequently and need to be captured using long-term ECG monitoring devices, aiming to provide complementary information to assist the diagnosis for cardiologists. For example, VEB, one type of non-life-threatening arrhythmias, means that there is a sign of disturbance in the depolarization process, which indicates a malignant cardia arrhythmia [84]. This chapter concentrates on designing classification strategies to discriminate VEBs and SVEBs so that appropriate intervention or therapy can be applied in advance.

The classification of ECG heartbeats generally consists of three stages [25, 75], i.e., preprocessing, feature extraction and classification. In the preprocessing stage, the signal is processed to reduce the influence of the noise, to remove the baseline wander and also to locate the fiducial points. Feature extraction aims to extract the most representative elements that can characterize the ECG heartbeats and is critical to successfully identify the heartbeats. The features commonly seen in the literature include ECG heartbeat morphological [71, 85] and dynamic features [86, 87], wavelet transform based features [87–89], frequency based features, projected features [5], etc. The classification part involves designing appropriate classifier to label each heartbeat according to the associated features

extracted. Classifiers in the literature include SVM [90, 91], linear discriminant [71, 86, 92], neural networks [68, 69, 89, 93], etc.

A lot of research efforts have been dedicated to investigating the detection and classification of VEBs and SVEBs. Basically, the classifiers can be separated into global classifiers [5, 71, 85, 87, 94–98] and patient-specific classifiers [68, 69, 86, 89, 93, 94, 99–103]. A global classifier is generally trained using the publicly available database without a prior incorporation of the ECG data of the patient to be monitored. Based on the transformed morphological and temporal features, the authors in [94] constructed a global classifier exploiting the self-organizing maps and learning vector quantization algorithms. Considering the unbalance property of different types of heartbeat arrhythmias, linear discriminant (LD) classifiers [71] with appropriate weighted likelihood functions are developed for two leads and classification is obtained by proper fusion of the two leads. Different from the generally used waveform shape related morphological features, the wavelet transformation and independent analysis [87] are used to extract the features, and the dimension of the features is further reduced and fed into a SVM based classifier exploiting two leads. Noting that the classification results in [71, 87, 94] are based on two leads, it is criticized in [97] that attaching two leads is not practical in some cases and the authors in [97] exploits the synchrosqueezing transform to derive phase and amplitude intervention of single-lead ECG heartbeats and perform the SVM-based classification.

Although some of the global classifiers reviewed above achieve good performance, the results are not consistent for each individual testing record, which might be caused by the inter-beat variation of the morphologies of ECG waveform. Henceforth, it is expected to obtain a better and consistent performance if the classifier is adjustable to specific patients. Recently, various forms of patient-specific classifiers which take into account the specific characteristic of the patient's ECG waveform, have been extensively studied. The authors in [94] proposed a patient-adaptable ECG beat classification algorithm, namely, a mixture

of experts (MOE) approach, in which a local classifier is constructed exploiting the first 5-minute annotated ECG beats taken from the specific patient and then combined with the global classifier to generate the classification results. To alleviate the workload of cardiologists, the authors in [86] first classify a small segment of ECG beats using a global classifier and then the ECG beats are examined and corrected if necessary to train a local classifier. Similar to [94], classification is performed using the combination of global and local classifiers. Different from the conventional methods, convolutional neural network based patient-specific classifiers [68, 104] integrate the feature extraction and classification, which can automatically learn the features from the input raw ECG beat. Still, a small segment of manually labeled patient-specific ECG beats should be provided. To fully avoid the intervention of cardiologists, the authors in [99] adopted a multiview approach to obtain the high-confidence patient-specific ECG beats which are used to train a local classifier. In general, the classification schemes that are aware of the patient-specific information yield better performance than the global classifiers.

This chapter studies the automatic patient-specific VEB and SVEB detection and classification algorithms. It is worth noting that although features extracted from multilead provide more comprehensive representations and thus yield better classification performance, the applicability is restricted due to the requirement to deploy more electrodes on the body. Inspired by [97], in this chapter, only single-lead ECG data is exploited. Similar to [86], global and local classifiers are designed to cooperatively classify each heartbeat. However, if there are VEB or SVEB beats in the first 5-minute ECG data, then the classification result is decided by the local classifier. On the other hand, if there are no VEB or SVEB beats in the first 5-minute ECG data, then the global classifier will dominate the classification results. In summary, the contributions of this chapter are itemized as follows:

- Two sets of features, intra-beat features and inter-beat features, are extracted. Intra-beat features characterize the distortion within the heartbeat, while inter-beat features

reflect the variation between successive heartbeats.

- A fully-automatic patient-specific classification strategy is studied. Specifically, the global classifier is firstly used to annotate the first 500 beats (above 5-minute length data) of the patient-specific data, and only the ECG beats with high posterior probabilistic estimate is used to train the local classifier. It turns out that the developed strategy yields better performance than that of the global classifier.

- The developed classification strategy only exploits single-lead ECG data, which is more practical. Simulation results show that the classification performance is comparable to that of using two-lead ECG data.

The rest of the chapter is organized as follows. Section 4.2 presents the ECG data information. Section 4.3 introduces the feature extraction and the classification model. Section 4.4 evaluates the classification performance and analyzes the results. Section 4.5 concludes this chapter.

## 4.2 Data Preparation

### 4.2.1 Database Information

The proposed algorithms are tested using the MITDB database, one of the most commonly-used public ECG databases. The database consists of 48 records from different patients with the exception that records 201 and 202 are from the same patient, and each record contains 30-minute 2-channel ECG data with a sampling rate of 360 Hz. Associated with each record, there is an annotation file containing the QRS position and the beat class information, which is verified by at least two cardiologists. Lead information for each record is listed in Table 4.1.

Table 4.1: Lead information of the records.

| **Lead A** | V5 | V5 | MLII | MLII | MLII | MLII |
|---|---|---|---|---|---|---|
| **Lead B** | V2 | MLII | V2 | V4 | V5 | V1 |
| **Records** | 102 104 | 114 | 103 117 | 124 | 100 123 | 101 105 106 107 108 109 111 112 113 115 116 118 119 121 122 200 201 202 203 205 207 208 209 210 212 213 214 215 217 219 220 221 222 223 228 230 231 232 233 234 |
| **Number** | 2 | 1 | 2 | 1 | 2 | 40 |

The record division schemes proposed by de Chazal *et al.* [71] is adopted in this chapter as shown in Table 4.2. These records are grouped into two sets, DS1 and DS2, respectively, for training a classification model and validating/testing the classification performance of this trained model. To comply with the ANSI/AAMI EC57: 1998 standard, paced records 102, 104, 107 and 217 are excluded as they display different characteristics from general ECG records. In addition, the first channel of the selected 44 records is used in this study.

Table 4.2: Database division.

| | **Total beats** | **Records included** |
|---|---|---|
| **D1** | 51508 | 101, 106, 108, 109, 112, 114, 115, 116, 118, 119, 122, 124, 201, 203, 205, 207, 208, 209, 215, 220, 223, 230. |
| **D2** | 49803 | 100, 103, 105, 111, 113, 117, 121, 123, 200, 202, 210, 212, 213, 214, 219, 221, 222, 228, 231, 232, 233, 234. |

### 4.2.2 Data Preprocessing

The ECG signal is affected by artifact signals including baseline wander, power line interference and high frequency noise as stated in [46] and it is also observed that the signal of interest falls in a specific frequency range [72]. Thus, to better reflect the dynamics of the heart, the raw ECG data is preprocessed to eliminate the influence of the external noise, which further facilitates the feature extraction of each heartbeat thereafter. To this end, the ECG data is preprocessed following the similar line in [53]: 1) the baseline wander is removed using a high-pass filter with the 1 Hz cut-off frequency; 2) the high-frequency noise is eliminated using a second-order Butterworth low-pass filter with the cut-off frequency at 40 Hz.

The ECG data is further segmented into consecutive heartbeats, so that the heartbeat-based feature extraction and classification can be employed. Various segmentation algorithms have been developed and great accuracy has been achieved [48,105]. In this chapter, to focus on the validation of the proposed classification method, the QRS positions in the annotation files provided in the database are used.

### 4.2.3 Beat Types

In the MITDB database, the heartbeats are categorized into 15 types. To be consistent with the AAMI recommendation and ensure a fair comparison with [68, 89, 94], the 15 types are mapped into 5 classes: N, V (VEB), S (SVEB), F, and Q, which is illustrated in detail in Table 4.3. Also, the heartbeat numbers of VEBs and SVEBs in the dataset DS1 and DS2 are presented in Table 4.2.

Table 4.3: Heartbeat class mapping.

| AAMI standards | Beats in DS1 | Beats in DS2 | MITDB annotations |
|---|---|---|---|
| N | 45825 | 34355 | • Normal beart (N) |
| | | | • Left bundle branch block beat (L) |
| | | | • Right bundle branch block beat (R) |
| | | | • Atrial escape beat (e) |
| | | | • Nodal (Junctional) escape beat (j) |
| V (VEB) | 4260 | 2578 | • Premature ventricular contraction (V) |
| | | | • Ventricular escape beat (E) |
| | | | • Ventricular flutter wave (!) |
| S (SVEB) | 1001 | 1573 | • Atrial premature beat (A) |
| | | | • Aberrated atrial premature beat (a) |
| | | | • Non-conducted P-wave (blocked APB) (x) |
| | | | • Nodal (junctional) premature beat (J) |
| F | 414 | 292 | • Fusion of ventricular and normal beat (F) |
| Q | 8 | 5 | • Fusion of paced and normal beat (f) |
| | | | • Unclassifiable beat (Q) |

### 4.2.4 Performance Evaluation

There are two different schemes to evaluate the classification algorithms, class-oriented [90, 98] and subject-oriented [71, 86, 87, 89, 93, 96, 97]. In the class-oriented scheme, the training set and the test set contain heartbeats from the same record, and thus, the information of a specific-patient is implicitly incorporated in the training stage. The class-oriented scheme tends to achieve an optimistic performance, however is not practical. The subject-oriented scheme, i.e. patient-specific scheme, on the other hand, conducts the training and testing in separate records, preventing the training process from being aware of specific patients' information, and thus offering a more realistic evaluation of the classifiers. The proposed

strategy is evaluated and compared with other strategies under the patient-specific scheme. Regarding the statistical indices to evaluate the classification algorithms, SE, SP, ACC, and PP, are used. For detailed definitions of SE, SP, ACC, and PP, readers can refer to [53].

## 4.3 Methodology

After the MITDB database is downloaded and preprocessed, i.e., the ECG signal is filtered and the ECG heartbeats are segmented, it is ready to extract the features that can characterize each heartbeat, and then conduct classification using the developed classifier.

### 4.3.1 Feature Extraction

Table 4.4: Features extracted.

| Class | Features |
|---|---|
| Intra-beat Features | • Amplitude of R, Q, and S peaks |
| | • QRS duration/width |
| | • Area and sample number of the QRS complex |
| | • Complexity parameters (CM) [19] |
| | • Frequency calculation (FreqBin) [106] |
| | • Kurtosis value [107] |
| | • Spectrum parameters [16] |
| Inter-beat Features | • Pre-RR interval |
| | • Post-RR interval |
| | • Ratio of RR interval from consecutive three heart beats [58] |
| | • Ratio of the amplitude from consecutive two R-peaks [58] |
| | • Waveform similarity of two consecutive heartbeat waveforms [58] |
| | • Dynamic time warping (DTW) between consecutive heartbeats |

The features extracted in this chapter (as shown in Table 4.4) are categorized into two types: intra-beat and inter-beat features. Intra-beat features are the features that can be obtained using a single heartbeat, while the inter-beat features are the features that are extracted using the current and the neighboring heartbeats. These two types of features are

illustrated in more detail as follows.

1) Intra-beat features: Intra-beat features reflect the distortion of the ECG signal within one heartbeat. In this chapter, seven intra-beat features are extracted, and are described as follows.

The amplitudes of Q, R and S peaks are simply obtained using the fiducial points provided in the annotation file associated with each record. The QRS duration/width refers to the number of sampling points between the QRS onset to the QRS offset.

Area of the QRS complex reflects a more comprehensive information and is obtained by summing up the amplitude of the sampling points between the QRS onset to the QRS offset.

Complexity measure (CM) [19] provides a precise characterization of the order or disorder of the evolution of the ECG signal, and is obtained by applying the detailed mathematical expression formulated by Lempel and Ziv to a finite symbol sequence transformed from the ECG heartbeat.

To obtain the frequency calculation (FreqBin) [106], a $0-1$ binary string is firstly obtained by comparing the ECG data with an appropriately chosen threshold, and then the number of binary signal transitions between '0' and '1' are counted and divided by the window length, which yields the normalized transitions for '1's.

Kurtosis value of the ECG signal [107] measures how Gaussian-like the ECG signal appears to be using its fourth standardized moment, which is obtained by calculating the relative peakedness of the ECG signal with respect to a Gaussian distribution

$$Kurt = E(x - \mu_x)^4/\sigma^4 - 3 \tag{4.1}$$

where $E$ is the mathematical expectation operator, $\mu_x$ and $\sigma$ are, respectively, the mean and standard deviation of the ECG signal.

Spectral parameters [16] assess the energy distribution in frequency domain for each heartbeat, which are obtained by firstly applying a Hamming window to achieve a high res-

olution and then implementing the FFT transformation. Particularly, spectral parameters extracted in this chapter consist of three parts: the first spectral moment normalized (denoted as $FSMN$), ratio of the area contained within the band delimited by the origin of the frequencies, and half the reference frequency (denoted as $A_1$), and ratio of the area contained in the range $0.7F$ to $1.4F$ (denoted as $A_2$). The mathematical expression for these three parts are presented as follows.

$$FSMN = \frac{1}{F}\frac{\sum_{0}^{\min(20F,100)} a_i * f_i}{\sum a_i} \tag{4.2}$$

$$A_1 = \frac{1}{F}\frac{\sum_{0.5}^{0.5F} a_i * f_i}{\sum_{0.5}^{20F} a_i} \tag{4.3}$$

$$A_2 = \frac{1}{F}\frac{\sum_{0.7F}^{1.4F} a_i * f_i}{\sum_{0.5}^{20F} a_i} \tag{4.4}$$

where $F$ is the frequency of the component with the greatest amplitude, namely, the peak frequency, in the range $0.5 - 9$ Hz; $f_i$ is the $i^{\text{th}}$ frequency in the FFT between 0 and 100 Hz; $a_i$ is the corresponding amplitude.

2) Inter-beat features: Inter-beat features characterize the variation of the heartbeat of interest with its neighboring heartbeats. The pre-RR interval refers to the RR interval between the current heartbeat and the previous heartbeat, while the post-RR interval examines the RR interval between the current heartbeat and the successive heartbeat. Ratio of the RR interval [58] measures the RR interval variation between the pre-RR interval and the post-RR interval, which involves three heartbeats. Ratio of the R-peaks amplitudes [58] reflects the amplitude change between the amplitude of the current R-peak and that of the previous R-peaks. Waveform similarity index (WSI) [58] determines the changes of consecutive

heartbeats due to the shape variations and is calculated as follows.

$$\Gamma = \frac{\sum_1^N [x_i(k) - \mu_{01}] \sum_1^N [x_{i-1}(k) - \mu_{02}]}{\sqrt{\sum_1^N [x_i(k) - \mu_{01}]} \sqrt{\sum_1^N [x_{i-1}(k) - \mu_{02}]}} \tag{4.5}$$

where $\Gamma$ represents the waveform similarity index; $\mu_{01}$ and $\mu_{02}$ denote the mean values of consecutive heartbeats, $x_i$ and $x_{i-1}$, respectively. For some ECG signal subject to large variation of the rhythm, WSI is sensitive to the length of the heartbeat. To overcome this problem, dynamic time warping (DTW) [6], another morphological feature, which can effectively compare two heartbeats in different lengths and at the same time alleviates the requirement to align two heartbeats, is also calculated.

### 4.3.2 Classifier Model

SVM is a type of effective machine learning based classification algorithms. Henceforth, SVM has been extensively studied in the academia and widely exploited in the practical classification problems.

Given the input vector $\mathbf{x}_i \in \mathbb{R}^{M \times 1}$, and the corresponding annotated labels $y_i \in \{+1, -1\}$. A trained model with calculated $\mu$ and $b$, is obtained by (2.6). For any feature vector $\hat{\mathbf{x}}$ with an unknown label, the corresponding decision value is estimated using the trained SVM model

$$\hat{f} \;=\; \sum_{i=1}^{N} \mu_i y_i K_G(\mathbf{x}_i, \hat{\mathbf{x}}) + b. \tag{4.6}$$

The above analysis shows that the heartbeat types are determined according to the distance from the point of interest to the separating boundary or the posterior probabilistic estimates of the point belonging to a certain type. Thus, it is concluded that SVM based classifiers are intrinsically binary classifiers.

The class-conditional densities $p(\hat{f}|y = \pm 1)$ between the margins are apparently exponential. A parametric model is directly used to fit the posterior probability $P(y_i = 1|\hat{f}_i)$ for the $i^{\text{th}}$ sample as

$$p_i = P(y_i = 1|\hat{x}_i) = P(y_i = 1|\hat{f}_i) = \frac{1}{1 + exp(A\hat{f}_i + B)}, \tag{4.7}$$

where $A$ and $B$ are parameters that maximize the log-likelihood function constructed using the training data, which is a cross-entropy error function:

$$\mathbf{max} \sum_{i=1}^{N} [t_i log(p_i) + (1 - t_i) log(1 - p_i)], \tag{4.8}$$

where $t_i = (y_i + 1)/2$ is a target probability for the $i^{\text{th}}$ sample, and a new training set is defined as $(\hat{f}_i, t_i)$.

In this paper, SVM classifiers are used to construct the global and the local classifiers. The LIBSVM package, one of the most popular SVM toolboxes, is exploited.

### 4.3.3 Classifying and Fusion of Classifiers

This subsection studies the classification strategy combining a global classifier and a local classifier. The above developed classifier can be used to predict the heartbeat types. However, the predicted result is not the final determination of the heartbeat type. The heartbeat type is determined by a classification strategy which involves the design of a global classifier, a local classifier and a fusion strategy combining the prediction results of the global and local classifiers.

The parameters associated with the global classifier is determined by exploiting the general public ECG database with heartbeat annotated by experts, which does not incorporate the patient-specific ECG information. There are two types of local classifiers: local classifiers with and without the intervention of the experts. For the local classifiers with the

intervention of experts, firstly the ECG data of the specific patient is classified by experts (or classified by the global classifier and then examined and corrected if necessary by experts) and then these data are exploited to train a local classifier. To make it fully-automatic, the local classifier without the intervention of the experts are formed this way: the ECG data of the specific patient is classified by the global classifier and only the predicted estimates with high probability, namely, high-confidence heartbeats are used to train a local classifier. It is obvious that the latter one is a fully automated local classifier, and thus it can be incrementally updated easily. In this paper, to facilitate the comparison, the same length of patient data is used to train a local classifier.

A novel fusion strategy is then proposed to combine more effectively the predicted estimates of the global and local classifiers. The principal is as follows: If the first small fraction of ECG data contains a certain number of VEB and non-VEB heartbeats, then the constructed local classifier may have a better performance. Otherwise, the local classifier constructed might not perform well. Thus, the novel strategy is: if the patient-specific training data contains the arrhythmia of interest to a certain portion, then the local classifier will decide the final results. Otherwise, the heartbeat type is determined by the global classifier.

The left chart of Fig. 4.1 shows how the local classifier is constructed. As can be seen, the global classifier is trained using the public database, and then the well-trained global classifier is used to predict the heartbeat type of a specific patients' ECG data. Only high-confidence heartbeats are exploited to train the local classifier. The right side of Fig. 4.1 shows the fusion of the global and local classifiers. The procedure is also illustrated in detail in Algorithm 3.

**Algorithm 3** Fusion strategy of global classifier (GC) and local classifier (LC).

**Input**

$DS1$ - training set;
$DS2$ - test set;
$DS21$ - the first 500 heartbeats in $DS2$;
$DS22$ - the remained data of $DS2$ excluding $DS21$;
$N_{lc}$ - number of heartbeats in DS21;
$I$ - number of heartbeats in $DS22$;
$\theta_p$ - the threshold for posterior probability.

**Output**

*output* - the fusion prediction of the global model and the local model.

Initialization: SVM classification configuration $params = [-s0 - t2 - b1]$;
Train the global classifier:

$$model_g = \mathbf{svmtrain}(y_i, \mathbf{x}_i, params), (\mathbf{x}_i, y_i) \in DS1;$$

Pick high-confidence personal training samples:

$$p_j = \mathbf{svmpredict}(\mathbf{x}_j, model_g, params), \mathbf{x}_j \in DS21;$$

**if** $p_j > \theta_p$ with $j \in \{1, 2, \cdots, N_{lc}\}$ **then**
    $D\hat{S}21 = \{(\mathbf{x}_j, y_j) | p_j > \theta_p\}$;
    $model_l = \mathbf{svmtrain}(y_j, \mathbf{x}_j, params), (\mathbf{x}_j, y_j) \in D\hat{S}21$;
**end if**
$i := 1$
For any $\hat{x} \in DS22$,
**if** $model_l$ exists **then**

$$output = \mathbf{svmpredict}(\hat{\mathbf{x}}, model_l, params);$$

**else**

$$output = \mathbf{svmpredict}(\hat{\mathbf{x}}, model_g, params);$$

**end if**
Return *output*.

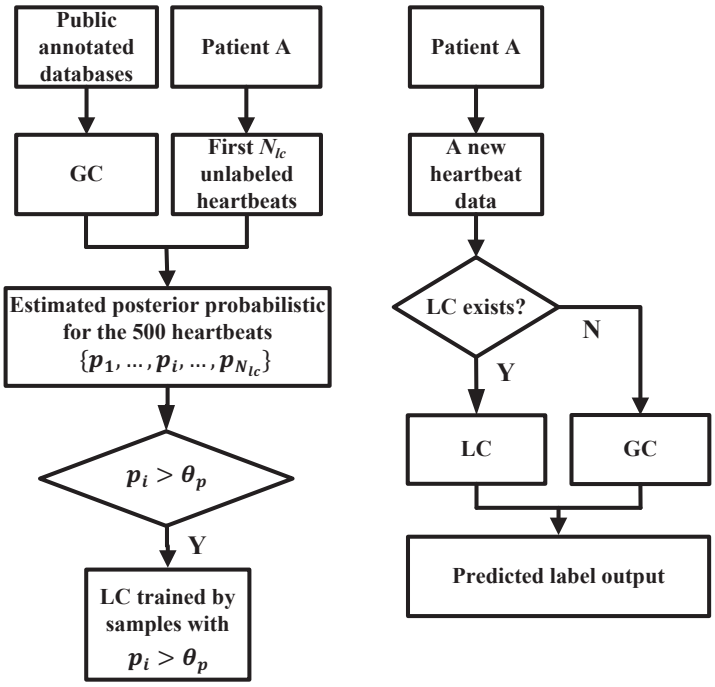


Figure 4.1: Proposed fusion strategy of the global classier and the local classifier.

### 4.3.4 Classification Performance Measures

Final assessment of the proposed algorithm is carried out in accordance with the AAMI recommendations [108]. Two sets of performance measurements are calculated. The performance measures focus on the ability of algorithms to distinguish VEBs from non-VEBs and SVEBs from non-SVEBs. Thus, two sets of performance measurements are calculated following the ways in Table V(a-b) of [71].

## 4.4 Simulation Results

### 4.4.1 Experiment Setup

As stated in Table 4.2, after four paced records are removed, the MITDB database is divided into DS1 and DS2, each of which contains 22 records. This data division scheme follows

prior investigations [86] [99] in order to facilitate the comparison. Data set DS1 is used to determine the parameters in the classification model, and DS2 is exploited to evaluate the developed classification model. Meanwhile, since the records in data sets DS1 and DS2 are not overlapped, the developed method belongs to the patient-specific classification strategy.

To construct a patient-adaptable classifier, the first 500 heartbeats in each record of the test set is annotated by experts or the global classifier so that the patient-specific information can be incorporated in the developed classification strategy. If the annotation is made by the experts, then the fused classification strategy is called experts intervention mode. If the annotation is made by the developed global classifier, then there is no need to involve the experts in the procedure, yielding the automatic adaptation mode.

### 4.4.2 Fixed Global Mode, Automatic Adaptation Mode and Expert Intervention Mode

Table 4.5 presents the classification accuracy using three classification modes for discriminating VEBs and SVEBs, respectively. The automatic adaptation mode yields an obvious performance improvement compared to the fixed global mode, especially for Records 105, 213 and 214. It is observed that in these three records, heartbeats of VEB appear in the first 500 heartbeats, which indicates that a patient-specific classifier can achieve a higher performance than a fixed global classifier due to the inevitable inter-beat variation. And thus, for the records containing VEB in their first 500 heartbeats, the local classifier without the experts' intervention dominates the classification results. However, for other records whose first 500 heartbeats do not contain VEB, the local classifier does not perform well. Similar phenomenon can also be seen for the classification of SVEB. The above observation motivates us to adopt novel fusion algorithms that can incorporate appropriately the patient-specific information.

Table 4.5 also presents the classification performance using the experts intervention mode,

which serves as a benchmark to evaluate the automatic adaptable mode. It is expected to see that the automatic adaptable mode yields a performance that falls in between the global classifier and the experts intervention mode, as shown in Table 4.7. Since more accurate heartbeat types can be provided in the experts' intervention mode, the constructed local classifier can accordingly generate good classification results. However, the experts intervention mode is not practical for the clinical center, since a large amount of physician's effort is needed. Furthermore, the classification results only exploiting single-lead ECG data in this chapter achieve a comparable or better results than those methods using two-lead ECG data in [86] [99] [109].

It is worth noting in Table 4.5 that our proposed methods does not yield a good performance for SVEB detection. As can be seen in the table, a super low SE for classification of SVEBs is obtained from the global classifier with an acceptable accuracy of 94.9%. This directly leads to a low SE value from the fused classifier under automatic adaptation mode, as the high-confidence local training samples cannot be guaranteed on which our proposed fusion strategy heavily relies on. However, the expert intervention mode achieves a comparable or even better performance than those of the reference works, i.e., with SVEBs existing in local personal training set, the trained local classifier works much better than the global classifier. This means the inter-beat variation has greater impact for SVEB detection than VEB detection. Both the VEB and SVEB classifiers show that the inter-beat variation cannot be ignored, which also validates the necessity of developing the proposed patient-specific classification strategy in this chapter.

Table 4.5: Classification accuracy of each record of DS22 under fixed global mode, expert intervention mode and automatic adaptation mode.

| Record | Total | DS21 (500 beats) | | DS22 (DS2-DS21) | | V | | | | | | S | | | | | |
|---|---|---|---|---|---|---|---|---|---|---|---|---|---|---|---|---|---|
| | | V | S | V | S | GC | | Auto | | Expert | | GC | | Auto | | Expert | |
| | | | | | | ACC | SE | ACC | SE | ACC | SE | ACC | SE | ACC | SE | ACC | SE |
| 100 | 2271 | 0 | 5 | 1 | 28 | 100 | 100 | 100 | 100 | 100 | 100 | 99.9 | 50 | 98.4 | 0 | 98.7 | 17.9 |
| 103 | 2082 | 0 | 0 | 0 | 2 | 100 | - | 100 | - | 100 | - | 99.8 | - | 99.9 | 50 | 99.9 | 50 |
| **105** | 2570 | 15 | 0 | 26 | 0 | 94.7 | 42.3 | 98.8 | 3.80 | 99.7 | 76.9 | 100 | - | 99.8 | - | 99.8 | - |
| 111 | 2122 | 0 | 0 | 1 | 0 | 99.3 | 100 | 99.9 | 0 | 99.3 | 100 | 99.8 | 0 | 100 | - | 100 | - |
| 113 | 1793 | 0 | 4 | 0 | 2 | 99.6 | - | 99.8 | - | 99.6 | - | 99.8 | 0 | 99.8 | 0 | 100 | 100 |
| 117 | 1533 | 0 | 0 | 0 | 1 | 99.9 | - | 99.9 | - | 99.9 | - | 99.9 | 100 | 99.8 | 0 | 99.8 | 0 |
| 121 | 1861 | 0 | 0 | 1 | 1 | 99.9 | 0 | 99.9 | 0 | 99.9 | 0 | 100 | - | 99.9 | 100 | 99.9 | 100 |
| 123 | 1516 | 1 | 0 | 2 | 0 | 100 | 100 | 100 | 100 | 100 | 100 | 97.9 | 39.3 | 100 | - | 100 | - |
| 200 | 2599 | 144 | 2 | 691 | 28 | 98 | 93.8 | 98 | 93.7 | 98.8 | 97.4 | 88.1 | 3.70 | 98.7 | 0 | 98.7 | 0 |
| 202 | 2134 | 7 | 1 | 12 | 54 | 99.2 | 91.7 | 99.7 | 66.7 | 99.7 | 66.7 | 97.8 | 60 | 88.1 | 3.70 | 96.7 | 0 |
| 210 | 2648 | 33 | 2 | 162 | 20 | 98.4 | 84.6 | 98.5 | 84.6 | 98.9 | 88.3 | 100 | - | 98.7 | 25 | 99.2 | 10 |
| 212 | 2746 | 0 | 0 | 0 | 0 | 100 | - | 100 | - | 100 | - | 99 | 0 | 100 | - | 100 | - |
| **213** | 3249 | 21 | 1 | 199 | 27 | 96.7 | 81.9 | 95.8 | 82.4 | 97.9 | 80.9 | 99.9 | - | 99 | 0 | 99 | 0 |
| **214** | 2260 | 59 | 0 | 199 | 0 | 97.4 | 77.7 | 97.9 | 82.2 | 99.7 | 97.5 | 82.7 | 5.90 | 99.9 | - | 99.9 | - |
| 219 | 2285 | 17 | 4 | 47 | 136 | 99.1 | 83 | 95.6 | 85.1 | 99.4 | 78.7 | 97.2 | - | 89.1 | 55.9 | 92.4 | 0 |
| 221 | 2425 | 95 | 0 | 302 | 0 | 99.8 | 99 | 99.8 | 99.3 | 99.8 | 99.7 | 83.2 | 71.8 | 98.8 | - | 97.2 | - |
| 222 | 2481 | 0 | 0 | 0 | 209 | 99.3 | - | 99.3 | - | 99.3 | - | 99.4 | 33.3 | 89.4 | 0 | 83.2 | 71.8 |
| 228 | 2051 | 113 | 0 | 269 | 3 | 99 | 94 | 99.6 | 98.4 | 99.8 | 98.8 | 100 | - | 99.8 | 0 | 99.4 | 33.3 |
| 231 | 1571 | 2 | 3 | 0 | 0 | 100 | - | 100 | - | 100 | - | 32.2 | 14.2 | 100 | - | 100 | - |
| 232 | 1778 | 0 | 373 | 0 | 1008 | 98.6 | - | 100 | - | 98.6 | - | 99.1 | 50 | 33.2 | 15.5 | 99.4 | 99.8 |
| 233 | 3077 | 134 | 3 | 700 | 4 | 98 | 93.5 | 99.6 | 99.3 | 99.6 | 99.1 | 97.8 | 10 | 99.1 | 50 | 99.8 | 0 |
| 234 | 2751 | 0 | 0 | 3 | 50 | 100 | 100 | 100 | 100 | 100 | 100 | 99.1 | 42.9 | 97.8 | 10 | 97.8 | 10 |
| Total | 49803 | 641 | 398 | 2578 | 1573 | 98.8 | **90.9** | 99.0 | **92.6** | 99.5 | **95.7** | 94.9 | 22.1 | 95.7 | 15.8 | 98.1 | 74.6 |

Note: '-' means invalid results as there are no VEB or SVEB in DS22; '0' means no VEB or SVEB correctly detected although they practically exist in DS22.

### 4.4.3 Performance Details under Automatic Adaptation Mode

Table 4.6 shows the performance assessment, as recommended by the AAMI standards. The first 500 beats in DS21 of the test subject are used to train the patient-specific local classifier and the classification performance is evaluated on the remaining data in DS22 of this subject. The final performance is obtained from the combination of the global classifier and the local classifier using the proposed fusion strategy.

Table 4.6: Classification performance details of each record of DS22.

| Record | V (Automatic Mode) | | | | S (Expert Intervention Mode) | | | |
|---|---|---|---|---|---|---|---|---|
| | ACC | SE | SP | PP | ACC | SE | SP | PP |
| 100 | 100 | 100 | 100 | 100 | 98.7 | 17.9 | 100 | 100 |
| 103 | 100 | - | 100 | - | 99.9 | 50 | 100 | 100 |
| 105 | 98.8 | 3.80 | 100 | 100 | 99.8 | - | 99.8 | 0 |
| 111 | 99.9 | 0 | 100 | - | 100 | - | 100 | - |
| 113 | 99.8 | - | 99.8 | 0 | 100 | 100 | 100 | 100 |
| 117 | 99.9 | - | 99.9 | 0 | 99.8 | 0 | 99.9 | 0 |
| 121 | 99.9 | 0 | 100 | - | 99.9 | 100 | 99.9 | 50 |
| 123 | 100 | 100 | 100 | 100 | 100 | - | 100 | - |
| 200 | 98 | 93.7 | 100 | 100 | 98.7 | 0 | 100 | - |
| 202 | 99.7 | 66.7 | 99.9 | 88.9 | 96.7 | 0 | 100 | - |
| 210 | 98.5 | 84.6 | 99.6 | 94.5 | 99.2 | 10 | 100 | 100 |
| 212 | 100 | - | 100 | - | 100 | - | 100 | 0 |
| 213 | 95.8 | 82.4 | 96.8 | 66.9 | 99 | 0 | 100 | - |
| 214 | 97.9 | 82.2 | 99.9 | 98.8 | 99.9 | - | 99.9 | 0 |
| 219 | 95.6 | 85.1 | 95.9 | 35.7 | 92.4 | 0 | 100 | - |
| 221 | 99.8 | 99.3 | 99.9 | 99.3 | 97.2 | - | 97.2 | 0 |
| 222 | 99.3 | - | 99.3 | 0 | 83.2 | 71.8 | 84.6 | 35.5 |
| 228 | 99.6 | 98.4 | 99.8 | 99.2 | 99.4 | 33.3 | 99.5 | 12.5 |
| 231 | 100 | - | 100 | - | 100 | - | 100 | - |
| 232 | 100 | - | 100 | - | 99.4 | 99.8 | 97.8 | 99.4 |
| 233 | 99.6 | 99.3 | 99.7 | 99.1 | 99.8 | 0 | 100 | - |
| 234 | 100 | 100 | 100 | 75.0 | 97.8 | 10.0 | 99.8 | 55.6 |
| Total | 99.0 | 92.8 | 99.5 | 92.6 | 98.1 | 74.6 | 99.1 | 76.9 |

### 4.4.4 Comparison with Other Reference Works

This subsection compares the classification performance of the proposed method with the related works in the literature. To facilitate the comparison, the ANSI/AAMI standards [108] are followed, and the classification performance for the types of SVEBs and VEBs which is our concern in this chapter, is evaluated in terms of ACC, SE, SP and PP. According to the data division scheme, the comparison is illustrated into two parts.

1) Comparison to the works under the same data division scheme

Table 4.7 presents the comparison results of the proposed methods with the works in the literature, where Proposed I, Proposed II and Proposed III refer to the fixed global mode, expert intervention mode and automatic adaptable mode, respectively. It can be observed that the fixed global mode proposed in this chapter using single lead achieves a better classification performance than that of Chazal [110] using single lead and Ye [109] exploiting two leads, which indicates that the features extracted in this chapter can provide a better discriminating capability of VEBs. However, the fixed global mode does not yield a good classification performance of SVEBs compared to the literature, which indicates that the features used do not capture the characteristics of SVEBs. The proposed expert intervention mode, as expected, yields better performance than the fixed global mode due to the reason that the classification strategy is aware of the patient-specific information. Particularly, the classification performance of the expert intervention mode generates a significant improvement for the SVEB detection, which shows that the inter-beat variation has a greater effect on the SVEB detection. That automatic adaptable mode, which does not need the intervention of physicians, yields a performance that is better than the fixed global mode, however, worse than the expert intervention mode, which is reasonable.

2) Compared with works using different data division scheme

To facilitate the comparison of different classification strategies, most of the research works follow the AAMI standards as well as the commonly used data division scheme. How-

ever, few works, for example, Hu [94] *et al.*, Ince *et al.* [89] [68], comply with the AAMI standards but employ different data division scheme. Specifically, Record 105 appears as a test record in [86] while a training record in [94]. Thus, it is not easy to directly compare their results with that of the proposed method. In the future, the proposed methods in Hu [94] *et al.*, Ince *et al.* [89] [68] will be examined using the commonly accepted data division scheme.

Table 4.7: Performance comparison of the proposed method and the major reference works.

| Methods | V | | | | S | | | | Leads | Mode |
|---|---|---|---|---|---|---|---|---|---|---|
| | ACC | SE | SP | PP | ACC | SE | SP | PP | | |
| Chazal [86] | 97.4 | 77.7 | 98.8 | 81.9 | 94.6 | 75.9 | 95.3 | 38.5 | 2 | Fixed |
| Ye [109] | 95.7 | 81.5 | 96.7 | 63.1 | 96.3 | 60.8 | 97.7 | 52.3 | 2 | Fixed |
| Ye [99] | 99.7 | 97.1 | 99.9 | 98.5 | 99.1 | 76.5 | 99.9 | 99.1 | 2 | Expert intervention |
| Chazal [86] | 99.4 | 94.3 | 99.7 | 96.2 | 95.9 | 87.7 | 96.2 | 47.0 | 2 | Expert intervention |
| Ye [99] | 99.4 | 91.8 | 99.9 | 98.0 | 98.3 | 61.4 | 99.8 | 90.7 | 2 | Automatic adaptation |
| Chazal [110] | 97.8 | 87.6 | 98.5 | 80.3 | 94.4 | 73.5 | 95.2 | 37.0 | 1 | Fixed |
| Proposed I | 98.8 | 90.9 | 99.4 | 90.8 | 95.6 | 21.2 | 98.4 | 32.8 | 1 | Fixed |
| Proposed II | 99.5 | 95.7 | 99.8 | 96.5 | 98.1 | 74.6 | 99.1 | 76.9 | 1 | Expert intervention |
| Proposed III | 99.0 | 92.8 | 99.5 | 92.6 | 95.6 | 19.8 | 98.5 | 32.7 | 1 | Automatic adaptation |

## 4.5 Conclusion

This chapter proposed an automatic patient-adaptable classification strategy to discriminate VEBs and SVEBs over the MITDB database. Firstly, a group of features consisting of several public intra-beat features by static measurement, such as the R-peak amplitude and spectral features, and some inter-beat features by dynamic measurement such as RR-interval, ratio of RR-interval, ratio of R-peak amplitude and waveform similarity. Dynamic measurement can better characterize intra-beat changes due to heart conditions or physical states in the

long-term ECG monitoring. Then, a novel classification strategy combining a global and a local classifiers is developed, where the global classifier is obtained using the public data and the local classifier is generated using the high-confidence data of a specific patient which is determined using the global classifier. Although the performance of the developed classifier is not as good as the expert intervention mode, it achieves fully-automatic classification, i.e., there is no need for the intervention of experts. Simulation results show that the classification strategy using single lead developed in this chapter for the detection of VEBs achieves comparable or even better than the results using single lead or two leads in the literature, due to the high generality of the extracted features and the novel fusion technique. However, the SVEB detection is not as good as the VEB detection, the possible reason might be: 1) the features do not capture the characteristic of SVEBs, 2) the inter-beat variation has a greater impact and 3) the high-confidence data does not have a high quality due to the low SE of SVEB detection using the global classifier.

In the future, firstly, the developed classification might be improved using multi-view feature sets for heartbeat classification. Especially for the detection of SVEBs, which is highly impacted by the inter-beat variation. Secondly, the features that can better capture the characteristics of the SVEBs need to be pursued so that the global classifier can achieve an acceptable SE, which will facilitate the design of the fully-automatic classification strategy. In the end, in some cases where there is no strict real-time performance requirement, the patient-specific data that has been classified by the global classifier can be used continuously to improve the developed classification strategy.

# Chapter 5

# Conclusions and Future Work

This dissertation concerns a resource-saving CLT-ECG system which consists of a raw ECG data acquisition system, a smartphone responsible for pre-processing of the signal and a server where advanced algorithms are implemented. This dissertation tackles some of the key problems existing in the resource-saving CLT-ECG scheme. However, there are still some issues to be dealt with before the system can be effectively and widely adopted. In this chapter, the research works that have been conducted in this dissertation are concluded. Furthermore, some possible research directions are also presented.

## 5.1 Conclusions

In this dissertation, three important issues that are closely related to the implementation of a resource-saving CLT-ECG system scheme are studied. Particularly, the detection of life-threatening algorithms, the discrimination of normal and abnormal heartbeats and classification of abnormal beats into different arrhythmia types are investigated. The conclusions are drawn as follows.

- **Life-Threatening Ventricular Arrhythmia Detection Using Personalized Features**

We have studied a detection algorithm of life-threatening ventricular arrhythmias exploiting two newly-extracted features, namely, aveCC and medianCC. These two features have been calculated based on the correlation coefficients between a patient-specific regular QRS-complex template and his/her real-time ECG data, which captures subtle differences in the QRS complexes among different people. SVM-based classification strategies have been developed exploiting a small set of most representative features selected from 11 newly extracted and 15 previously existing features. The effectiveness of the proposed algorithms has been validated under both the record-based and database-based data divisions. Specifically, under random record-based data divisions, the classification algorithm using two features, VFleak and aveCC, achieves an AUC value of $98.56\% \pm 0.89\%$, SP of $94.80 \pm 2.15\%$, and ACC of $94.66\% \pm 1.97\%$; and the classification algorithm using three features, VFleak, MEA, and aveCC, yields an AUC of $98.98\% \pm 0.58\%$, SP of $95.56\% \pm 1.45\%$, and ACC of $95.46\% \pm 1.36\%$. Similar results are also obtained under the database-based division scheme. It has been observed that the results outperform the available classification performance in the literature.

- **A Novel Normal and Abnormal Heartbeat Classification Method for a Resource-Saving CLT-ECG System Using OC-SVMs**

  We have developed a patient-specific arrhythmia detection algorithm using OC-SVMs, aiming to improve the resource-saving rate in the CLT-ECG monitoring system. Two types of heartbeat variations have been explored: WCI, which reflects a waveform change in one of the three segments (P/QRS/T segments) within one heartbeat, and modRRIR, which characterizes the successive heartbeat interval variation. The classification strategy has been designed by tuning the classifier adopting separately WCI and modRRIR, and then combining them to obtain the overall classification results. Evaluation of the proposed results using the publicly available MITDB database has

yielded an ACC of 78.4%, SE of 76.5%, SP of 93.2%, and PP of 98.9%, and, and has outperformed the results in the literature. Furthermore, the effectiveness of the proposed algorithms using the data collected from the ECG platform Heartcarer built has also been validated.

- **Patient-Specific VEBs and SVEBs Classification of ECG Heartbeats Exploiting a Single Lead**

  We have examined a patient-specific single-lead ECG heartbeat classification strategy, which discriminates VEBs and SVEBs. We have extracted intra-beat features, which characterize the distortion of the waveform within one heartbeat, and inter-beat features, which reflect the variation between successive heartbeats. The generality and effectiveness of the extracted feature set has been verified by VEB detection using the global classifier. Furthermore, we have proposed a novel fusion strategy combining a global classifier and a local classifier, which takes into account of the patient-specific information and thus can potentially improve the classification performance. By exploiting the high-confidence heartbeats to train the local classifier, fully-automatic classification is realized without the intervention of physicians. Simulation results have shown that comparable or even better classification performance is achieved, which validates the effectiveness of the proposed strategy.

## 5.2 Future Work

The work presented in this dissertation has addressed some critical issues concerning the implementation of the CLT-ECG monitoring system. However, there are still some open problems pertaining to the effectiveness of the monitoring system. Specifically, the following three research topics will be further studied.

- **Exploitation of Disease-Specific Features and Integration of Experienced**

**Classifiers**

The standard ECG heartbeat classification algorithm consists of extracting features of the heartbeat and then applying a certain classifier to identify the arrhythmia types. In most of the literature, the authors extract the features from the signal processing point of view, and the features extracted do not have an explicit relationship with the arrhythmias considered. It is of great value to understand in-depth the dynamics of the heart and the mechanics of how a certain type of arrhythmias affects the ECG signal. Based on the understanding, disease-specific features can be extracted that better reflect the arrhythmias of interest. Furthermore, in the clinical practice, for some heartbeats that are not easy to identify, several experienced cardiologists will discuss and then reach a final decision. This idea can also be adopted, i.e., several classifiers that based on different sets of features conduct the classification and the classification results are obtained by integrating comprehensively each of the experienced 'classifiers'.

- **Behavior-Adaptive Arrhythmia Classification Algorithms**

  The classification strategy, based on the training dataset, can be categorized into global classifiers and local classifiers. The global classifier captures the general characteristics of the heartbeats, whereas the local classifier takes the patient-specific characteristics into account. However, when a specific patient is in different conditions, for example, running, walking, standing or lying down, the characteristics may change. The current classification strategy does not consider such situations, which is necessary to investigate since for some mild arrhythmias, long-term ECG signal needs to be monitored. There are possibly two directions or the combination of them to solve this problem: 1) some advanced adaptive algorithms need to be developed that can automatically identify the subjects' condition change and conduct the classification accordingly and 2) supplementary information such as the gestures, speed of the subjective needs to be provided to the classification algorithm so that the current algorithm is aware of

the condition change. In general, the patient-specific classification algorithms that are capable of adapting to the patients' behavior are definitely promising methods and will be adopted in the clinical practice for the long-term ECG signal monitoring system.

- **Heart Disease Risk Prediction**

  The current ECG signal processing works mainly focus on heart disease classification for patients. Another potential research direction is to predict a heart disease risk for normal people, which means a potential health suggestion will be provided in advance to slow down the process of the heart getting ill. This direction will become more and more important in the future and benefit a larger group of people.

**Patents and Publications**

- Ping Cheng and Xiaodai Dong, "A Personalized Template Based Method for Electrocardiogram Ventricular Arrhythmia Detection," U.S. provisional patent application No. 62471334 filed in Mar. 2017.

- P. Cheng and X. Dong, "Life-Threatening Ventricular Arrhythmia Detection with Personalized Features," in *IEEE Access*, pp. 14195–14203, Jul. 2017.

- P. Cheng, and X. Dong, "A Novel Normal and Abnormal Heartbeat Classification Method for a Resource-Saving Cloud based Long-Term ECG Monitoring System Using One-Class Support Vector Machines," in preparation to submit.

- P. Cheng, and X. Dong, "A Patient-Specific Single-Lead ECG Heartbeat Classification Using Support Vector Machines," in preparation to submit.

# Bibliography

[1] Karpagachelvis, *Effective Arrhythmia Classification in ECG Using Machine Learning Techniques*. PhD thesis, KSR College of Arts and Science, Tamilnadu, India, Jun. 2012.

[2] J. Barron, "Secrets of the heart." `http://jonbarron.org/article/secrets-heart\#.ViAsVPlVhHw`.

[3] A. Sparshott, "A quick guide to ECG." `http://www.ivline.org/2010/05/quick-guide-to-ecg.html`.

[4] U. R. Acharya, *Advances in Cardiac Signal Processing*. NY, USA: Springer-Verlag, Apr. 2007.

[5] X. Chen, J. Ji, K. Loparo, and P. Li, "Real-time personalized cardiac arrhythmia detection and diagnosis: a cloud computing architecture," in *IEEE Int. Conf. Eng. Med. Biol. Soc.*, pp. 201–204, Feb. 2017.

[6] D. Ngo and B. Veeravalli, "Design of a real-time morphology-based anomaly detection method from ECG streams," in *IEEE Int. Conf. Bioinform. Biomed.*, pp. 829–836, Nov. 2015.

[7] A. Huang, W. Xu, Z. Li, L. Xie, M. Sarrafzadeh, X. Li, and J. Cong, "System light-loading technology for mHealth: manifold-learning-based medical data cleansing

and clinical trials in WE-CARE project," *IEEE J. Biomed. Health Inform.*, vol. 18, pp. 1581–1589, Sept. 2014.

[8] E. B. Mazomenos, D. Biswas, A. Acharyya, T. Chen, and K. Maharatna, "A low-complexity ECG feature extraction algorithm for mobile healthcare applications," *IEEE J. Biomed. Health Inform.*, vol. 17, pp. 459–469, Mar. 2013.

[9] A. V. Halteren, R. Bults, K. Wac, D. Konstantas, I. Widya, N. Dokovski, G. Koprinkov, V. Jones, and R. Herzog, "Mobile patient monitoring: The mobiHealth system," *J. Inform. Technol. Healthc.*, vol. 2, pp. 365–373, Oct. 2004.

[10] Resuscitation Council (UK), *Resuscitation guidelines 2000*, vol. 102. Aug. 2000.

[11] A. Amann, R. Tratning, and K. Unterkofler, "Reliability of old and new ventricular fibrillation detection algorithms for automated external defibrillation," *BioMed. Eng. OnLine*, vol. 60, pp. 1–15, Oct. 2005.

[12] F. J. Chin, Q. Fang, T. Zhang, and I. Cosic, "A fast critical arrhythmic ECG waveform identification method using cross-correlation and multiple template matching," in *IEEE Int. Conf. Eng. Med. Biol. Soc.*, pp. 1922–1925, Aug. 2010.

[13] M. A. Arafat, A. W. Chowdhury, and M. K. Hasan, "A simple time domain algorithm for the detection of ventricular fibrillation in electrocardiogram," *Signal Image Video Process.*, vol. 5, pp. 1–10, Sept. 2011.

[14] N. Thakor, Y. Zhu, and K. Pan, "Ventricular tachycardia and fibrillation detection by a sequential hypothesis testing algorithm," *IEEE Trans. Biomed. Eng.*, vol. 37, pp. 837–843, Sept. 1990.

[15] E. M. A. Anas, S. Y. Lee, and M. K. Hasan, "Sequential algorithm for life threatening cardiac pathologies detection based on mean signal strength and EMD functions," *BioMed. Eng. OnLine*, vol. 9, Sept. 2010.

[16] S. Barro, R. Ruiz, D. Cabello, and J. Mira, "Algorithmic sequential decision making in the frequency domain for life threatening ventricular arrhythmias and imitative artifacts: a diagnostic system," *J. of Biomed. Eng.*, vol. 11, pp. 320–328, Jul. 1989.

[17] R. Dzwonczyk, C. G. Brown, and H. A. Werman, "The median frequency of the ECG during ventricular fibrillation: its use in an algorithm for estimating the duration of cardiac arrest," *IEEE Trans. Biomed. Eng.*, vol. 37, pp. 640–646, Jun. 1990.

[18] I. Jekova and V. Kraseva, "Real time detection of ventricular fibrillation and tachycardia," *Physiol. Meas.*, vol. 25, pp. 1167–1178, Aug. 2004.

[19] X. Zhang, Y. Zhu, N. Thakor, and Z. Wang, "Detecting ventricular tachycardia and fibrillation by complexity measure," *IEEE Trans. Biomed. Eng.*, vol. 46, pp. 548–555, May 1999.

[20] A. Amann, R. Tratning, and K. Unterkofler, "Detecting ventricular fibrillation by time-delay methods," *IEEE Trans. Biomed. Eng.*, vol. 54, pp. 174–177, Jan. 2007.

[21] H. Li, W. Han, C. Hu, and Q. Meng, "Detecting ventricular fibrillation by fast algorithm of dynamic sample entropy," in *IEEE Int. Conf. Robot. Biomimet.*, Dec. 2009.

[22] I. Jekova, "Comparison of five algorithms for the detection of ventricular fibrillation from the surface ECG," *Physiol. Meas.*, vol. 21, pp. 429–439, Aug. 2000.

[23] F. Alonso-Atienza, E. Morgado, L. Fernandez-Martinez, A. Garcia-Alberola, and J. L. Rojo-Alvarez, "Detection of life-threatening arrhythmias using feature selection and support vector machines," *IEEE Trans. Biomed. Eng.*, vol. 61, pp. 832–840, Mar. 2014.

[24] N. A. M. S. Islam, N. Ammour and M. Abdullah-Al-Wadud, "Selection of heart-biometric templates for fusion," *IEEE Access*, vol. 5, pp. 1753–1761, Feb. 2017.

[25] S. H. Jambukia, V. K. Dabhi, and H. B. Prajapati, "Classification of ECG signals using machine learning techniques: A survey," in *Int. Conf. Advances in Comput. Eng. and Appl.*, pp. 714–721, Mar. 2015.

[26] C. Figuera, U. Irusta, E. Morgado, E. Aramendi, U. Ayala, L. Wik, J. Kramer-Johansen, T. Eftestol, and F. Alonso-Atienza, "Machine learning techniques for the detection of shockable rhythms in automated external defibrillators," *Plos ONE*, vol. 11, pp. 1–17, Jul. 2016.

[27] H. Peng, F. Long, and C. Ding, "Feature selection based on mutual information criteria of max-dependency, max-relevance, and min-redundancy," *IEEE Trans. Pattern Anal. Mach. Intell.*, vol. 27, pp. 1226–1238, Aug. 2005.

[28] Q. Gu, Z. Li, and J. Han, "Generalized fisher score for feature selection," in *Conf. Uncertainty in Artificial Intell.*, pp. 266–273, Jul. 2011.

[29] S. Chen, N. Thakor, and M. Mover, "Ventricular fibrillation detection by a regression test on the autocorrelation function," *Med. Biol. Eng. Comput.*, vol. 25, pp. 241–249, May 1987.

[30] K. Minami, H. Nakajima, and T. Toyoshima, "Real-time discrimination of ventricular tachyarrhythmia with fourier-transform neural network," *IEEE Trans. Biomed. Eng.*, vol. 46, pp. 179–185, Feb. 1999.

[31] Q. Li, C. Rjagopalan, and G. Clifford, "Ventricular fibrillation and tachycardia classification using a machine learning approach," *IEEE Trans. Biomed. Eng.*, vol. 61, pp. 1607–1613, Jun. 2014.

[32] R. Clayton, A. Murray, and R. Campbell, "Recognition of ventricular fibrillation using neural networks," *Med. Biol. Eng. Comput.*, vol. 32, pp. 217–220, Mar. 1994.

[33] E. Aramendi, U. Irusta, E. Pastor, A. Bodegas, and F. Benito, "ECG spectral and morphological parameters reviewed and updated to detect adult and paediatric life-threatening arrhythmia," *Physiol. Meas.*, vol. 31, pp. 749–761, Apr. 2010.

[34] U. Irusta, J. Ruiz, E. Aramendi, S. R. de Gauna, U. Ayala, and E. Alonso, "A high-temporal resolution algorithm to discriminate shockable from nonshockable rhythms in adults and children," *Resuscitation*, Jan. 2012.

[35] M. Faezipour, A. Saeed, S. C. Bulusu, a. H. M. M. Nourani, and L. Tamil, "A patient-adaptive profiling scheme for ECG beat classification," *IEEE Trans. Inf. Technol. Biomed.*, vol. 14, pp. 1153–1165, Sept. 2010.

[36] J. Park and K. Kang, "PcHD: Personalized classification of heartbeat types using a decision tree," *Comput. Biol. Med.*, vol. 54, pp. 79–88, Aug. 2014.

[37] S. A. Israel, J. M. Irvine, A. Cheng, M. D. Wiederhold, and B. K. Wiederhold, "ECG to identify individuals," *Pattern Recognit.*, vol. 38, pp. 133–142, Jan. 2005.

[38] T. Last, C. D. Nugent, and F. J. Owens, "Multi-component based cross correlation beat detection in electrocardiogram analysis," *BioMed. Eng. OnLine*, vol. 3, p. 26, Jul. 2004.

[39] E. Laciar, R. Jané, and D. H. Brooks, "Improved alignment method for noisy high-resolution ECG and holter records using multiscale cross-correlation," *IEEE Trans. Biomed. Eng.*, vol. 50, pp. 344–353, Mar. 2003.

[40] S. Dutta, A. Chatterjee, and S. Munshi, "Correlation technique and least square support vector machine combine for frequency domain based ECG beat classification," *Med. Eng. Phys.*, vol. 32, pp. 1161–1169, Dec. 2010.

[41] N. S. Hammed and M. I. Owis, "Patient adaptable ventricular arrhythmia classifier using template matching," in *IEEE Conf. Biomed. Circuits and Systems*, pp. 1–4, Oct. 2015.

[42] A. Page, T. Soyata, J. P. Couderc, and M. Aktas, "An open source ECG clock generator for visualization of long-term cardiac monitoring data," *IEEE Access*, vol. 3, pp. 2704–2714, Dec. 2015.

[43] G. Moody and R. Mark, "The impact of the MIT-BIH arrhythmia database," *IEEE Eng. Med. Biol. Mag.*, vol. 20, pp. 45–50, May-Jun. 2001.

[44] F. M. Nolle, F. K. Badura, J. M. Catlett, R. W. Bowser, and M. H. Sketch, "CREI-GARD, a new concept in computerized arrhythmia monitoring systems," in *IEEE Conf. Comput. Cardiol.*, vol. 13, pp. 515–518, 1986.

[45] S. Greenwald, "The development and analysis of a ventricular fibrillation detector," Master's thesis, Massachusetts Institute of Technology, MA, USA, May 1986.

[46] J. Li, G. Deng, W. Wei, H. Wang, and Z. Ming, "Design of a real-time ECG filter for portable mobile medical systems," *IEEE Access*, vol. 5, pp. 696–704, Mar. 2016.

[47] A. Amann, R. Tratnig, and K. Unterkofler, "A new ventricular fibrillation detection algorithm for automated external defibrillators," in *IEEE Conf. Comput Cardiol.*, pp. 559–562, Sept. 2005.

[48] J. Pan and W. J. Tompkins, "A real-time QRS detection algorithm," *IEEE Trans. Biomed. Eng.*, vol. 32, pp. 230–236, Mar. 1985.

[49] G. Camps-Balls, J. L. Rojo-Alvarez, and M. Martinez-Ramon, *Kernel Methods in Bioengineering, Communications and Image Processing.* PA, USA: Idea Group Inc., Jan. 2007.

[50] V. N. Vapnik, *The Nature of Statistical Learning Theory*. NY, USA: Springer-Verlag, Mar. 1995.

[51] W. Lu, "Support Vector Machines," in *Leture Notes of Machine Learning for Signal Processing*, ch. 5, pp. 140–161, BC, Canada: University of Victoria, Jan. 2015.

[52] Y. S. Abu-Mostafa, M. Magdon-Ismail, and H.-T. Lin, "Training versus testing," in *Learning From Data*, ch. 2, pp. 39–76, Berlin, Germany: AMLBook, Mar. 2012.

[53] P. Cheng and X. Dong, "Life-threatening ventricular arrhythmia detection with personalized features," *IEEE Access*, vol. 5, pp. 14195–14203, Jul. 2017.

[54] G. Belforte, R. D. Mori, and F. Ferraris, "A contribution to the automatic processing of electrocardiograms using syntactic methods," *IEEE Trans. Biomed. Eng.*, vol. 26, pp. 125–136, Mar. 1979.

[55] P. Trahanias and E. Skordalakis, "Syntactic pattern recognition of the ECG," *IEEE Trans. Pattern Anal. Mach. Intell.*, vol. 12, pp. 648–657, Jul. 1990.

[56] P. Macfarlane, B. Devine, and E. Clark, "The university of glasgow Uni-G ECG analysis program," in *IEEE Conf. Comput. Cardiol.*, vol. 32, pp. 451–454, Sept. 2005.

[57] A. R. Houghton and D. Gray, *Making Sense of the ECG: A Hands-On Guide*. Lincolnshire, UK: CRC Press, 4nd ed., Jan. 2014.

[58] U. Satija, B. Ramkumar, and M. S. Manikandan, "Robust cardiac event change detection method for long-term healthcare monitoring applications," *IET Healthc. Technol. Lett.*, vol. 3, pp. 116–123, Dec. 2016.

[59] C. Li, C. Zheng, and C. Tai, "Detection of ECG characteristic points using wavelet transforms," *IEEE Trans. Biomed. Eng.*, vol. 42, pp. 21–28, Jan. 1995.

[60] J. Martinez and P. Laguna, "A wavelet-based ECG delineator: evaluation on standard databases," *IEEE Trans. Biomed. Eng.*, vol. 51, pp. 570–581, Mar. 2004.

[61] B. Weng, M. Blanco-Velasco, and K. Barner, "ECG denoising based on the empirical mode decomposition," in *IEEE Int. Conf. Eng. Med. Biol. Soc.*, pp. 1–4, Aug.-Sept. 2006.

[62] N. Srinivasan, D. F. Ge, and S. M. Krishnan, "Autoregressive modeling and classification of cardiac arrhythmias," in *IEEE Int. Conf. Eng. Med. Biol. Soc.*, vol. 2, pp. 1405–1406, Oct. 2002.

[63] H. Hussain and L. L. Fatt, "Efficient ECG signal classification using sparsely connected radial basis function neural network," in *Int. Conf. Circuits Syst. Electron. Contr. Sig. Process.*, pp. 412–416, Dec. 2007.

[64] R. R. Marcello, S. F. Jamil, and S. J. Philip, "Beat detection and classification of ECG using self organizing maps," *IEEE Int. Conf. Eng. Med. Biol. Soc.*, vol. 1, pp. 89–91, Oct.-Nov. 1997.

[65] Y. Ozbay, R. Ceylan, and B. Karlik, "Integration of type-2 fuzzy clustering and wavelet transform in a neural network based ECG classifier," *Expert Syst. Appl.*, vol. 38, pp. 1004–1010, Jan. 2011.

[66] H. M. Rai, A. Trivedi, and S. Shukla, "ECG signal processing for abnormalities detection using multi-resolution wavelet transform and artificial neural network classifier," *Measurement*, vol. 46, pp. 3238–3246, Nov. 2013.

[67] S. Chauhan and L. Vig, "Anomaly detection in ECG time signals via deep long short-term memory networks," in *IEEE Int. Conf. Data Science and Advanced Analytics*, pp. 1–7, Oct. 2015.

[68] S. Kiranyaz, T. Ince, and M. Gabbouj, "Real-time patient-specific ECG classification by 1-d convolutional neural networks," *IEEE Trans. Biomed. Eng.*, vol. 63, pp. 664–675, Mar. 2016.

[69] P. Li, Y. Wang, J. He, L. Wang, Y. Tian, T. Zhou, T. Li, and J. Li, "High-performance personalized heartbeat classification model for long-term ECG signal," *IEEE Trans. Biomed. Eng.*, vol. 64, pp. 78–86, Jan. 2017.

[70] P. de Chazal, B. G. Celler, and R. B. Rei, "Using wavelet coefficients for the classification of the electrocardiogram," in *IEEE Int. Conf. Eng. Med. Biol. Soc.*, vol. 1, pp. 64–67, Jul. 2000.

[71] P. de Chazal, M. O'Dwyer, and R. B. Reilly, "Automatic classification of heartbeats using ECG morphology and heartbeat interval features," *IEEE Trans. Biomed. Eng.*, vol. 51, pp. 1196–1206, Jul. 2004.

[72] L. Sörnmo and P. Laguna, *Bioelectrical Signal Processing in Cardiac and Neurological Applications*, ch. 6, pp. 411–452. Academic Press, 1st ed., Jun. 2005.

[73] M. A. Escalona-Moran, M. C. Soriano, I. Fischer, and C. R. Mirasso, "Electrocardiogram classification using reservoir computing with logistic regression," *IEEE J. Biomed. Health Inform.*, vol. 19, pp. 892–898, May 2015.

[74] C. M. Yu, H. Lin, Q. Zhang, and J. E. Sanderson, "High prevalence of left ventricular systolic and diastolic asynchrony in patients with congestive heart failure and normal QRS duration," *Cardiovasc. Med.*, vol. 89, pp. 54–60, Mar. 2003.

[75] E. J. da S. Luz, W. R. Schwartz, G. Camara-Chavez, and D. Menotti, "ECG-based heartbeat classification for arrhythmia detection: A survey," *Comput. Methods and Programs Biomed.*, vol. 127, pp. 144–164, Apr. 2016.

[76] C. Ye, M. T. Coimbra, and B. V. K. V. Kumar, "Arrhythmia detection and classification using morphological and dynamic features of ECG signals," in *IEEE Int. Conf. Eng. Med. Biol. Soc.*, pp. 1918–1921, Aug. 2010.

[77] S. Yu and K. Chou, "Integration of independent component analysis and neural networks for ECG beat classification," *Expert Syst. Appl.*, vol. 34, pp. 2841–2846, May 2008.

[78] S. Yu and Y. Chen, "Electrocardiogram beat classification based on wavelet transformation and probabilistic neural network," *Pattern Recognit. Lett.*, vol. 28, pp. 1142–1150, Jul. 2007.

[79] I. Guler and E. D. Ubeyli, "ECG beat classifier designed by combined neural network model," *Pattern Recognit.*, vol. 38, pp. 199–208, Feb. 2005.

[80] M. H. Song, J. Lee, S. P. Cho, K. J. Lee, and S. K. Yoo, "Support vector machine based arrhythmia classification using reduced features," *Int. J. Control, Autom. Syst.*, vol. 3, pp. 571–579, Dec. 2005.

[81] K. Robert and E. C. Colleen, *Basis and Treatment of Cardiac Arrhythmias.* NY, USA: Springer, 1st ed., Sept. 2005.

[82] S. Evans, H. Hastings, and M. Bodenheimer, "Differentiation of beats of ventricular and sinus origin using a self-training neutal network," *PACE*, vol. 17, pp. 611–626, Apr. 1994.

[83] K. Minami, H. Nakajima, and T. Toyoshima, "Real-time discrimination of ventricular tachyarrhythmia with Fourier-transform neural network," *IEEE Trans. Biomed. Eng.*, vol. 46, pp. 179–185, Feb. 1999.

[84] G. A. Ng, "Treating patients with ventricular ectopic beats," *Heart*, vol. 92, pp. 1707–1712, Nov. 2006.

[85] I. Christov, I. Jekova, and G. Bortolan, "Premature ventricular contraction classification by the $k$th nearest-neighbours rule," *Physiol. Meas.*, vol. 26, pp. 123–130, Jan. 2005.

[86] P. de Chazal and R. B. Reilly, "A patient-adaptive heartbeat classifier using ECG morphology and heartbeat interval features," *IEEE Trans. Biomed. Eng.*, vol. 53, pp. 2535–2543, Dec. 2006.

[87] C. Ye, B. V. K. V. Kumar, and M. T. Coimbra, "Heartbeat classification using morphological and dynamic features of ECG signal," *IEEE Trans. Biomed. Eng.*, vol. 59, pp. 2930–2941, Oct. 2012.

[88] L. Senhadji, G. Carrault, J. J. Bellanger, and G. Passariello, "Comparing wavelet transforms for recognizing cardiac patterns," *IEEE Trans. Biomed. Eng.*, vol. 14, pp. 167–173, Mar.-Apr. 1995.

[89] T. Ince, S. Kiranyaz, and M. Gabbouj, "A generic robust system for automated patient-specific classification of electrocardiogram signals," *IEEE Trans. Neural Netw.*, vol. 56, pp. 1415–1426, May 2009.

[90] S. Osowski, L. T. Hoa, and T. Markiewic, "Support vector machine-based expert system for reliable heartbeat recognition," *IEEE Trans. Biomed. Eng.*, vol. 51, pp. 582–589, Apr. 2004.

[91] X. Jiang, L. Q. Zhang, Q. B. Zhao, and S. Albayrak, "ECG arrhythmia recognition system based on independent component analysis feature extraction," in *IEEE Region 10 Conf.*, pp. 1–4, Nov. 2006.

[92] M. Llamedo and J. P. Martinez, "Heartbeat classification using feature selection driven by database generalization criteria," *IEEE Trans. Biomed. Eng.*, vol. 58, pp. 616–625, Mar. 2011.

[93] W. Jiang and S. G. Kong, "Block-based neural networks for personalized ECG signal classification," *IEEE Trans. Neural Netw.*, vol. 18, pp. 1750–1761, Nov. 2007.

[94] Y. H. Hu, S. Palreddy, and W. J. Tompkins, "A patient-adaptable ECG beat classifier using a mixture of experts approach," *IEEE Trans. Biomed. Eng.*, vol. 44, pp. 891–900, Sept. 1997.

[95] H. EI-Saadawy, M. Tantawi, H. A. Shedeed, and M. F. Tolba, "Electrocardiogram (ECG) classification based on dynamic beats segmentation," in *Int. Conf. Inf. Syst.*, pp. 75–80, May 2016.

[96] Z. Zhang, J. Dong, X. Luo, K. Choi, and X. Wu, "Heartbeat classification using disease-specific feature selection," *Comput. Biol. Med.*, vol. 46, pp. 79–89, Mar. 2014.

[97] C. L. Herry, M. Frasch, A. J. Seely, and H. Wu, "Heart beat classification from single-lead ECG using the synchrosqueezing transform," *Physiol. Meas.*, vol. 38, pp. 171–178, Jan. 2017.

[98] M. Lagerholm, C. Peterson, G. Braccini, L. Edenbrandt, and L. Sörnmo, "Clustering ECG complexes using Hermite functions and self-organizing maps," *IEEE Trans. Biomed. Eng.*, vol. 47, pp. 838–848, Jul. 2000.

[99] C. Ye, B. V. K. V. Kumar, and M. T. Coimbra, "An automatic subject-adaptable heartbeat classifier based on multiview learning," *IEEE J. Biomed. Health Inform.*, vol. 20, pp. 1485–1492, Nov. 2016.

[100] M. Llamedo and J. P. Martinez, "Automatic patient-adapted ECG heartbeat classifier allowing expert assistance," *IEEE Trans. Neural Netw.*, vol. 59, pp. 2312–2320, Aug. 2012.

[101] S. Kiranyaz, T. Ince, and M. Gabbouj, *Multi-Dimensional Partical Swarm Optimization for Machine Learning and Pattern Recognition*. New York, USA: Springer, Jul. 2013.

[102] E. D. Ubeyli, "Eigenvector methods for automated detection of electrocardiographic changes in partial epileptic patients," *IEEE Trans. Inf. Technol. Biomed.*, vol. 13, pp. 478–485, Jul. 2009.

[103] V. Krasteva and I. Jekova, "QRS template matching for recognition of ventricular ectopic beats," *Ann. Biomed. Eng.*, vol. 35, pp. 2065–2076, Dec. 2007.

[104] M. Zubair, J. Kim, and C. Yoon, "An automated ECG beat classification system using convolutional neural networks," in *Int. Conf. IT Convergence Security*, pp. 1–5, Sept. 2016.

[105] C. Li, C. Zheng, and C. Tai, "Detection of ECG characteristic points using wavelet transforms," *IEEE Trans. Biomed. Eng.*, vol. 42, pp. 21–28, Jan. 1998.

[106] I. Jekova, "Shock advisory tool: Detection of life-threatening cardiac arrhythmias and shock success prediction by means of a common parameter set," *Biomed. Signal Process. Control*, vol. 2, pp. 25–33, Jan. 2007.

[107] Q. Li, R. G. Mark, and G. D. Clifford, "Robust heart rate estimation from multiple asynchronous noisy sources using signal quality indices and a kalman filter," *Physiol. Meas.*, vol. 29, pp. 15–32, Jan. 2008.

[108] AAMI, *Testing and Reporting Performance Results of Cardiac Rhythm and ST Segment Measurement Algorithms Association for the Advancement of Medical Instrumentation*. Arlington, VA: ANSI/AAMI EC57, 1998.

[109] C. Ye, *Advanced Heartbeat Classification Models for Reliable Electrocardiogram Analysis in Ambulatory Health Monitoring.* PhD thesis, Carnegie Mellon University, PA, USA, Nov. 2013.

[110] P. de Chazal, "Detection of supraventricular and ventricular ectopic beats using a single lead ECG," in *IEEE Int. Conf. Eng. Med. Biol. Soc.*, pp. 45–48, Jul. 2013.